JAERI-M
7364

NUMERICAL STRESS ANALYSIS OF TOROIDAL COIL BY THREE DIMENSIONAL FINITE ELEMENT METHOD

October 1977

Hidetomo NISHIMURA* and Susumu SHIMAMOTO

日本原子力研究所
Japan Atomic Energy Research Institute

この報告書は，日本原子力研究所が JAERI-M レポートとして，不定期に刊行している研究報告書です．入手，複製などのお問合わせは，日本原子力研究所技術情報部（茨城県那珂郡東海村）あて，お申しこしください．

JAERI-M reports, issued irregularly, describe the results of research works carried out in JAERI. Inquiries about the availability of reports and their reproduction should be addressed to Division of Technical Information, Japan Atomic Energy Research Institute, Tokai-mura, Naka-gun, Ibaraki-ken, Japan.

JAERI-M 7364

Numerical Stress Analysis of Toroidal Coil by Three-Dimensional Finite Element Method

Hidetomo NISHIMURA* and Susumu SHIMAMOTO

Division of Thermonuclear Fusion Reseach,
Tokai Reseach Establishment, JAERI

(Received October 8, 1977)

A structure analysis program based on finite element method for toroidal coils, developed in JAERI, and its example application to a medium-size tokamak are described. In this application, the effects of material anisotropy, poloidal field and spring constant value were studied, and also the influence of toroidal coil failure on the peak stress.

The following were revealed. The effect of anisotropy on the peak stress in reinforcement must be considered. The effect of poloidal field on the peak stress is small compared with that of toroidal field. The spring constant value between coil and support does not much influence the peak stress value. The peak stress in reinforcement rises with increasing number of failed coils.

In the case of 2000 nodes on the structure, CPU time with the program is about 40 min.

Keywords; Structure Analysis, Finite Element Method, Poloidal Coil, Spring Constant, Anisotropy, Support, Coil Failure, Stresses

---

*On leave from Hitachi Reseach Laboratory, Hitachi Ltd.

JAERI－M　7364

三次元有限要素法によるトロイダル・コイルの応力解析

日本原子力研究所東海研究所核融合研究部

西村　秀知*・島本　　進

（1977年10月8日受理）

原研で開発されたトロイダル・コイルのための，有限要素法を利用した構造解析プログラムと中規模トロイダル・コイルへのこのプログラムの応用例について述べた。この例で材料の異方性，ポロイダル磁界，バネ定教の値の影響について探求した。また，トロイダル・コイルの故障が最大応力にどの様な影響を与えるかも探求した。

次の結論を得た。異方性が補強材の最大応力に与える影響は無視できない。ポロイダル磁界による応力はトロイダル磁界による応力と比べると非常に小さい。支持部でのバネ定数の値の変化は最大応力に大きな変化を与えない。故障コイルの数が多くなると最大応力も増加する。

なお，コイルの節点数が2000ほどの場合には，CPU時間は約40分であった。

* 外来研究員：日立製作所　日立研究所

Contents

1. Introduction

The absence of applicable computer programs has been a major obstacle to the performance of detailed structural analyses of toroidal coils. This obstacle has recently been overcome by the development of the finite element method and its applications.[1,2,3] JAFUSAC (JAERI Fusion Structure Analysis on Coil), a computer program developed in JAERI for three dimensional stress calculation by the finite element method, is available to estimate the stress distribution in a toroidal coil. As this program is able to run not only batch mode but also time sharing mode in conjunction with a graphic display terminal, it is possible to get graphic output data by plotter, computer output microfilm (COM) in batch center or hard copy on the graphic display terminal. Though its capability and an example toroidal coil analysis was already discussed,[4] more detailed results are presented in this paper.

2. Computer Program JAFUSAC

The program JAFUSAC is actually a set of programs that are related to each other and must be execute in the proper order as shown in Fig.1. The five independent computer programs are structured to be compatible with respect to input and output. Each of the five programs has a separate identity and can be run independently. Each program has been set up so that, when applicable, it can be also run with edited output data generated by one of the other programs. The functions of these programs are described briefly in the following paragraphs.

2.1 Input Generater

The first program, the user must execute, is IG (Input Generating program) which is used to describe the geometry of a toroidal coil shaped circular, oval or D-shape. By means of this program IG, it is not necessary to assemble a deck of typically hundreds or thousands of cards in order to sepcify the toroidal coil geometry. Because this program generates almost all node and element data of the coil geometry automatically itself except several data-cards of key-points. And magnetic field is calculated by volume current integration method. Furthermore, electromagnetic, gravitational and seismic forces on the center of gravity in each element are given simultaneously. Then, other

1. Introduction

The absence of applicable computer programs has been a major obstacle to the performance of detailed structural analyses of toroidal coils. This obstacle has recently been overcome by the development of the finite element method and its applications.[1,2,3] JAFUSAC (JAERI Fusion Structure Analysis on Coil), a computer program developed in JAERI for three dimensional stress calculation by the finite element method, is available to estimate the stress distribution in a toroidal coil. As this program is able to run not only batch mode but also time sharing mode in conjunction with a graphic display terminal, it is possible to get graphic output data by plotter, computer output microfilm (COM) in batch center or hard copy on the graphic display terminal. Though its capability and an example toroidal coil analysis was already discussed,[4] more detailed results are presented in this paper.

2. Computer Program JAFUSAC

The program JAFUSAC is actually a set of programs that are related to each other and must be execute in the proper order as shown in Fig.1. The five independent computer programs are structured to be compatible with respect to input and output. Each of the five programs has a separate identity and can be run independently. Each program has been set up so that, when applicable, it can be also run with edited output data generated by one of the other programs. The functions of these programs are described briefly in the following paragraphs.

2.1 Input Generater

The first program, the user must execute, is IG (Input Generating program) which is used to describe the geometry of a toroidal coil shaped circular, oval or D-shape. By means of this program IG, it is not necessary to assemble a deck of typically hundreds or thousands of cards in order to sepcify the toroidal coil geometry. Because this program generates almost all node and element data of the coil geometry automatically itself except several data-cards of key-points. And magnetic field is calculated by volume current integration method. Furthermore, electromagnetic, gravitational and seismic forces on the center of gravity in each element are given simultaneously. Then, other

data, for example, support condition, thermal force, and anisotorpy, must be added to the previous data.

2.2 Input Data Check Program

The second program is IDAC (Input Data Check program) which is used to check up the data generated by the program IG. According to the data, this program plots the toroidal coil structure on the paper of plotter, film of COM or cathode-ray tube of graphic display terminal so that debugging work is easy. An examination of the picture plotted by this program makes easy to find whether the data are good or not.

2.3 Matrix Solving Program

The third program is MESA (Member, Element, Solid Analysis program) which is general purpose finite element method program for static load analysis of linear elastic structures. This program is permitted consideration of isotropic and/or anisotropic materials and calculation of principal stresses and Von Mises stress in each element. The wave front method is used in order to solve a giantic size stiffness matrix equation in this program. At the present time, size 6000×6000 matrix equation can be solved by less than 40 minutes CPU time.

2.4 Plotting Program

One of the outputting programs for resultant data of the MESA is called MOP (MESA Output Plotting program) that can plot induced nodal translational displacements magnified by a specified scale factor and superimpose on a plot of the toroidal coil structure. The user select the view to be plotted.

Another outputting program the user must execute is SPP (Stress Printing and Plotting program) that can print and plot stresses, Von Mises stress and other principal stresses, in any elements, the user specified along the toridal coil perimeters. In a figure plotted by this program SPP, a longitudinal axis and a transversal axis signifies the Von Mises stress and a fraction of the perimeter, respectively.

3. Toroidal Coil Analysis

As an example of the JAFUSAC calculation, a medium size full toroidal coil system is chosen. In this systems, it can be taken into account four types, inner poloidal coils and continuous support type, inner poloidal coils and two points support type, outer poloidal coils and continuous support type and outer poloidal coils and two points support type. The inner poloidal coils and the outer poloidal coils means that poloidal coils do and do not inter-link with toroidal coils, respectively. And a comparison of the continuous support with the two points support is shown in Fig.2. A detailed drawing of the two points support is shown in Fig.3.

The size and disposition of the coil systems are shown in Fig.4. and Fig.5; i.e., vertical field (VF) coils are not drawn explicitly. Positions and cross section of the VF coils are shown in table 1 with the ohmic heating (OH) coils. A toroidal field induced by the coil systems is shown in Fig.6. The electromagnetic force calculation on a point in the conductor area gives average value.

3.1 Parameters

The parameters used this calculation are as follows:

Toroidal Coil

number of coils	18
external height	4450 mm
external width	2729 mm
winding cross section	480×100 mm^2
overall cross section approximately	540×100 mm^2
current density	24.5 A/mm^2
weight	7.03 ton

OH Coil

number of coils	100
winding cross section	100×40 mm^2
current density	25.0 A/mm^2

VF Coil

number of coils	88
winding cross section	40×20 mm^2
current density	26.8 A/mm^2

The program JAFUSAC can solve theoretically any problems on stress in a toroidal coil. But, at the present time, as our computers are not so fast enough to give proper answers to complex problems, a coil structure of this numerical analysis must be modeled more simple than the actual coil structure, as shown in Fig.7.

3.2 Effect of Poloidal Field

In this analysis, the OH coils and VF coils are called as the poloidal coils. From Fig. 8 to Fig.12, the field and force distributions are shown, and the total field is a vector summation of other fields. The toroidal field is a field parallel with a toroidal direction. And the normal field and the tangential field is a field perpendicular to current directions and a field parallel with current directions, respectively. The hoop force is a force perpendicular to current directions and makes hoop stress in windings. The compressive force is a force caused by the pinch effect on windings. And the tangential force is a force parallel with current directions and must be always zero as far as this calculation is executed without errors. With these figures, it is found that force distributions are not so different each other without reference to types of the coil systems.

With the poloidal field, out-of-plane forces are generated in windings of toroidal field coils. However vector summation of these forces is smaller than that of in-plane forces that are generated by the toroidal field and act on a center core. The values of these vector summations are

out-of-plane force (FO)	1093 ton
in-plane force (Fi)	
in case of outer VF coils	110 ton
inner VF coils	98 ton
outer OH coils	90 ton
inner OH coils	150 ton

Total vector summation F is

$$F = FO^2 + Fi^2$$

When FO>>Fi, the equation can be rewritten as

$$F = FO + Fi^2/2FO$$

The second term is very small as compared with the first term, so that the effect of the poloidal field on forces can be negligible. And the effect of the poloidal field on stresses in winding of toroidal coils is not very significant, too.

3.3 Effect of Support

It is evident that the stress concentration with the two points support differs much from that with the continuous support. In case of this analysis, the former value is about four times greater than the latter value. The detailed maximum displacements and maximum stresses are as follows:

two points support

by electromagnetic force	4.891 mm	22.8	kg/mm^2
by gravitational force	0.021 mm	0.102	kg/mm^2
by seismic (1G) force	0.061 mm	0.090	kg/mm^2

continuous support

by electromagnetic force	1.063 mm	6.2	kg/mm^2
by gravitational force	0.021 mm	0.102	kg/mm^2
by seismic (1G) force	0.030 mm	0.027	kg/mm^2

The appearances of displacements induced by these forces are shown in from Fig.13 to Fig.18. Furthermore, difference of a peak stresses value between infinite spring constant and practical value of spring constnat, which is called 'difference of stress' herein, depends on the spring constant as shown in Fig.19. The peak stress with infinite spring constant is 15.36 kg/mm^2, and it is found that the effect of the spring constant is small.

3.4 Effect of Anisotropy

In fact, the conductor shown in Fig. 7 consists of insulating layers and cooling helium channels, therefore it must be characterized by anisotropy. In this calculation with anisotropy effect moduli of elasticity Ex, Ey, and Ez, are assumed as 5×10^3kg/mm^2, 5×10^3kg/mm^2 and 1.12×10^4kg/mm^2, respectively, and isotropic modulus of elasticity E is 1.12×10^4kg/mm^2. The results of the numerical analysis are presented in from Fig.27 to Fig.30. It is found that in continuous support type the values of peak stress are not different between isotropic and anisotropic moduli but in two points support type they are different as followings: with isotropic modulus 19.9kg/mm^2 and with anisotropic moduli 22.8kg/mm^2. Therefore, the calculated value with isotropic modulus is not enough for a design of practical coil which has anisotropy.

3.5 Sudden Coil Failure

The stress distributions are changed when some coils are suddenly in failure. In this case, the analysis is assumed as a static problem; i.e., some coils in failure have no currents and other coils have nominal currents. Examples of toroidal fields and electromagnetic forces distributions in windings of neighboring failed or break down coils are shown in from Fig. 20 to Fig. 24. The failure is explained in Fig.25.

Stresses and electromagnetic forces are shown as a function of number of breakdown coils in Fig.26. It is found that increasing in number of breakdown coils results in rising unbalanced force and stresses in the parts of reinforcement, inner, outer and side plane. The values of centripetal force and unbalanced force are

number of failed coils	centripetal (out-of-plane) force	unbalanced (in-plane) force
0	1093 ton	0 ton
1	954 ton	550 ton
2	845 ton	795 ton
3	761 ton	922 ton
4	701 ton	984 ton
.	.	.
.	.	.
.	.	.

Then, some strength margin of reinforcement should be taken as a margin against this sudden coil failure.

3.6 Detailed Data

Finally, other detailed data concerning principal stress and Von Mises stress distributions are known in from Fig.27 to Fig.50. The cases of no poloidal coils under other given conditions are shown in from Fig.27 to Fig.30. The stresses caused by seismic or gravitational force are shown in from Fig.31 to Fig.34. The case of inner poloidal coils, OH coils or VF coils, are shown in from Fig.35 to Fig.42. The case of outer poloidal coils are shown in from Fig.43 to Fig.50. And in Fig.51, the data are summarized with maximum Von Mises stress.

4. Conclusions

The usability of the three dimensional stress analysis program JAFUSAC, which has room for improvement of saving CPU time and core memory in order to solve more complex problems still as far as our conventional computers are used hereafter, is demonstrated by its application to an example, a medium size full toroidal coil system. And from this analysis following conclusions are obtained.

The effect of poloidal field on the peak stress is small as compared with that of toroidal field.

The variation of spring constant value does not give an important influence on the peak stress.

The peak stress value in reinforcement increases with growth of failed coil number.

Then, some strength margin of reinforcement should be taken as a margin against this sudden coil failure.

3.6 Detailed Data

Finally, other detailed data concerning principal stress and Von Mises stress distributions are known in from Fig.27 to Fig.50. The cases of no poloidal coils under other given conditions are shown in from Fig.27 to Fig.30. The stresses caused by seismic or gravitational force are shown in from Fig.31 to Fig.34. The case of inner poloidal coils, OH coils or VF coils, are shown in from Fig.35 to Fig.42. The case of outer poloidal coils are shown in from Fig.43 to Fig.50. And in Fig.51, the data are summarized with maximum Von Mises stress.

4. Conclusions

The usability of the three dimensional stress analysis program JAFUSAC, which has room for improvement of saving CPU time and core memory in order to solve more complex problems still as far as our conventional computers are used hereafter, is demonstrated by its application to an example, a medium size full toroidal coil system. And from this analysis following conclusions are obtained.

The effect of poloidal field on the peak stress is small as compared with that of toroidal field.

The variation of spring constant value does not give an important influence on the peak stress.

The peak stress value in reinforcement increases with growth of failed coil number.

Acknowledgement

We would like to acknowledge our gratitude to Dr. S. Mori and Dr. Y. Obata, head and deputy head of our division respectively, for their continuing encouragement.

Reference

1) R. Pohlchen, and M. Huguet: Fifth International Conference on Magnet Technology (MT-5) p325-p331 (1975)
2) M. Söll, O. Jandal, and H. Gorenflo: IPP-report 4/142, III/31 (1975)
3) Nishimura. H, and Shimamoto. S: JAERI-M 6865 (1977) (in Japanese)
4) Shimamoto. S, and Nishimura. H: to be presented in Sixth International Conference on Magnet technology (MT-6) (1977)

Acknowledgement

We would like to acknowledge our gratitude to Dr. S. Mori and Dr. Y. Obata, head and deputy head of our division respectively, for their continuing encouragement.

Reference

1) R. Pohlchen, and M. Huguet: Fifth International Conference on Magnet Technology (MT-5) p325-p331 (1975)
2) M. Söll, O. Jandal, and H. Gorenflo: IPP-report 4/142, III/31 (1975)
3) Nishimura. H, and Shimamoto. S: JAERI-M 6865 (1977) (in Japanese)
4) Shimamoto. S, and Nishimura. H: to be presented in Sixth International Conference on Magnet technology (MT-6) (1977)

Table and Figures Captions

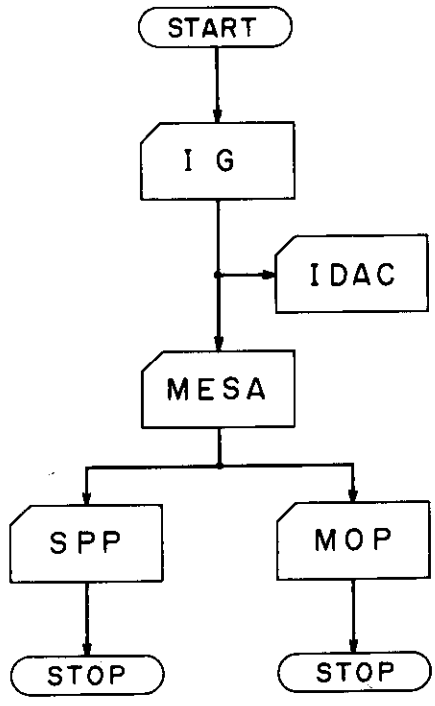

Fig. 1 Calculation procedure of JAFUSAC

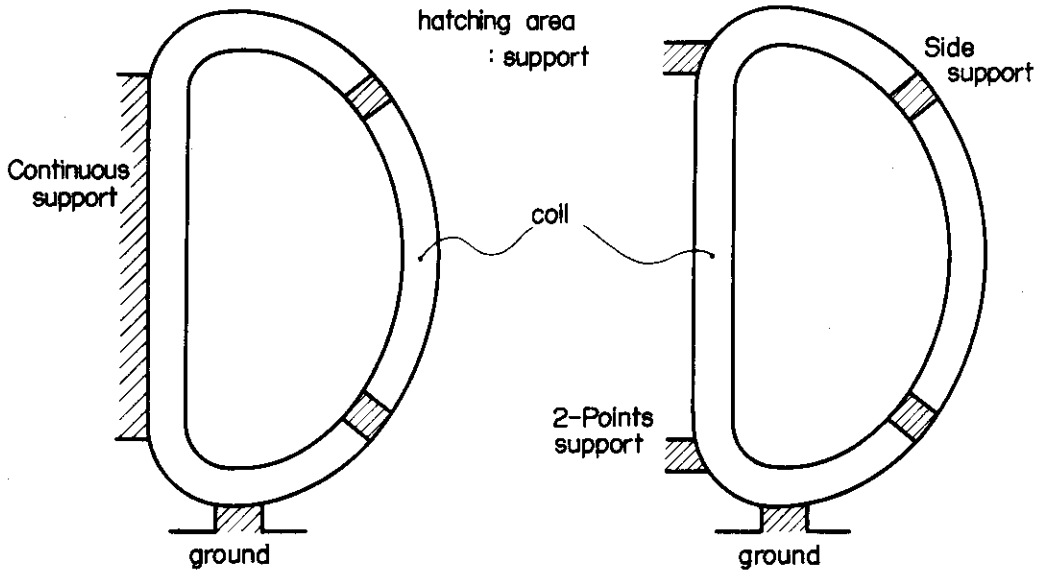

Fig. 2 Supporting method

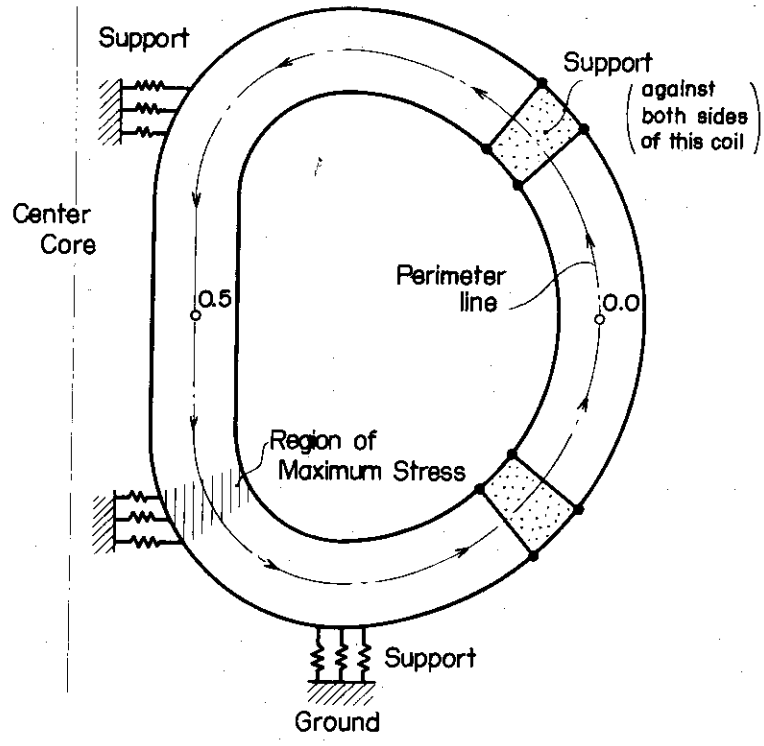

Fig. 3 Detailed drawing of two points support

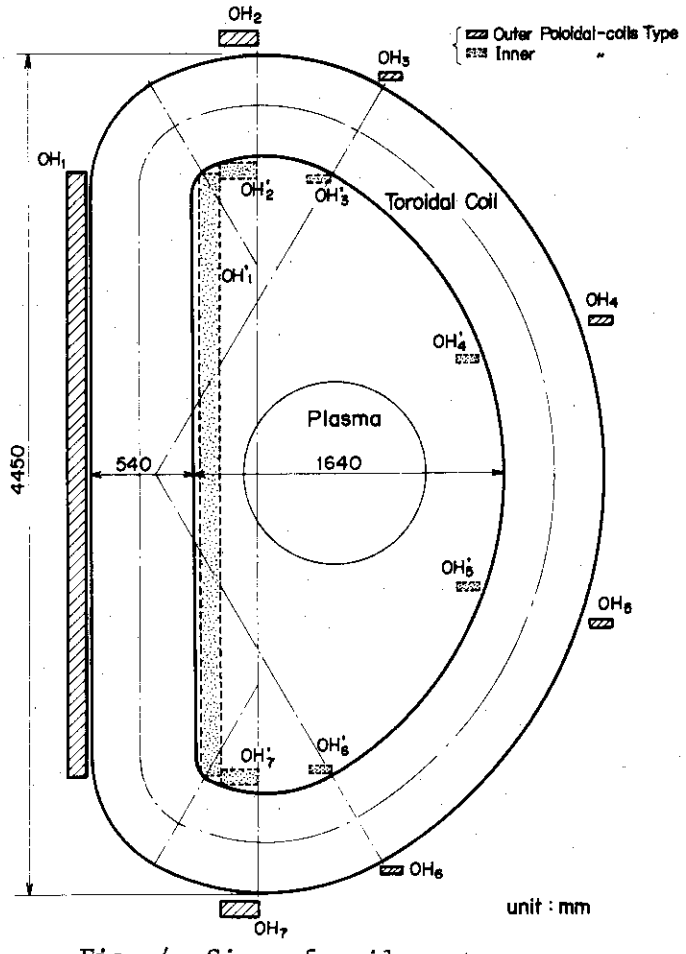

Fig. 4 Size of coil systems

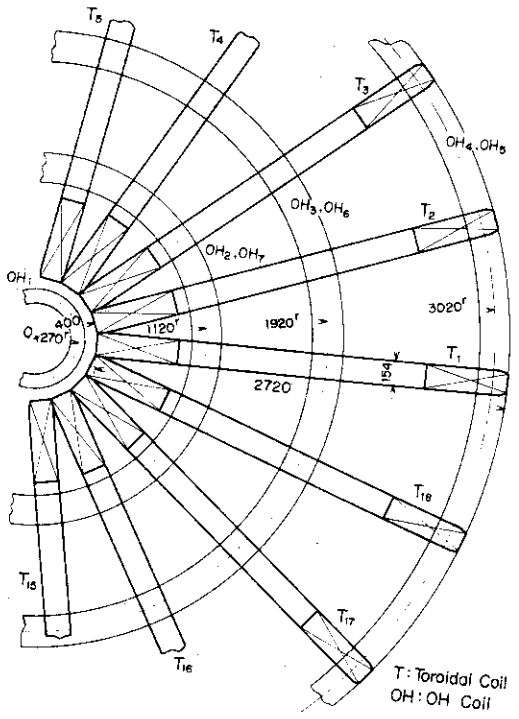

Fig. 5 Disposition of coil systems

Table 1 Position and Cross section of Poloidal Coils

	Inner Poloidal-coils Type			Outer Poloidal-coils Type		
	No.	Position	w×h	No.	Position	w×h
OH-coil	1	(1120, 1600)	200×150	1	(1120, 2300)	200×150
	2	(1540, 1560)	100× 30	2	(1920, 2100)	100× 30
	3	(2320, 600)	100× 30	3	(3020, 800)	100× 30
	4	(2320, 600)	100× 30	4	(3020,- 800)	100× 30
	5	(1540,-1560)	100× 30	5	(1920,-2100)	100× 30
	6	(1120,-1600)	200×150	6	(1120,-2300)	200×150
	7	(970, 0)	100×3200	7	(270, 0)	100×3200
V-coil	1	(1700, 1400)	100× 72	1	(2100, 2100)	100× 72
	2	(2300, 700)	48×100	2	(3000, 1000)	48×100
	3	(2300, 300)	60×100	3	(3100, 500)	60×100
	4	(2300,- 300)	60×100	4	(3100,- 500)	60×100
	5	(2300,- 700)	48×100	5	(3000,-1000)	48×100
	6	(1700,-1400)	100× 72	6	(2100,-2100)	100× 72
	7	(960, 0)	15×2400	7	(270, 0)	15×2400

unit:mm

Origin is set at the plasma center, and some coils are gathed up.

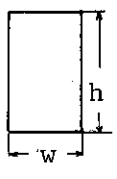

cross section

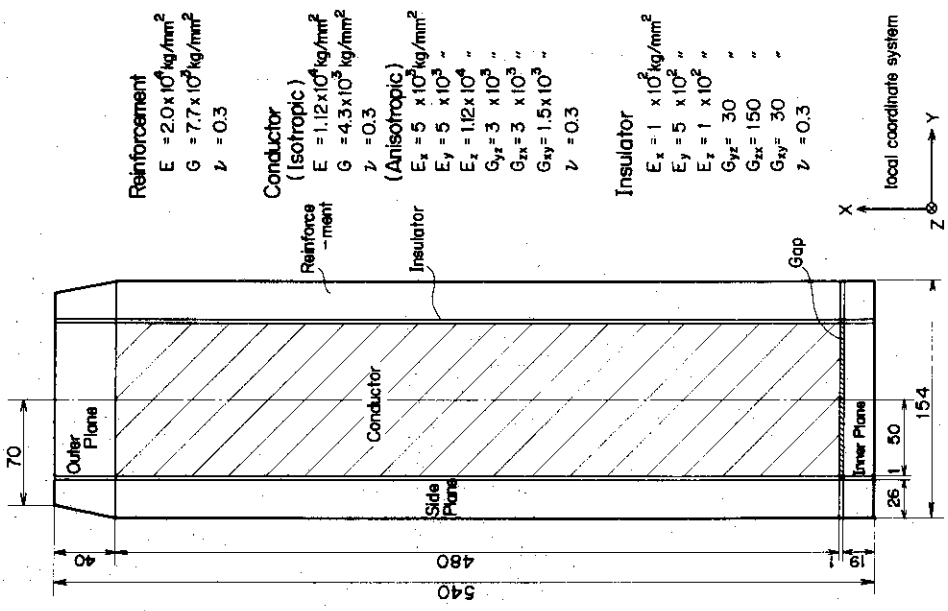

Fig. 7 Cross section of toroidal coil

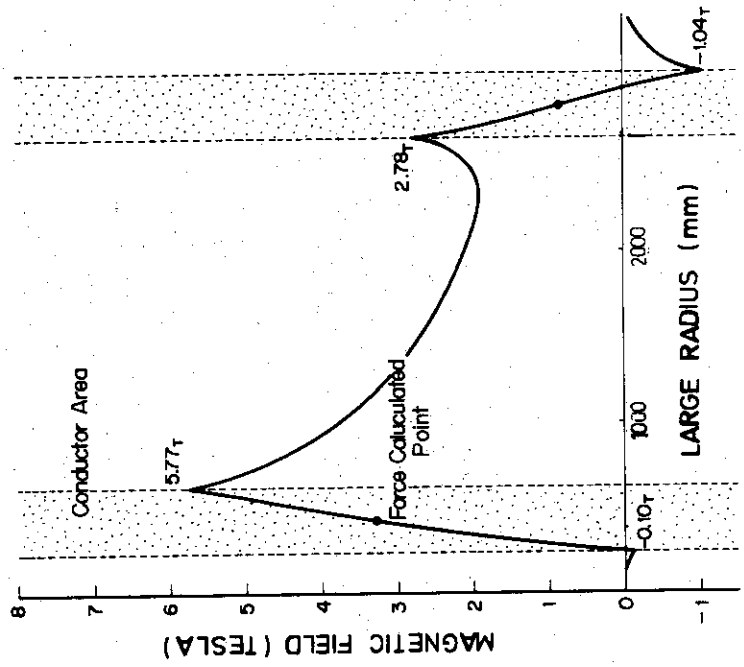

Fig. 6 Toroidal field distribution

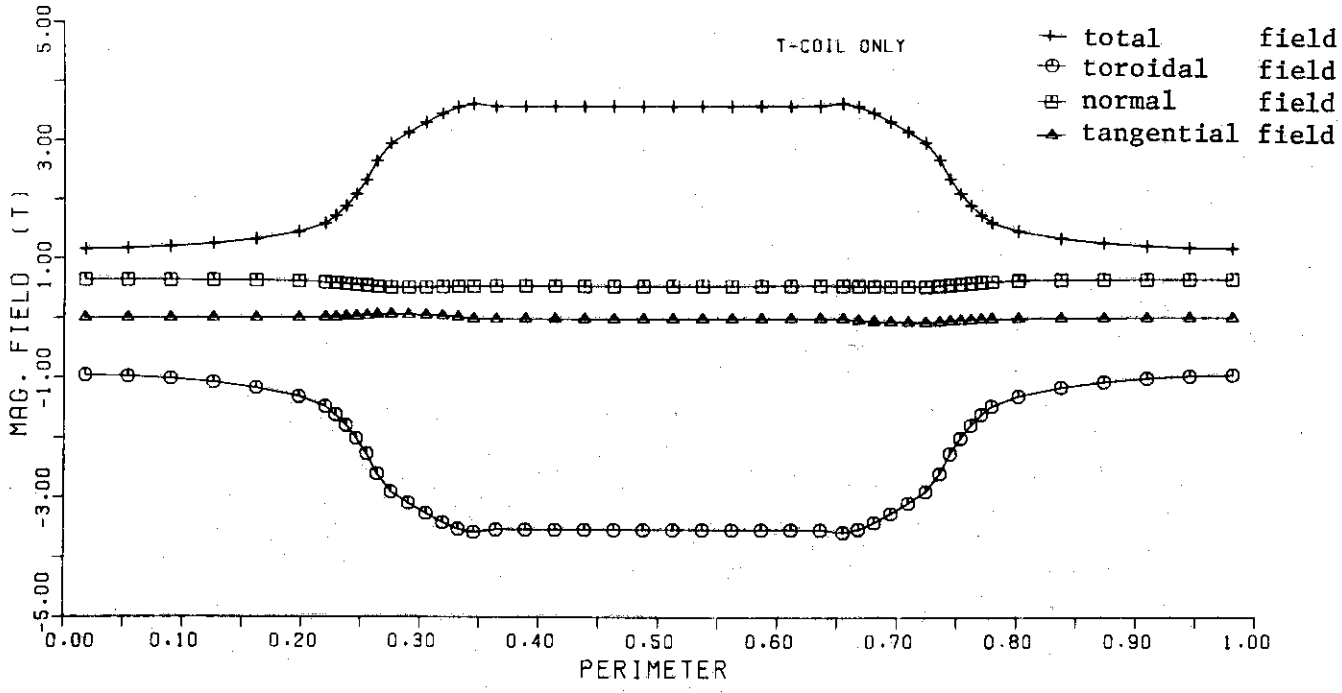

Fields Distribution in Toroidal Coil

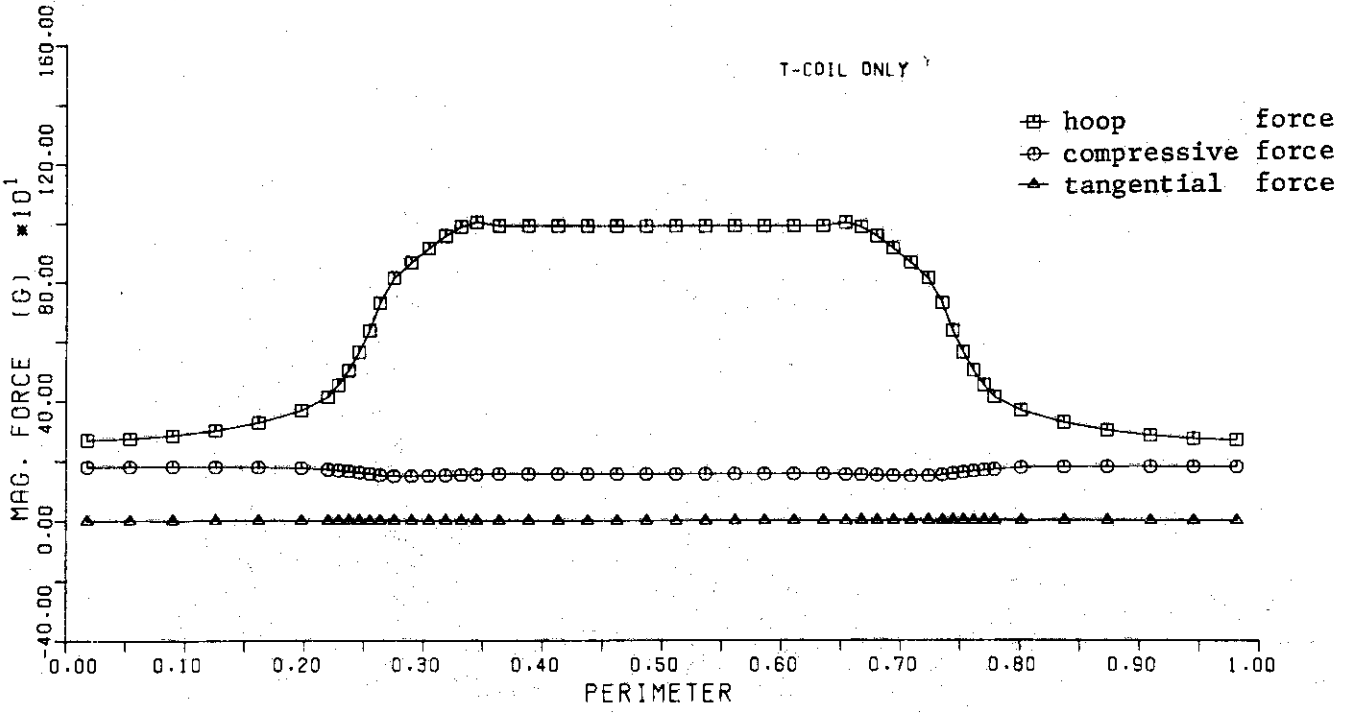

Forces Distribution in Toroidal Coil

Fig. 8 Distribution in case of toroidal coil only

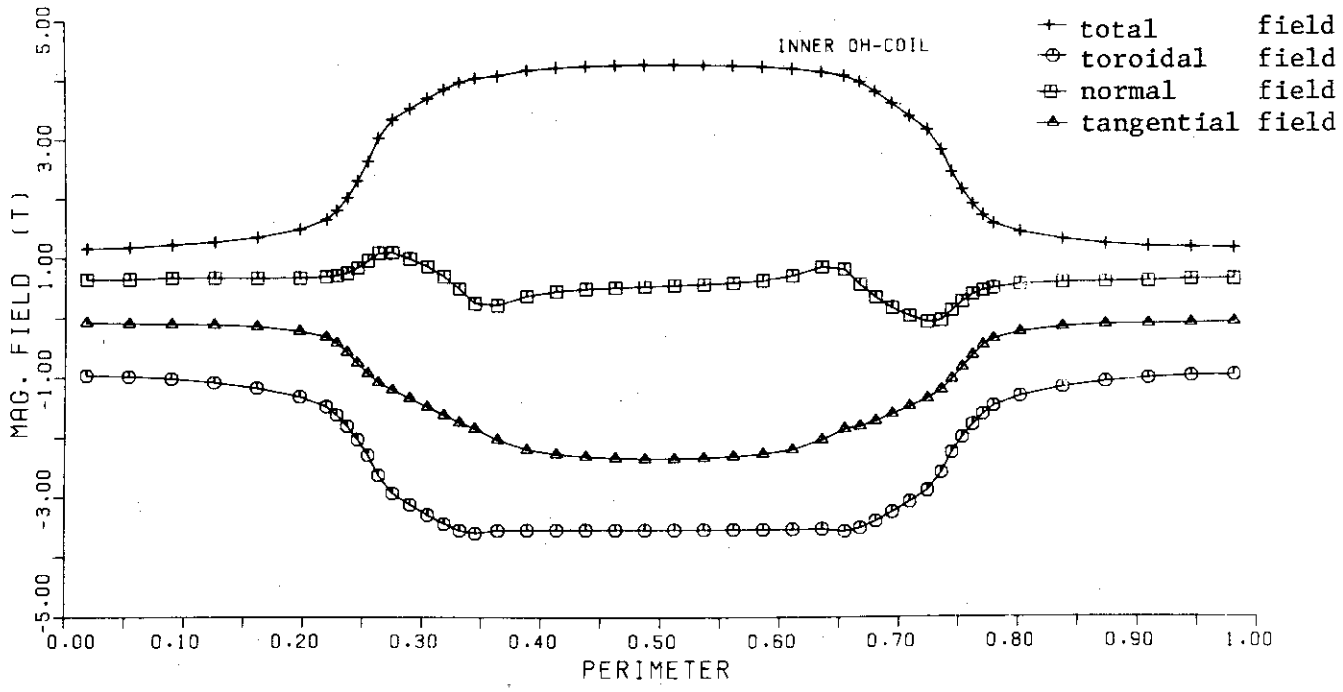

Fields Distribution in Toroidal Coil

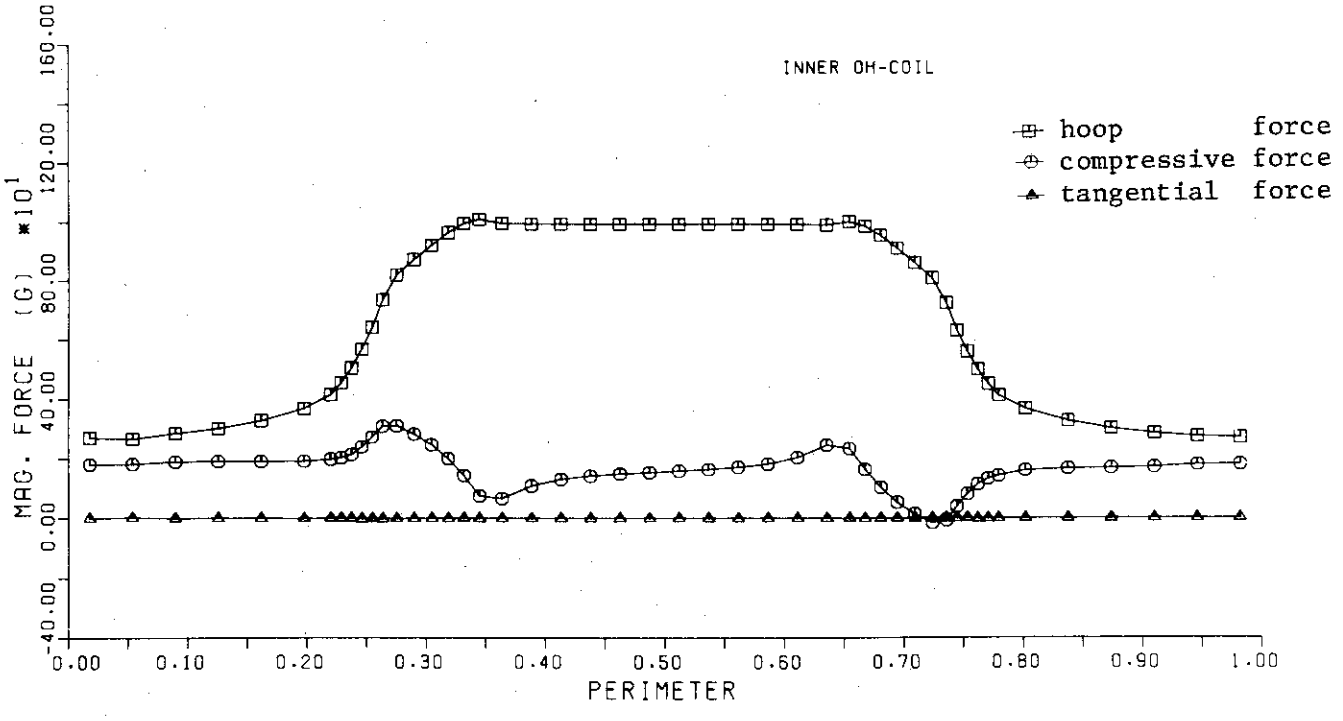

Forces Distribution in Toroidal Coil

Fig. 9 Distribution in case of inner OH coil type

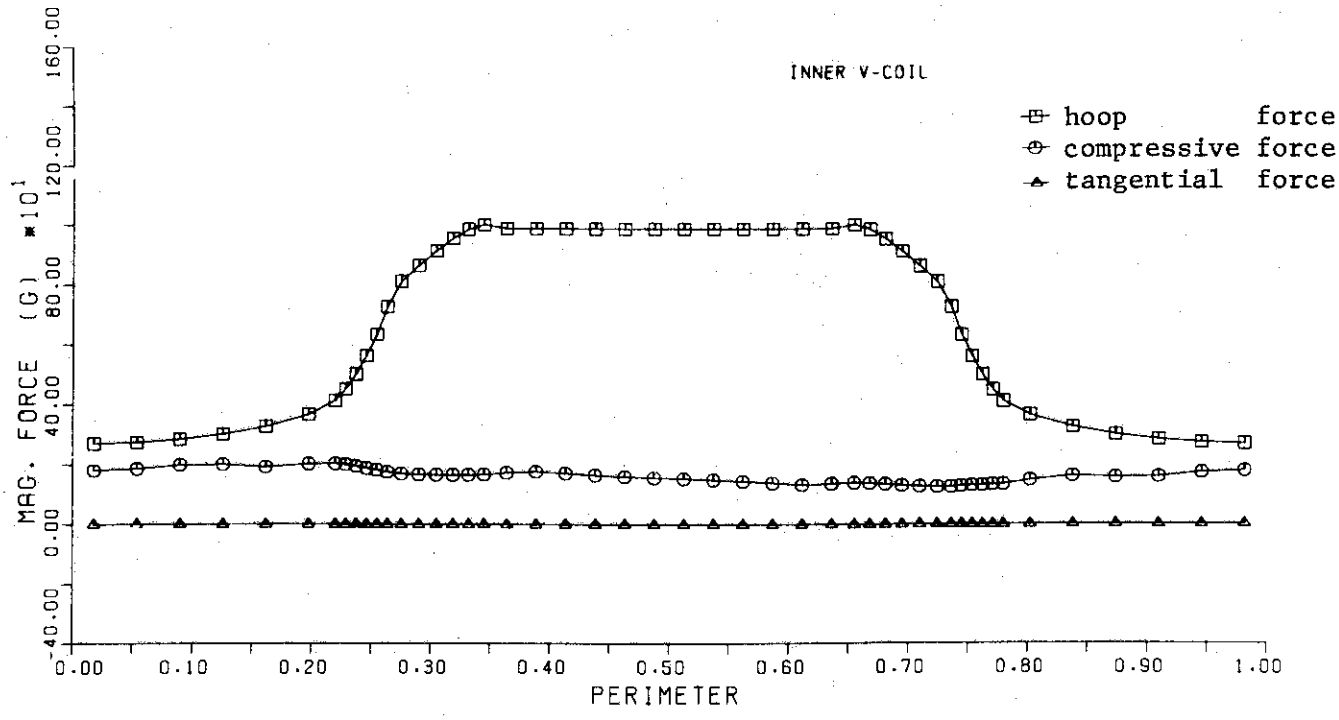

Forces Distribution in Toroidal Coil

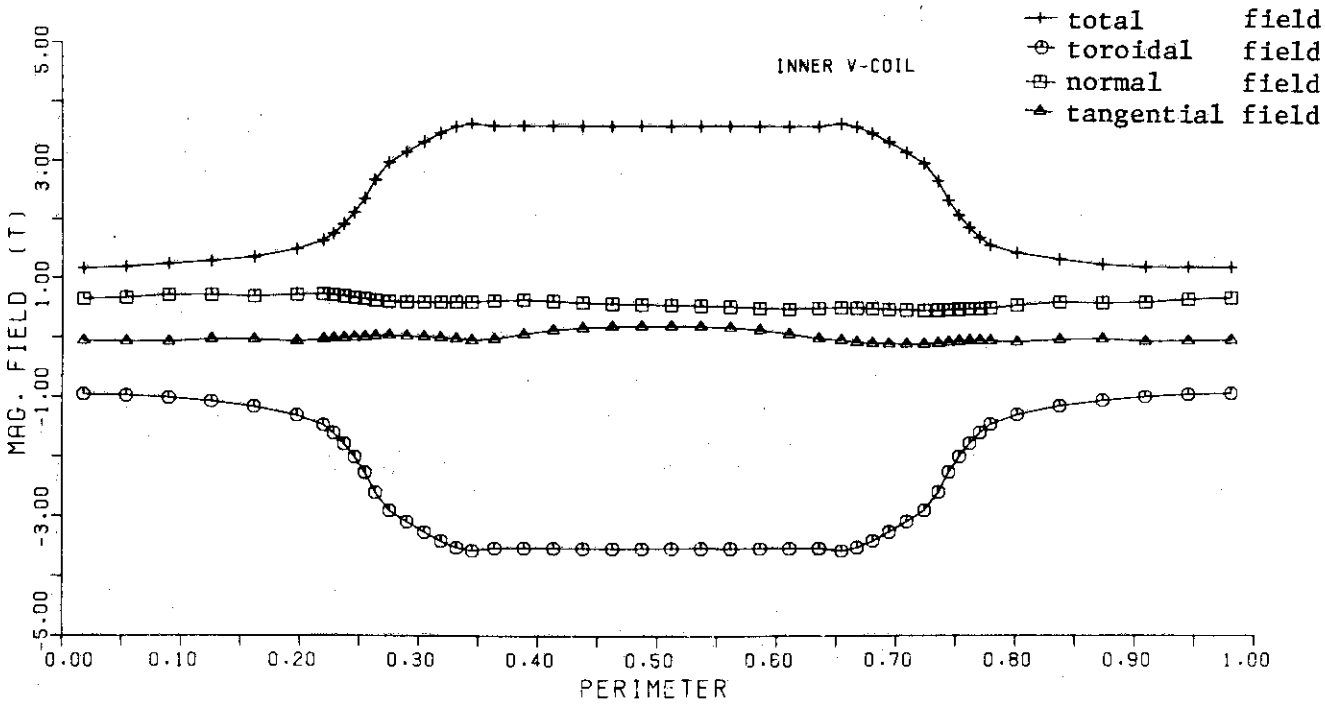

Fields Distribution in Toroidal Coil

Fig. 10 Distribution in case of inner VF coil type

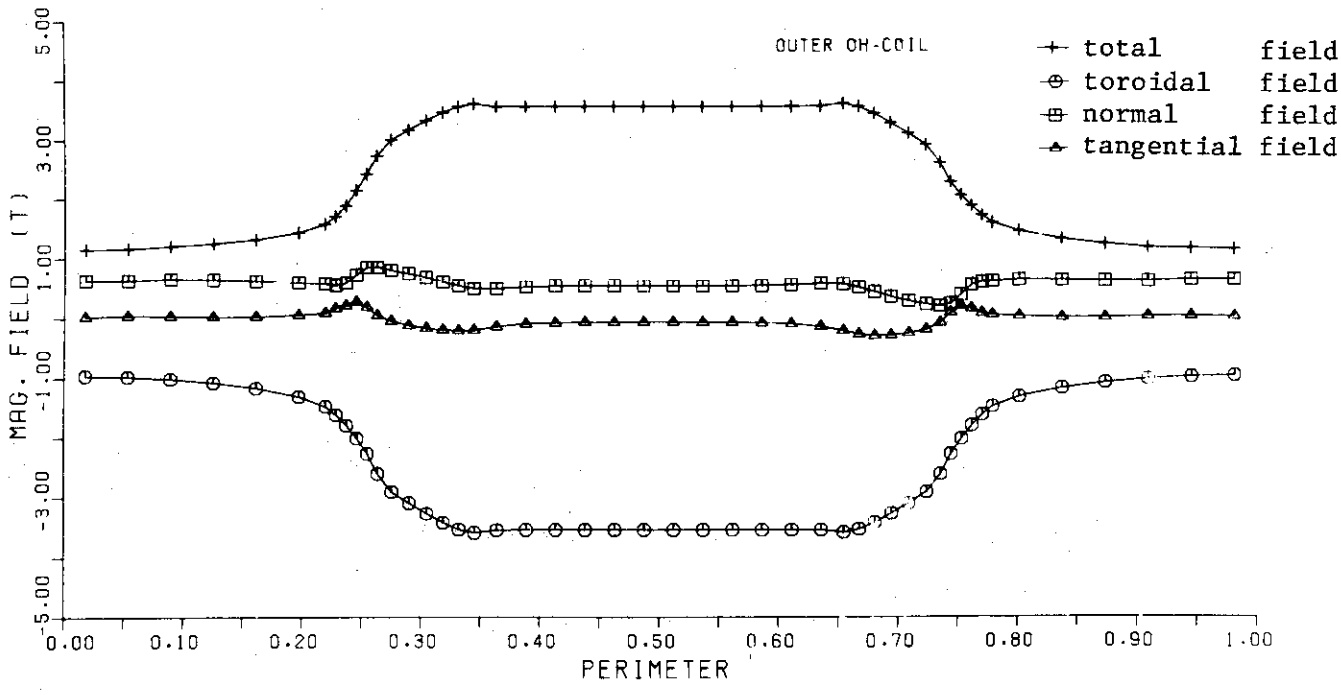

Fields Distribution in Toroidal Coil

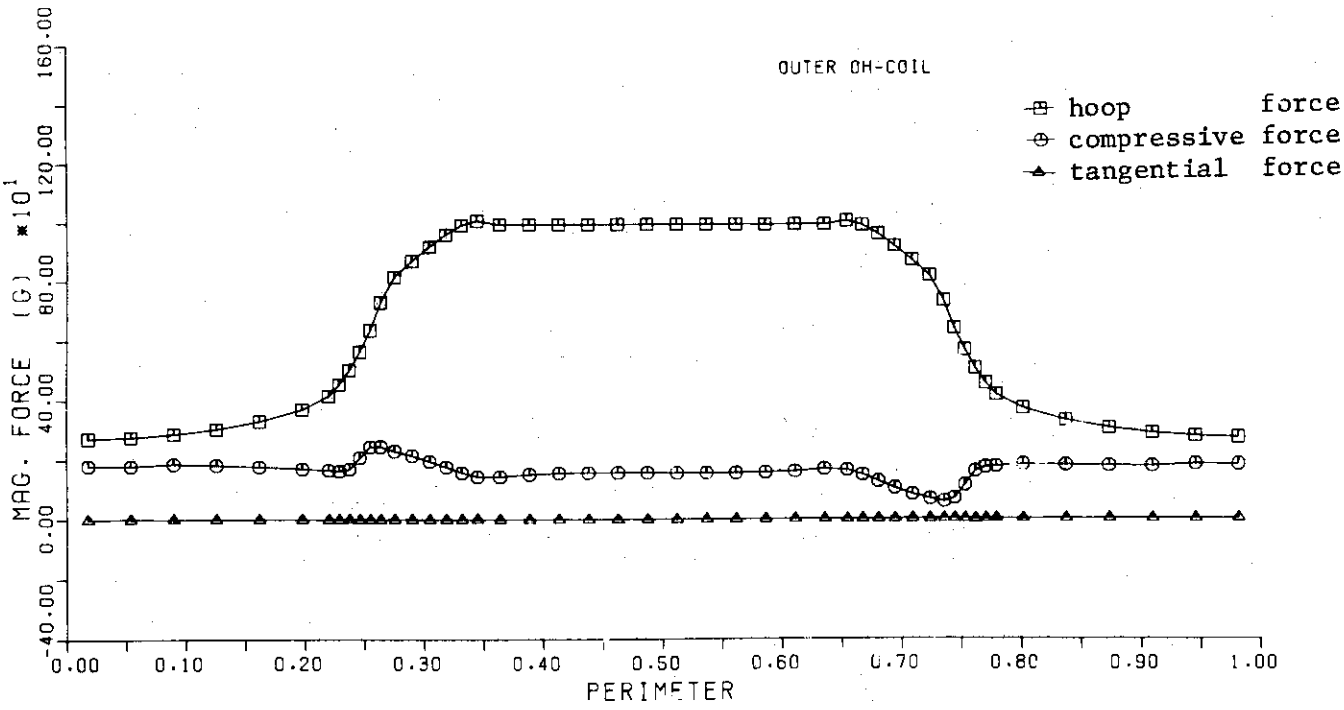

Forces Distribution in Toroidal Coil

Fig. 11 Distribution in case of outer OH coil type

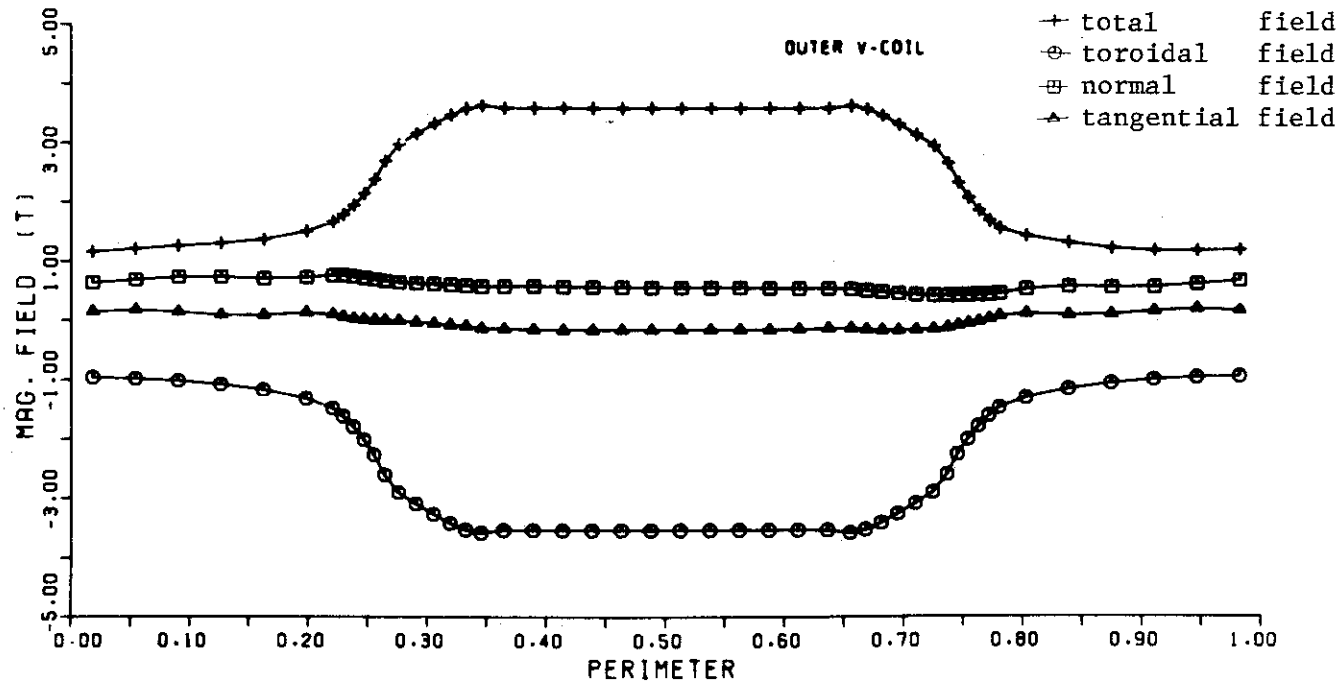

Fields Distribution in Toroidal Coil

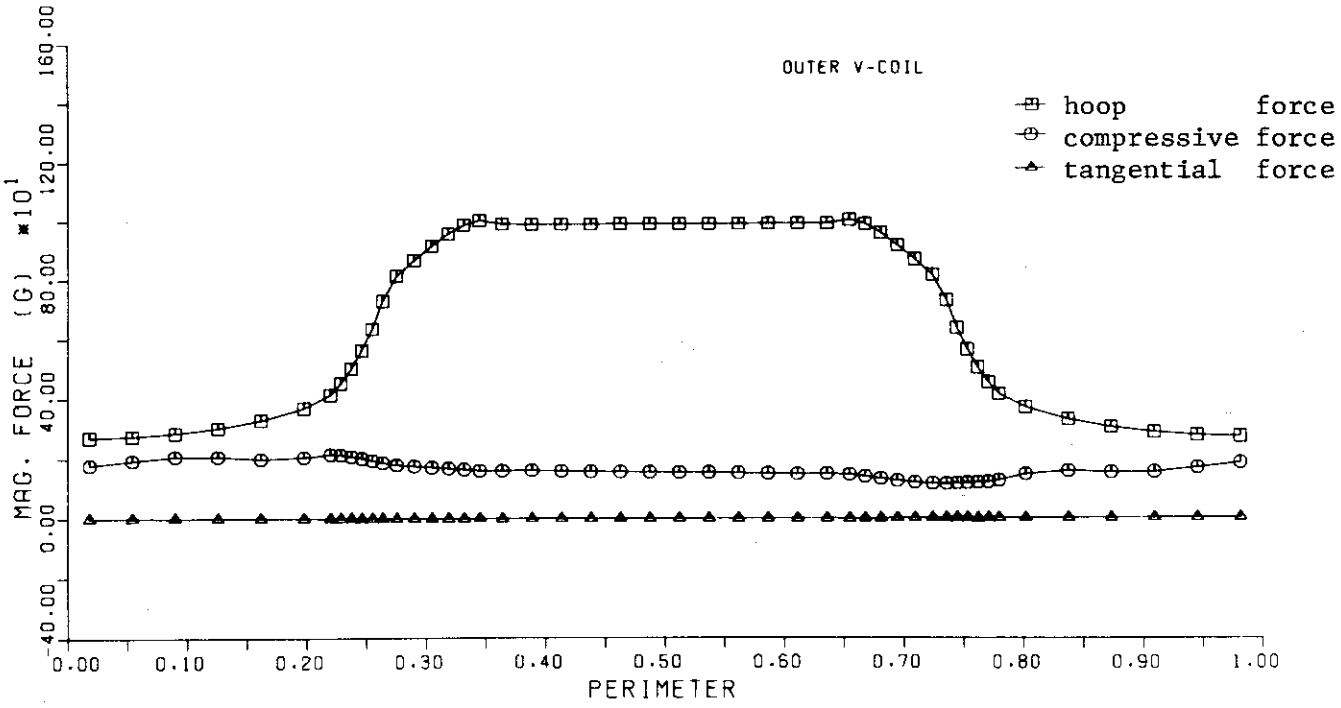

Forces Distribution in Toroidal Coil

Fig. 12 Distribution in case of outer VF coil type

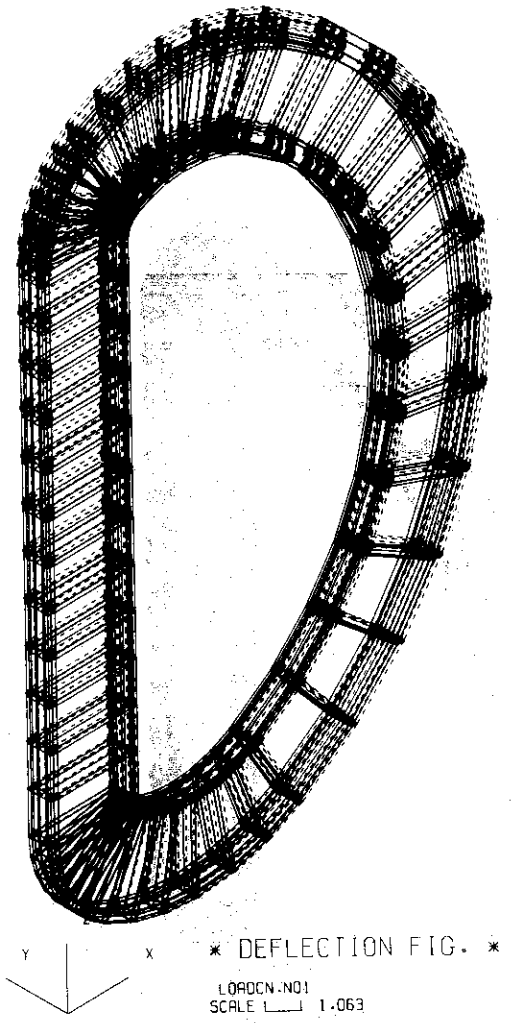

Fig. 13 Deflection induced by electromagnetic force on continuous support

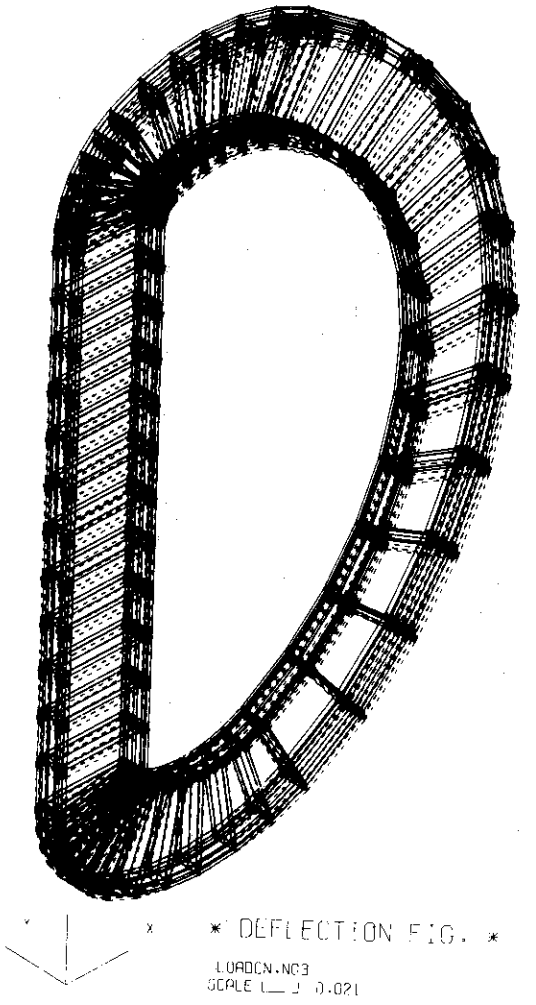

Fig. 14 Deflection induced by seismic force on continuous support

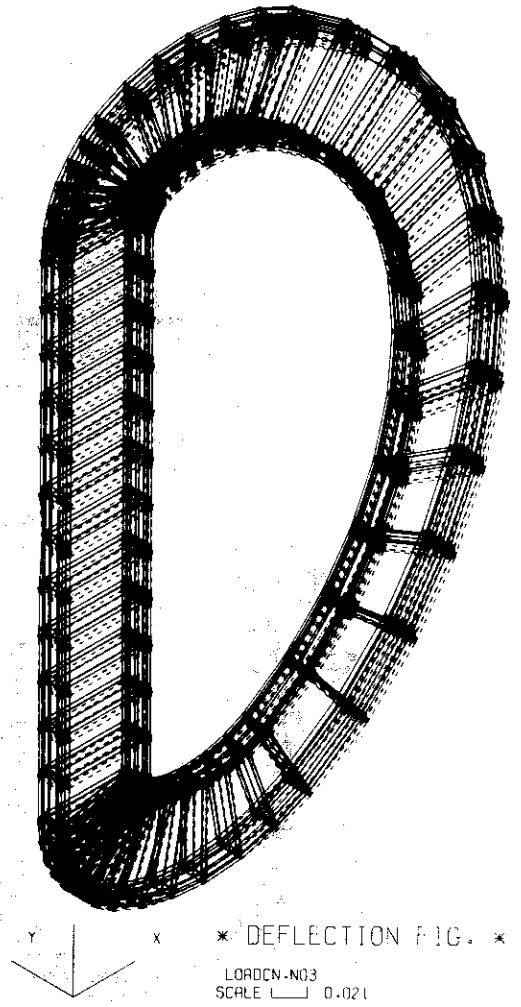

Fig. 15 Deflection induced by gravitational force on continuous support

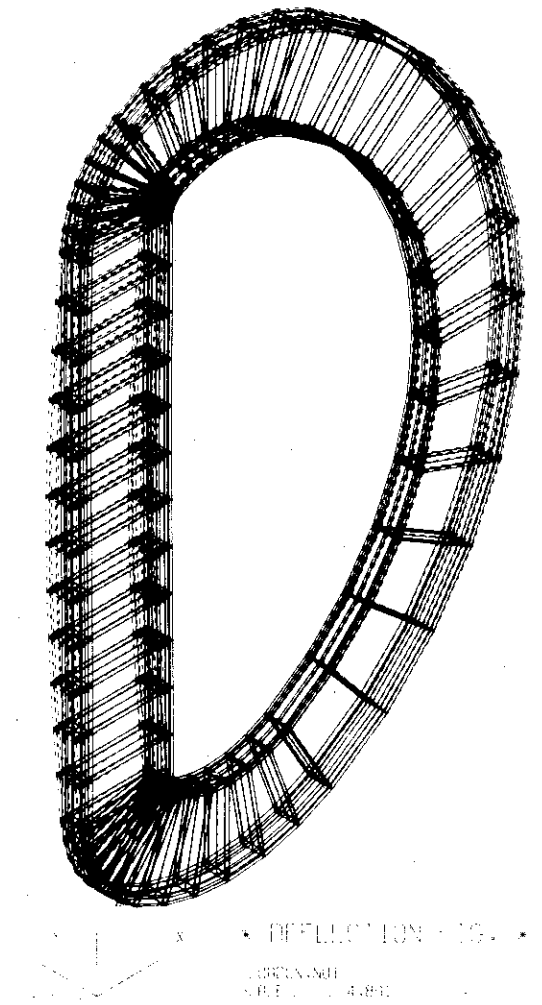

Fig. 16 Deflection induced by electromagnetic force on two points support

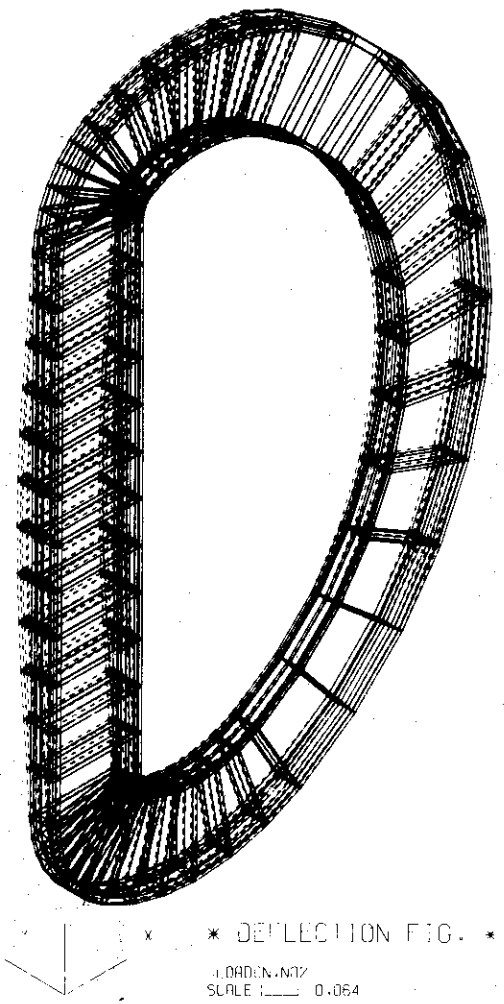

Fig. 17 Deflection induced by seismic force on two points support

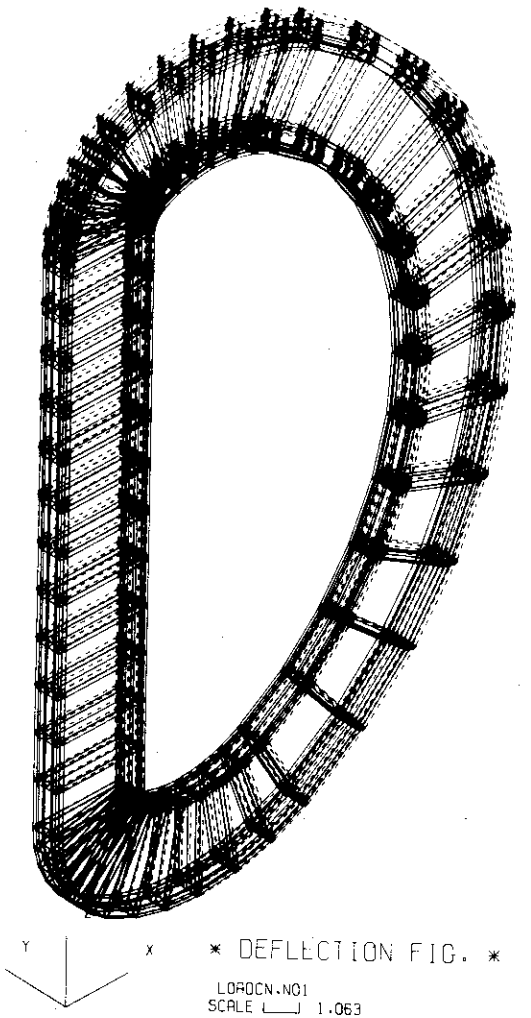

Fig. 18 Deflection induced by gravitational force on two points support

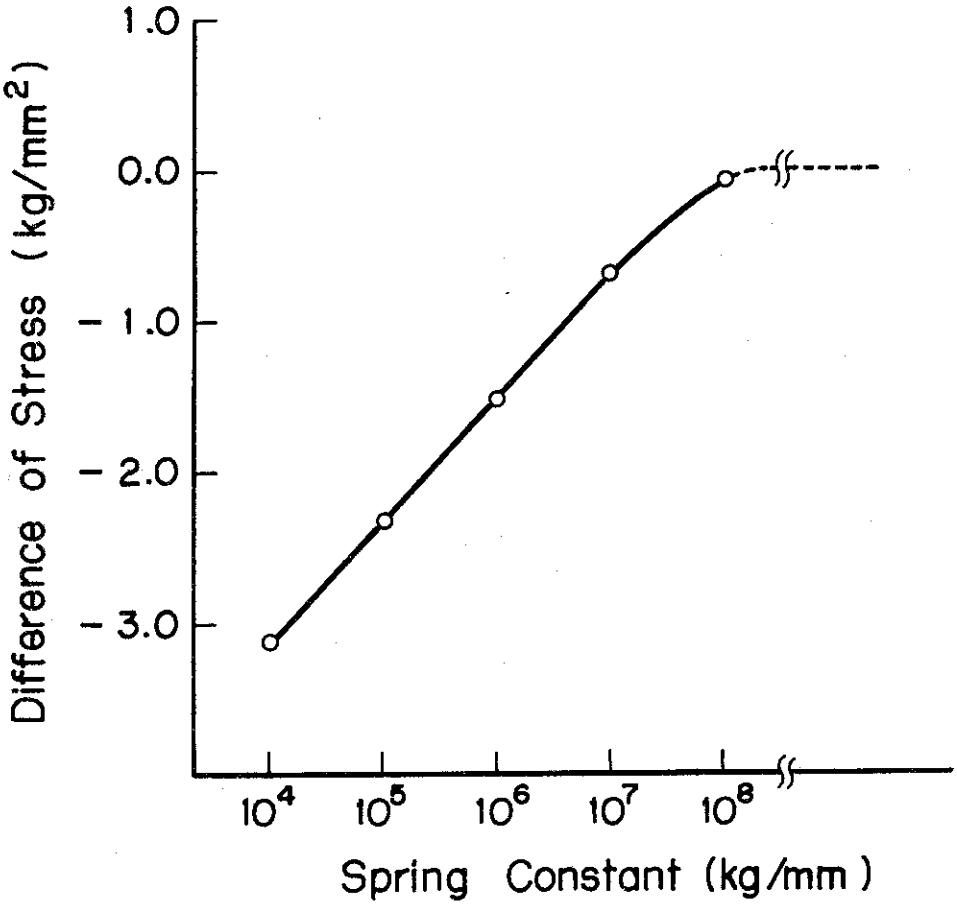

Fig. 19 'difference of peak stress' as a function of the spring constant (the stress with infinite spring constant is 15.36kg/mm^2)

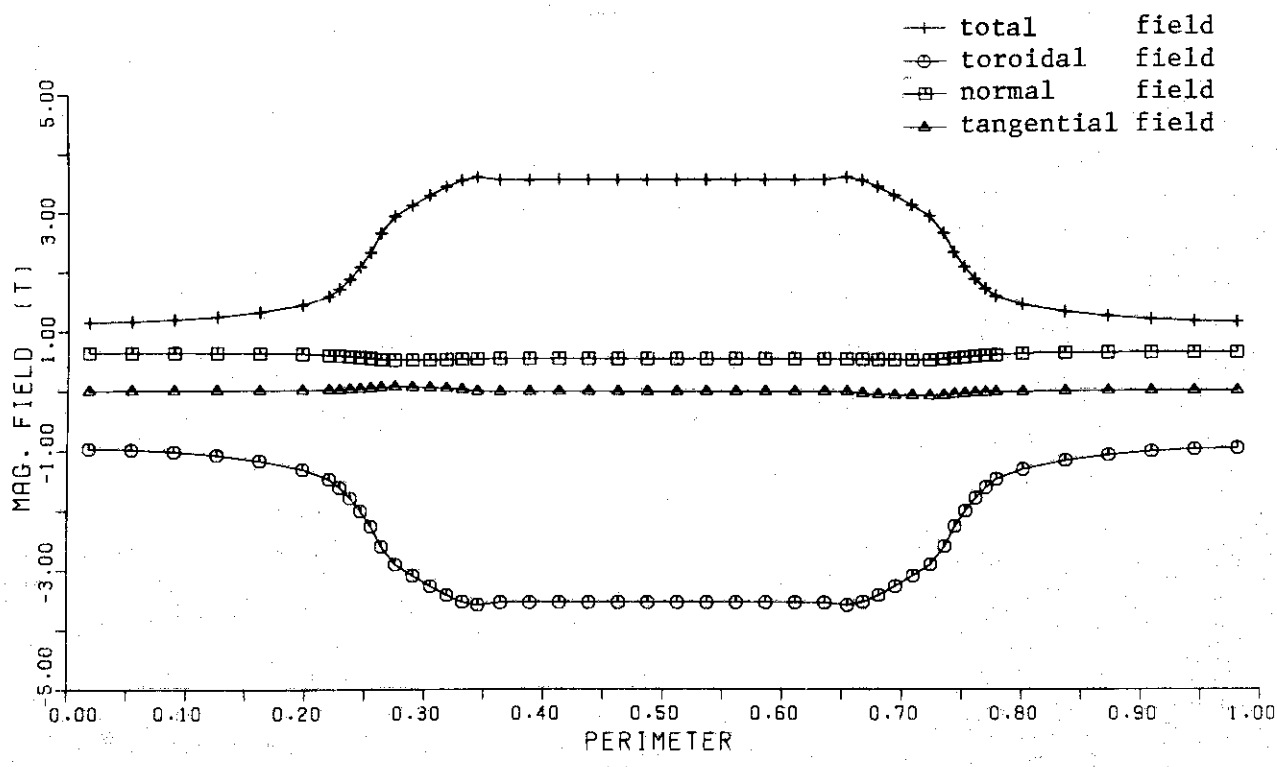

Fields Distribution in Toroidal Coil

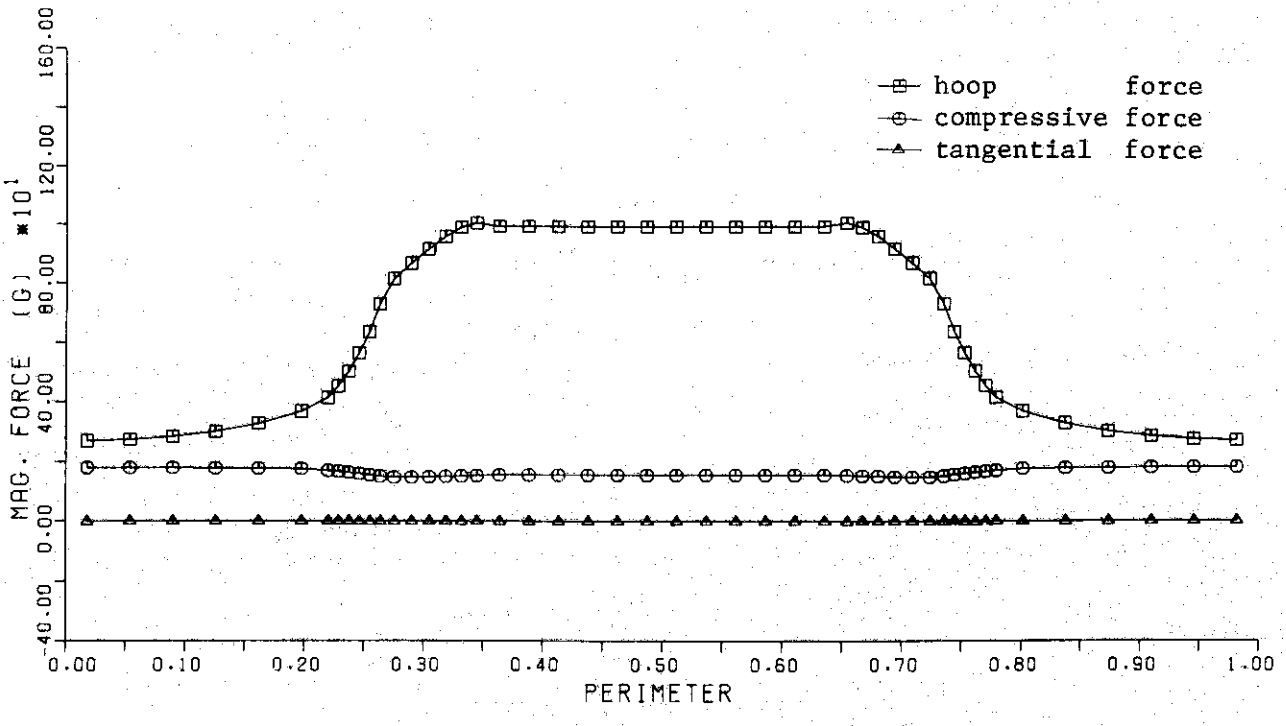

Forces Distribution in Toroidal Coil

Fig. 20 Field and force distributions (no failed coils)

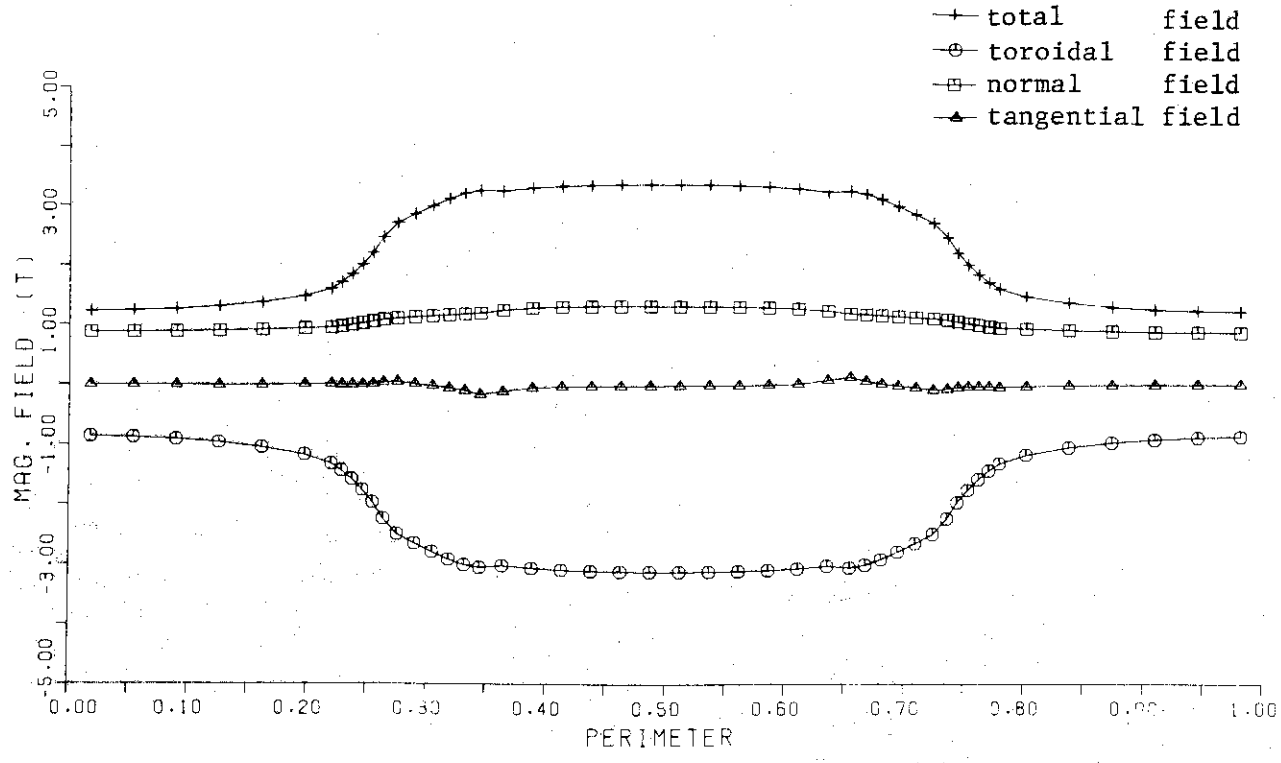

Fields Distribution in Toroidal Coil

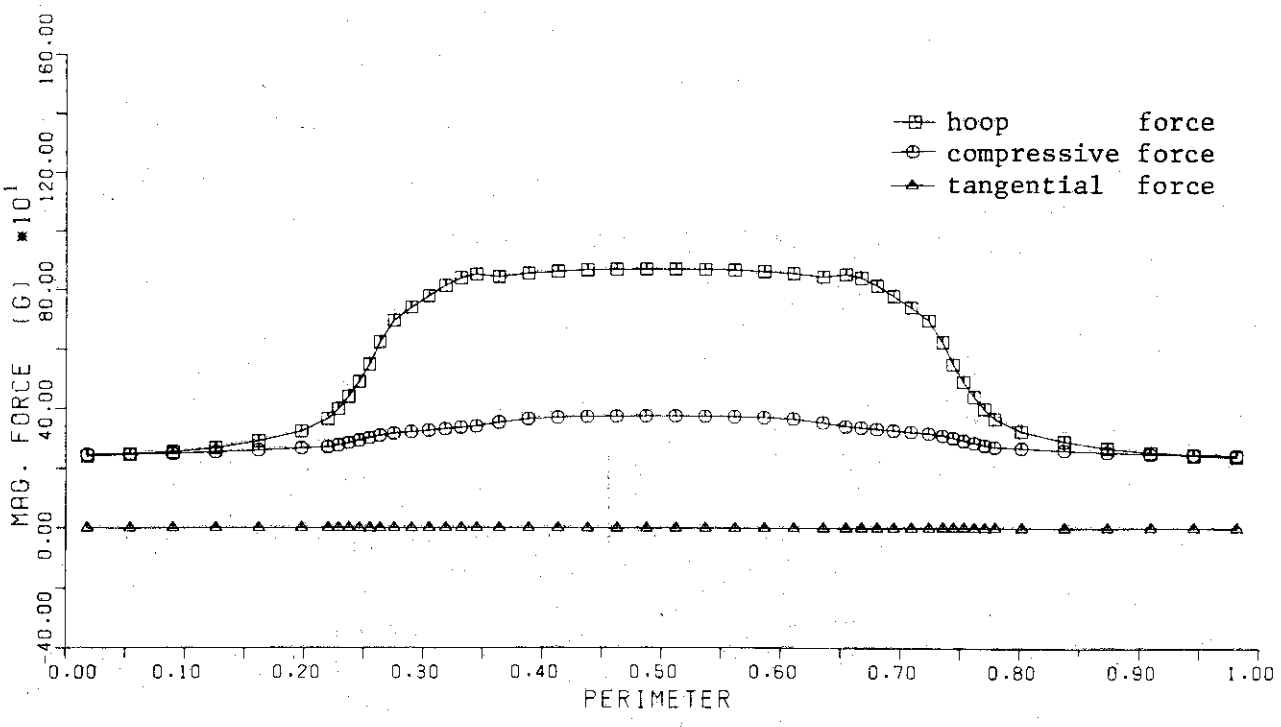

Forces Distribution in Toroidal Coil

Fig. 21 Field and force distributions (one failed coil)

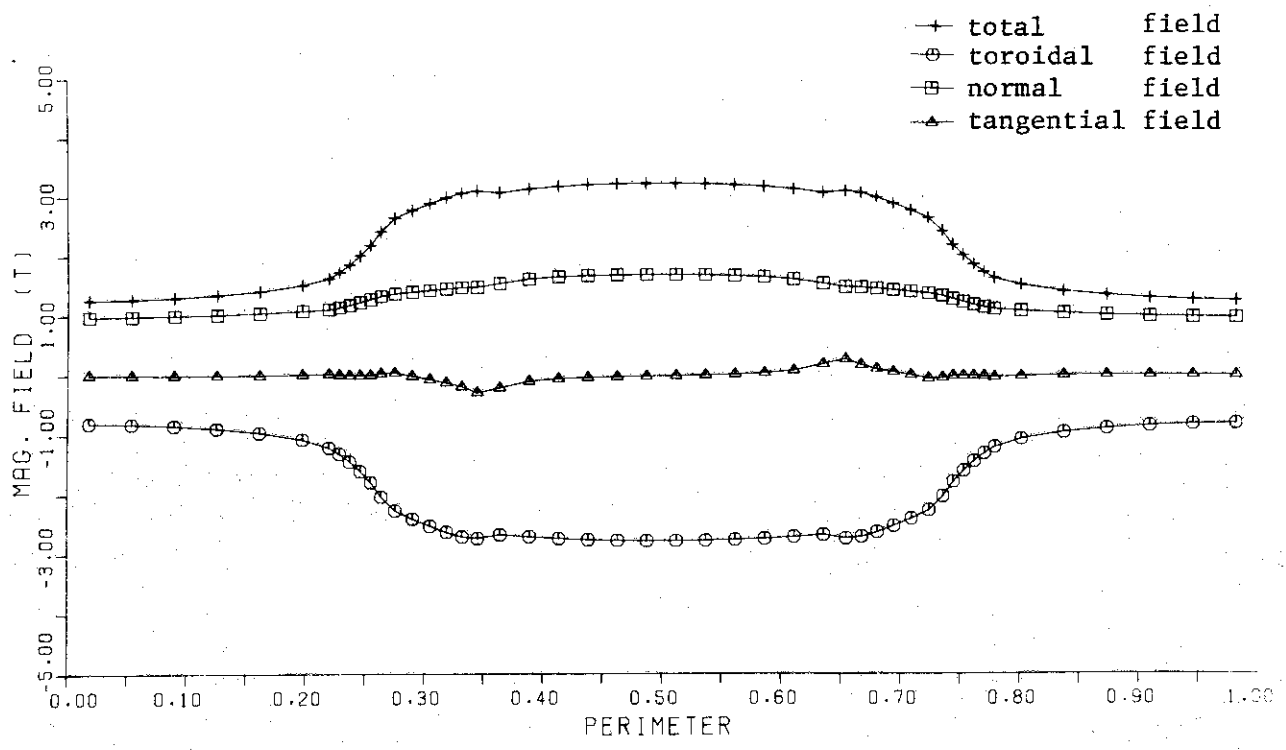

Fields Distribution in Toroidal Coil

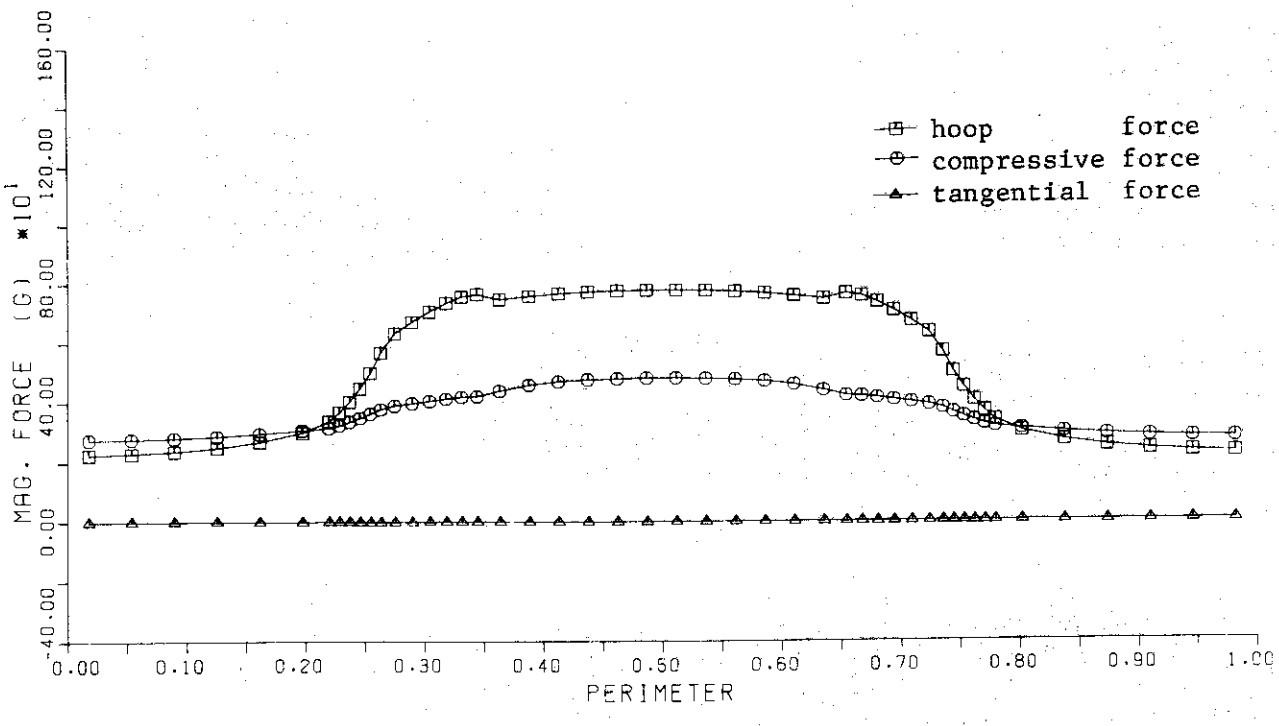

Forces Distribution in Toroidal Coil

Fig. 22 Field and force distributions (two failed coil)

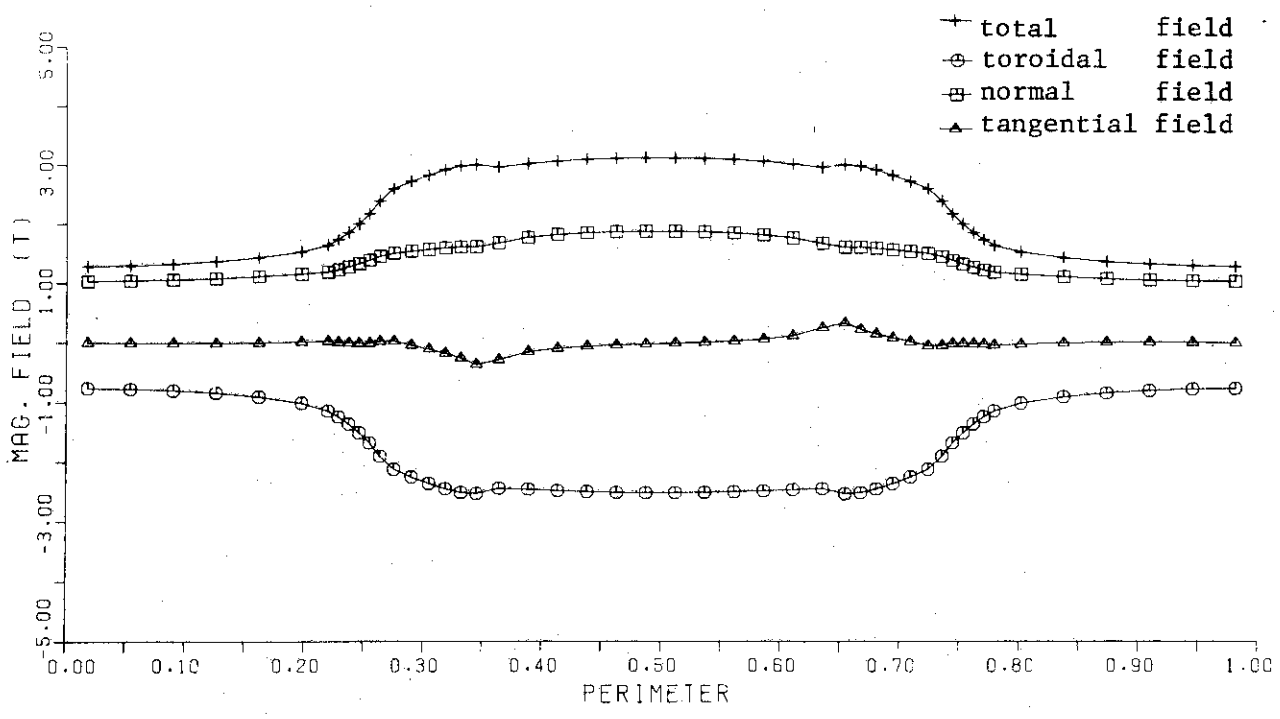

Fields Distribution in Toroidal Coil

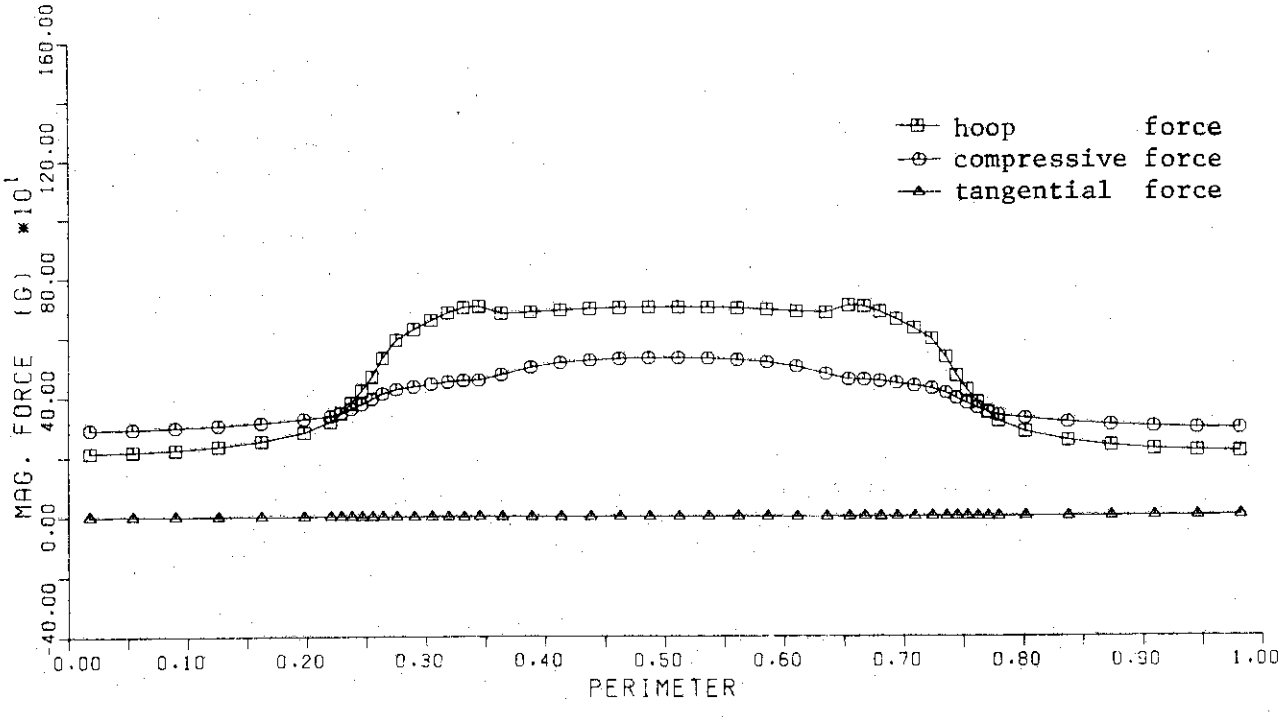

Forces Distribution in Toloidal Coil

Fig. 23 Field and force distributions (three failed coils)

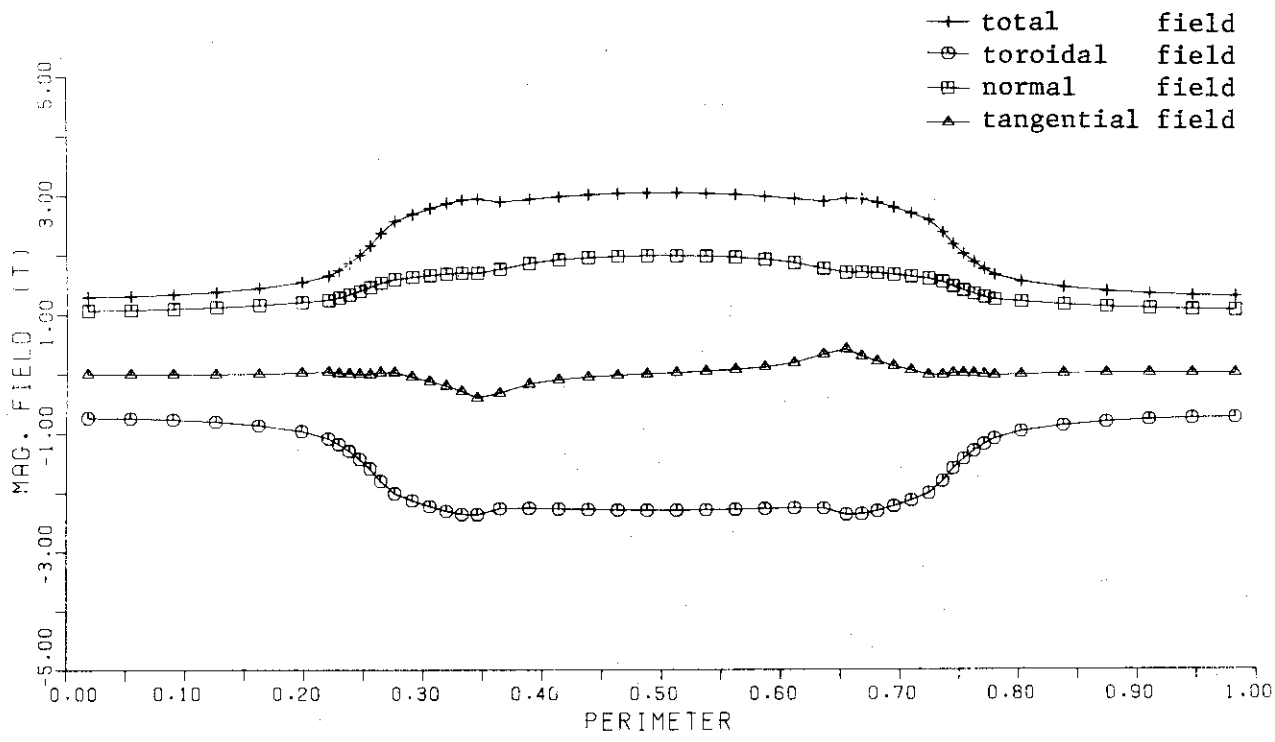

Fields Distribution in Toroidal Coil

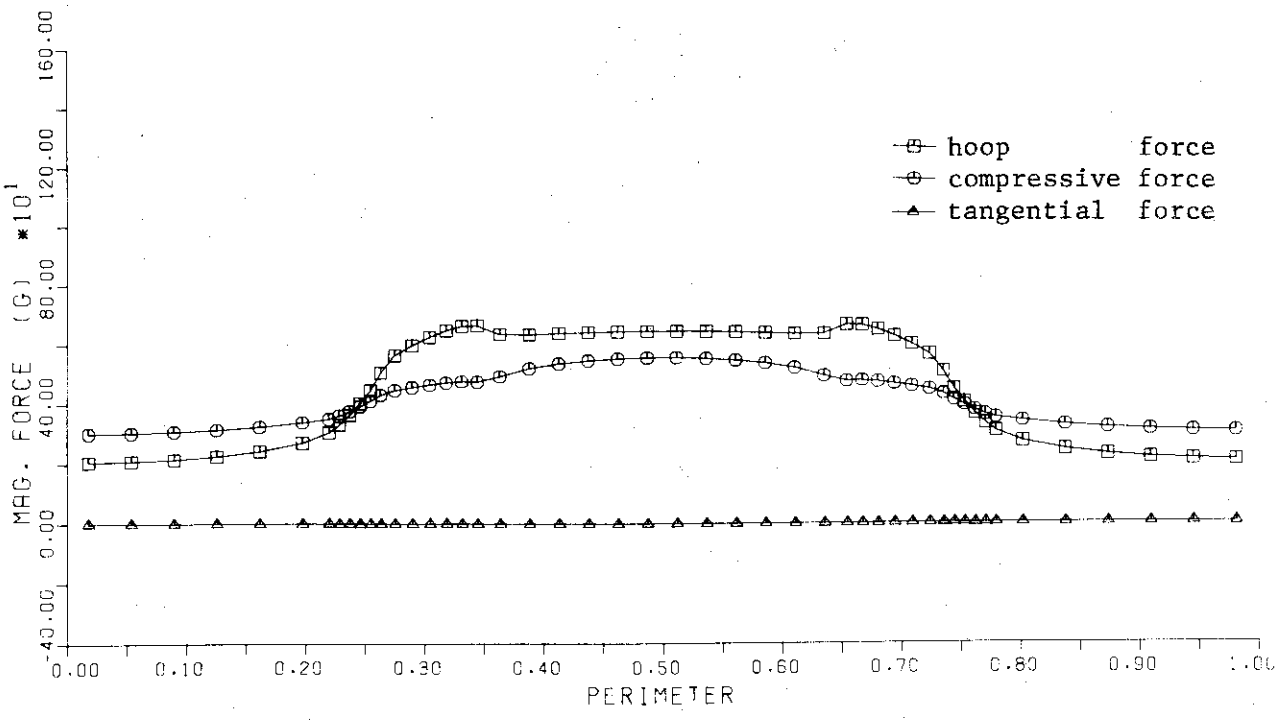

Forces Distribution in Toroidal Coil

Fig. 24 Field and force distributions (four failed coils)

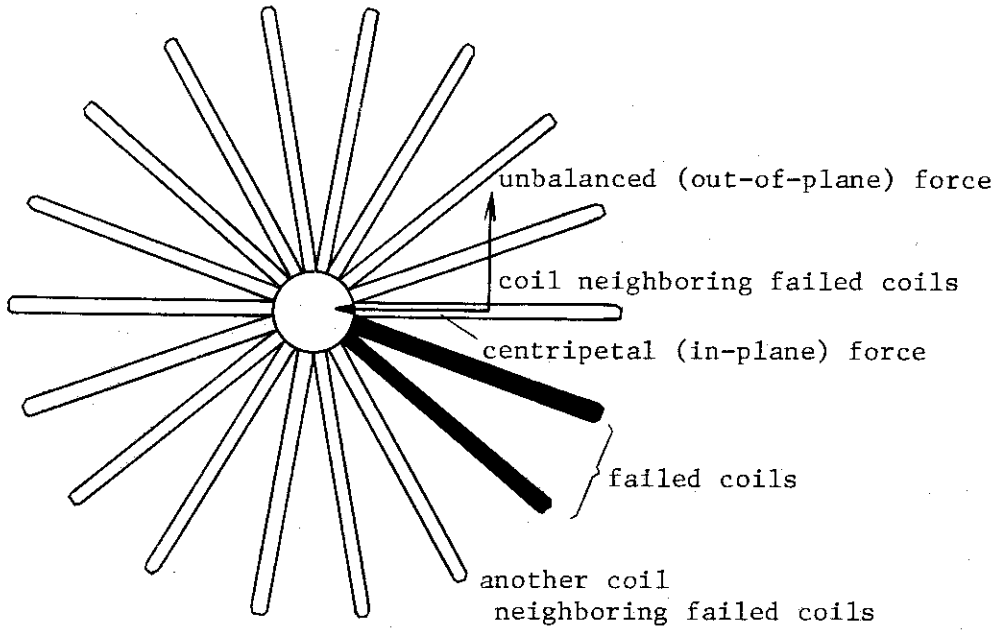

Fig. 25 Explanation of the failure (in case of two coils in failure)

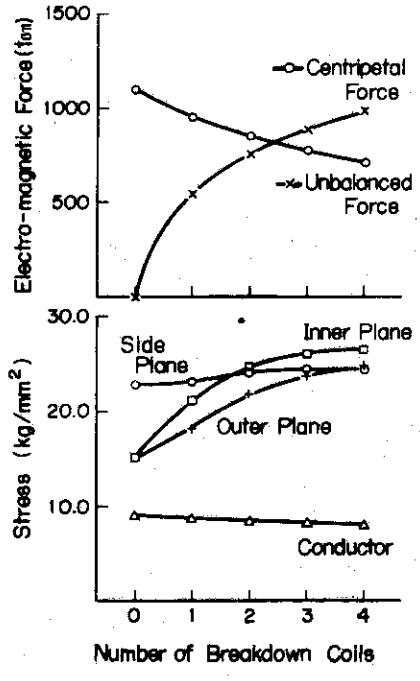

Fig. 26 Stress and electromagnetic forces in a coil neighboring failed coils as a function of failed coil number

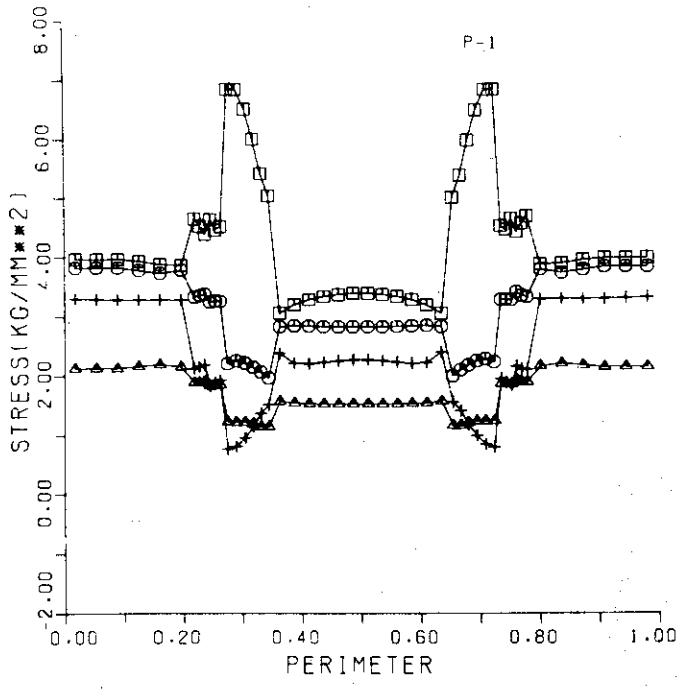

Principal Stress σ1

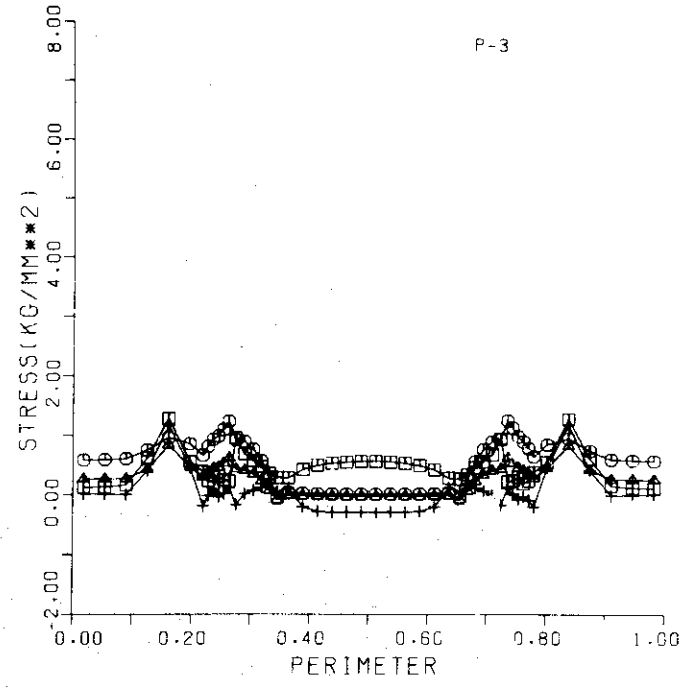

Principal Stress σ3

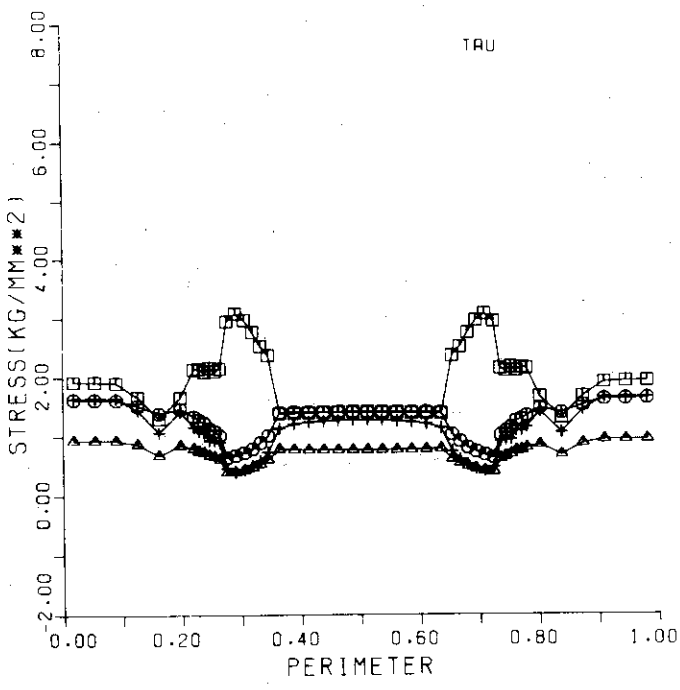

Principal Shear Stress τ

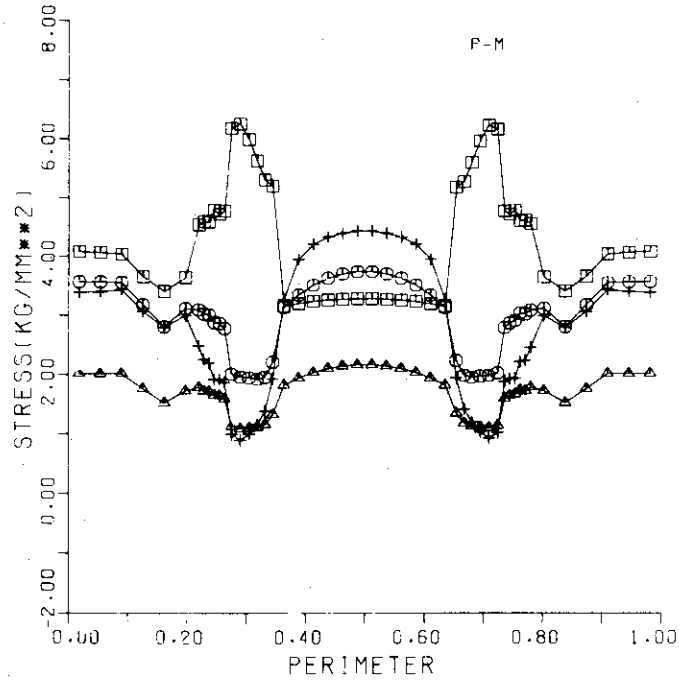

Von Mises Stress

⊟⊟ is inner plane, ⊣⊢ is outer plane, ⊖⊖ is side plane and ▲▲ is conductor. These symbols are same in following figures.

Fig. 27 Stresses in case of no poloidal coils, isotropy and continuous support

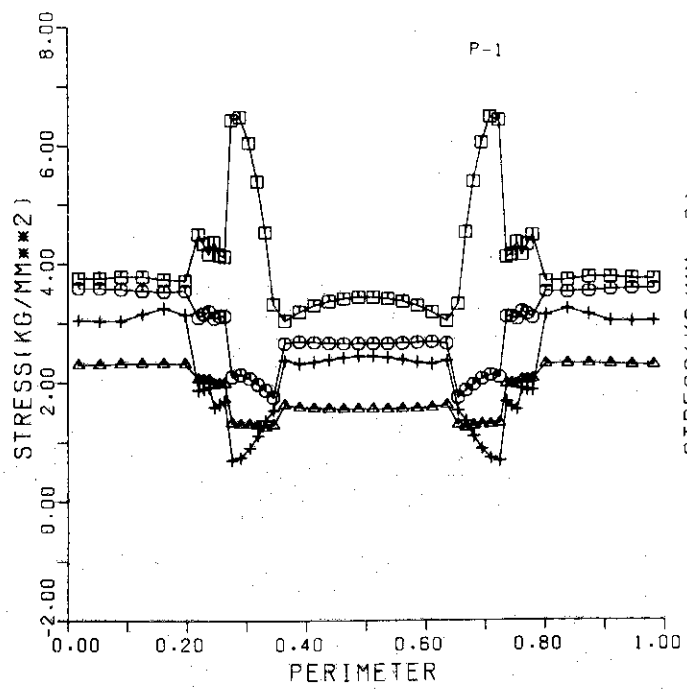

Principal Stress σ1

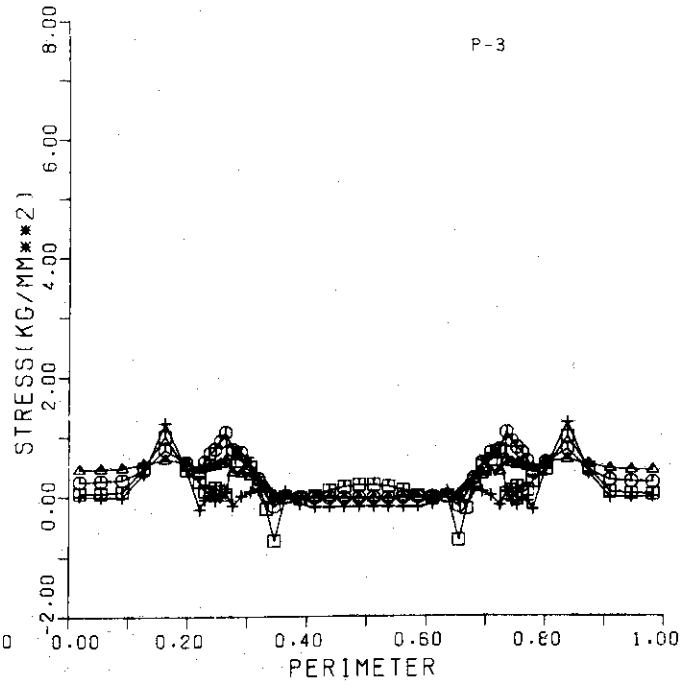

Principal Stress σ3

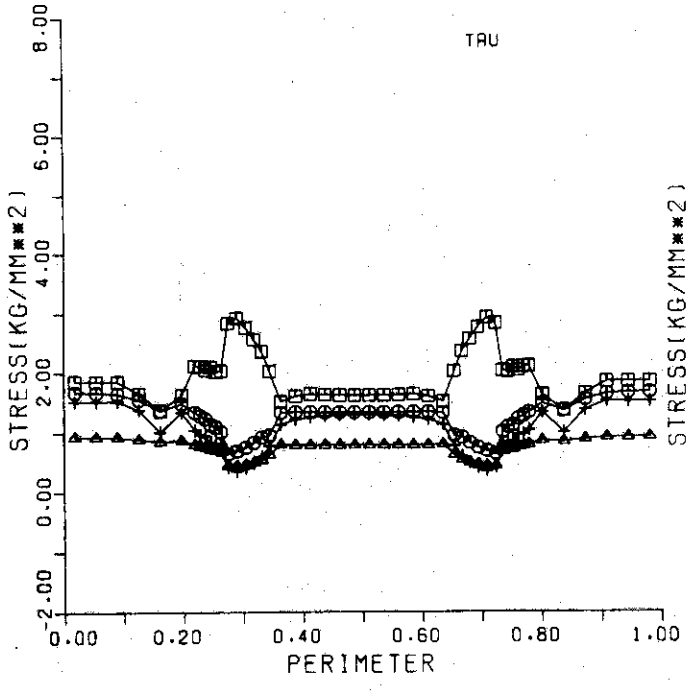

Principal Shear Stress τ

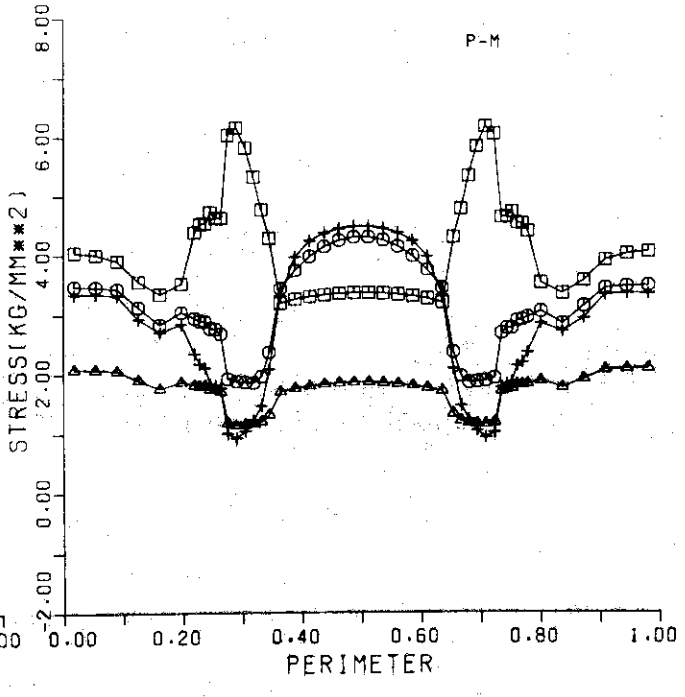

Von Mises Stress

Fig. 28 Stresses in case of no poloidal coils, anisotropy and continuous support

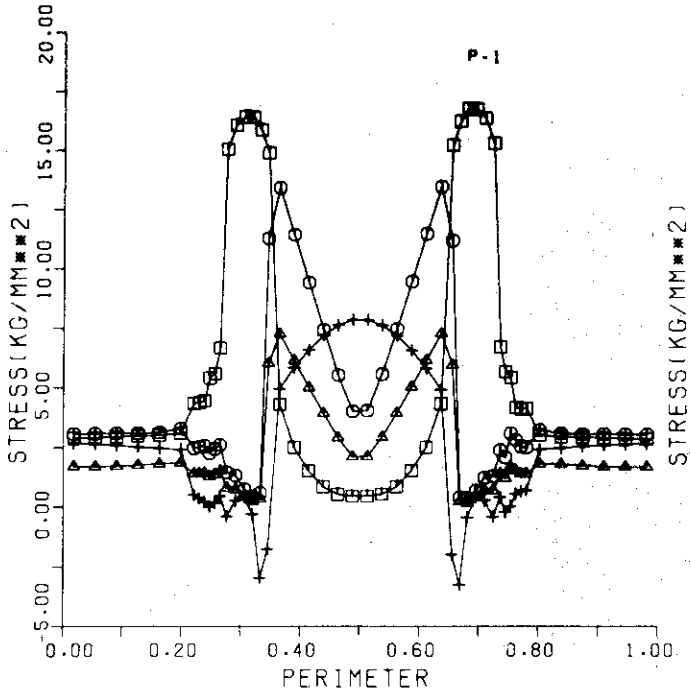

Principal Stress σ1

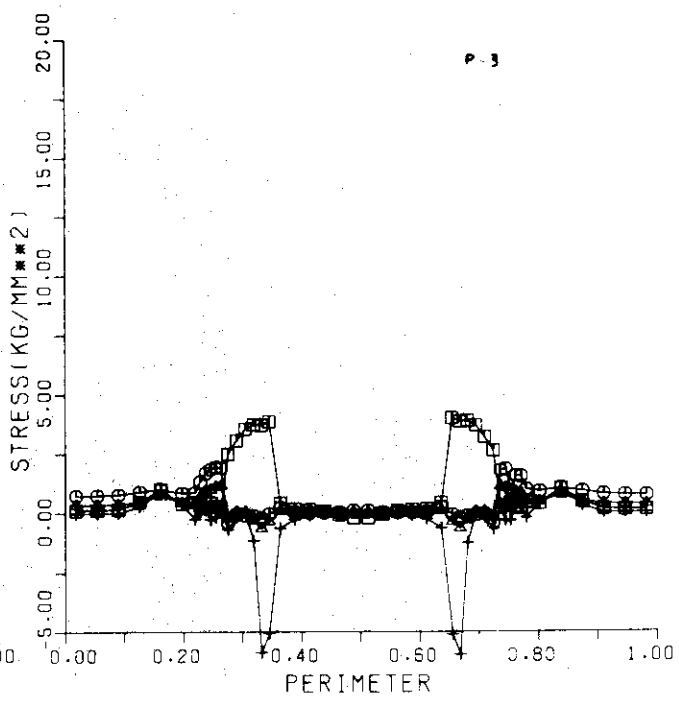

Principal Stress σ3

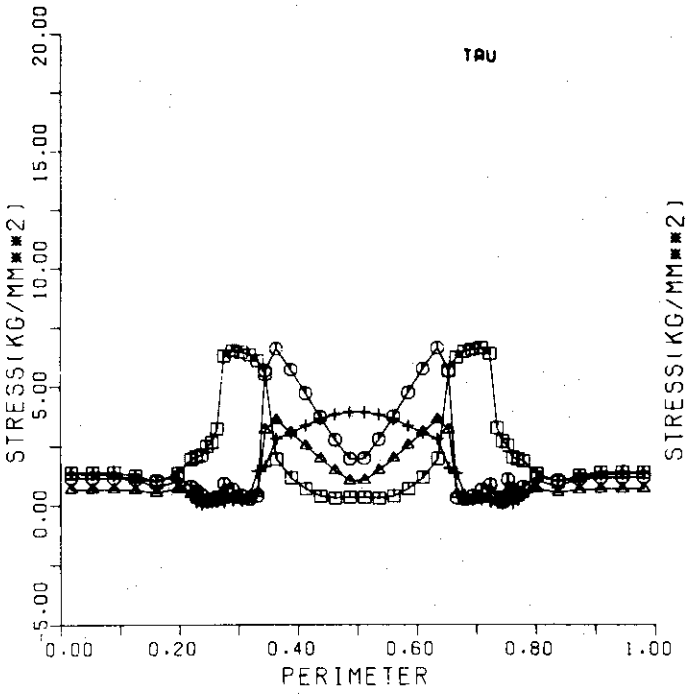

Principal Shear Stress τ

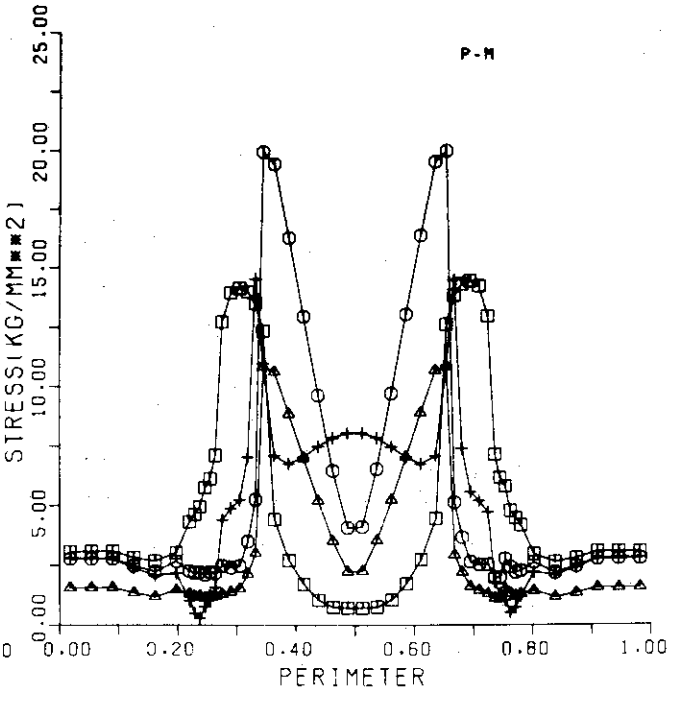

Von Mises Stress

Fig. 29 Stresses in case of no poloidal coils, isotropy and two points support

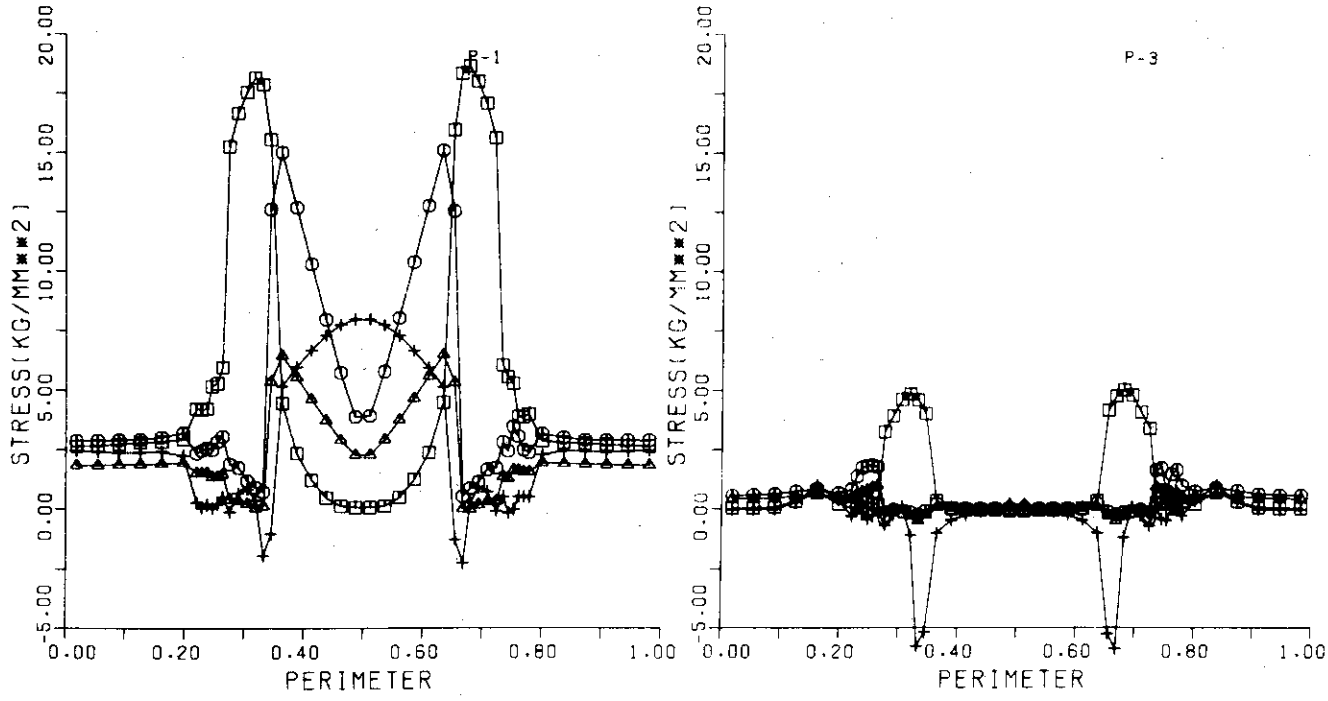

Principal stress σ1 Principal Stress σ3

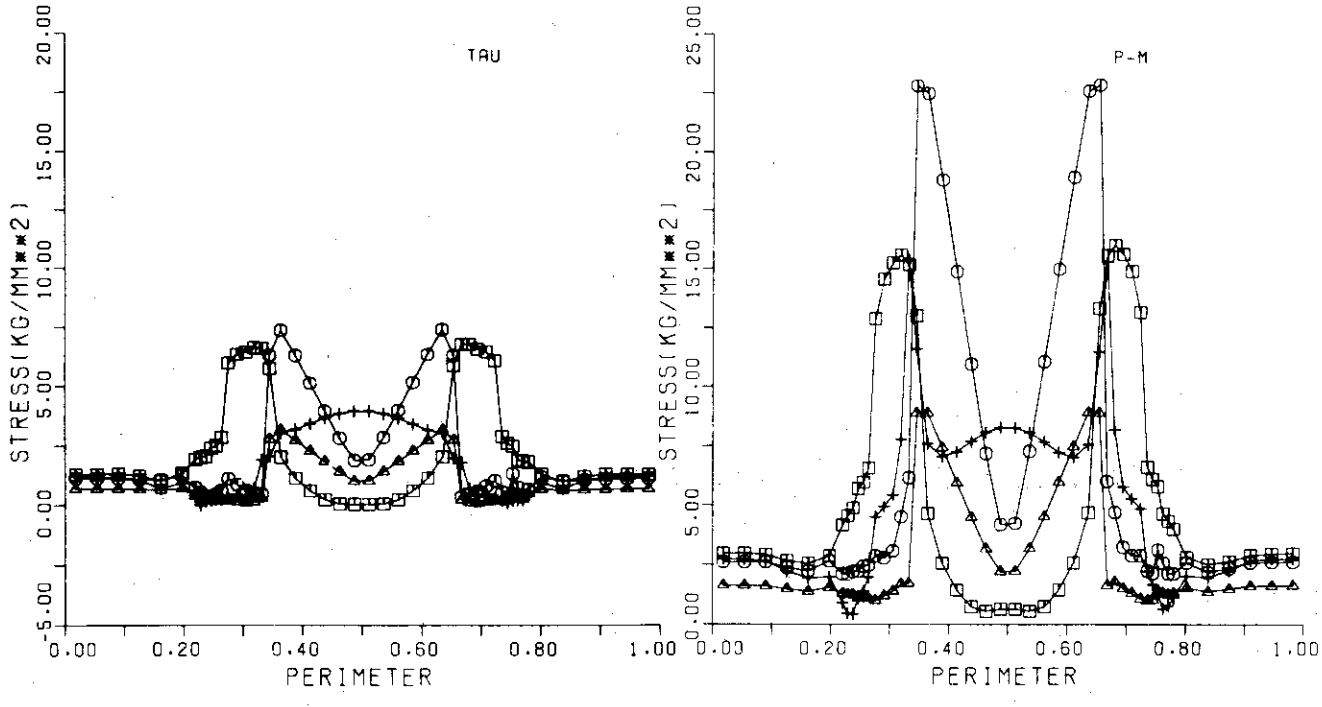

Principal Shear Stress τ Von Mises Stress

Fig. 30 Stresses in case of no poloidal coils, anisotropy and two points support

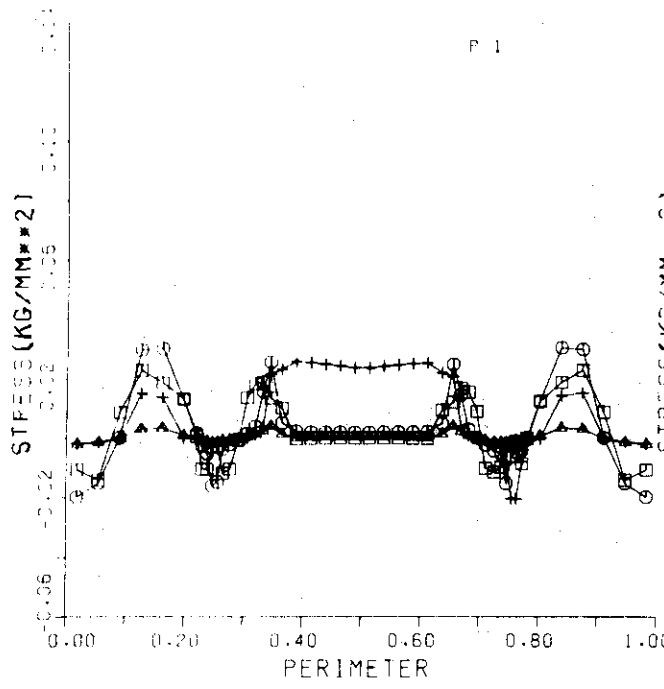

Principal Stress σ1

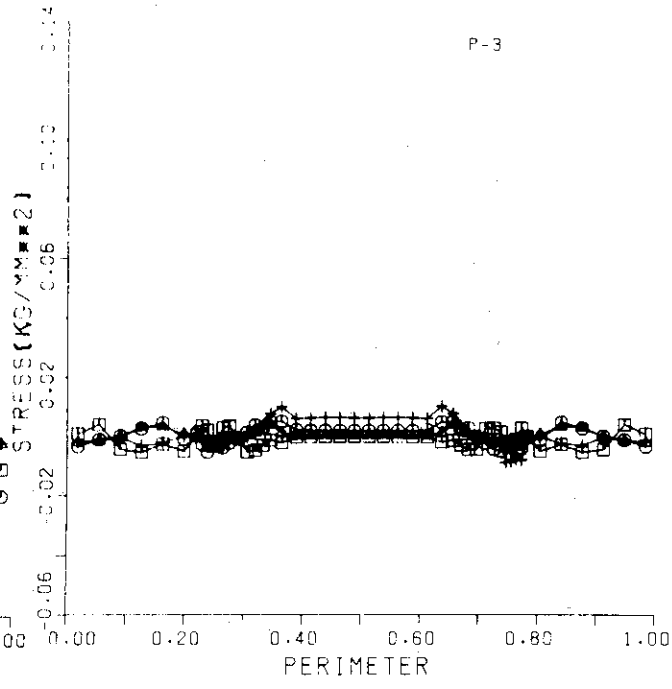

Principal Stress σ3

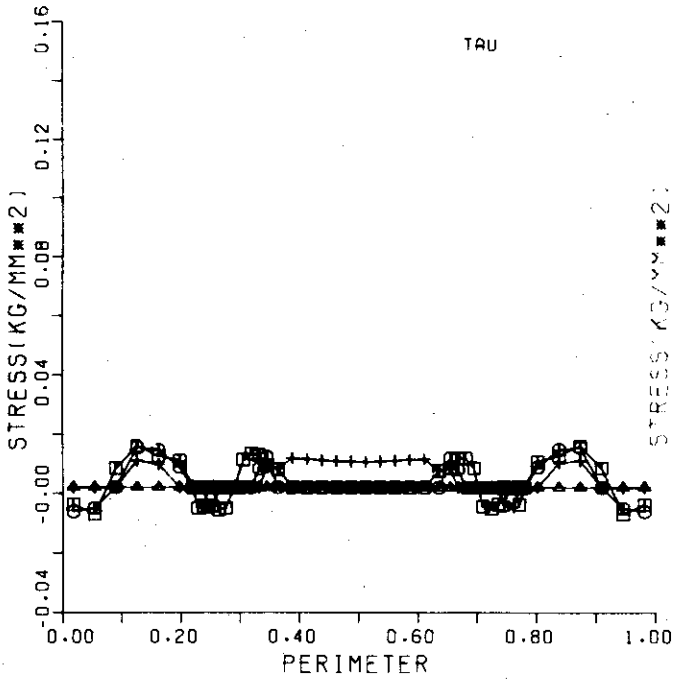

Principal Shear Stress τ

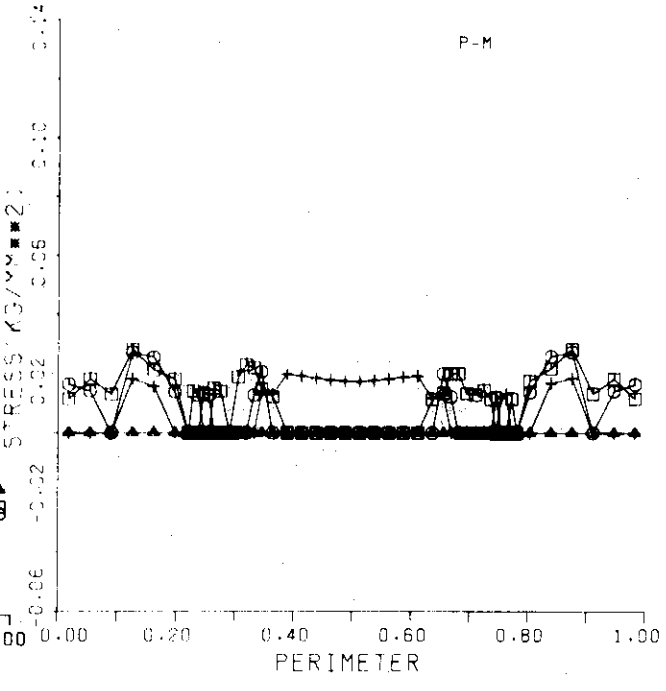

Von Mises Stress

Fig. 31 Stresses in case of seismic force and continuous support

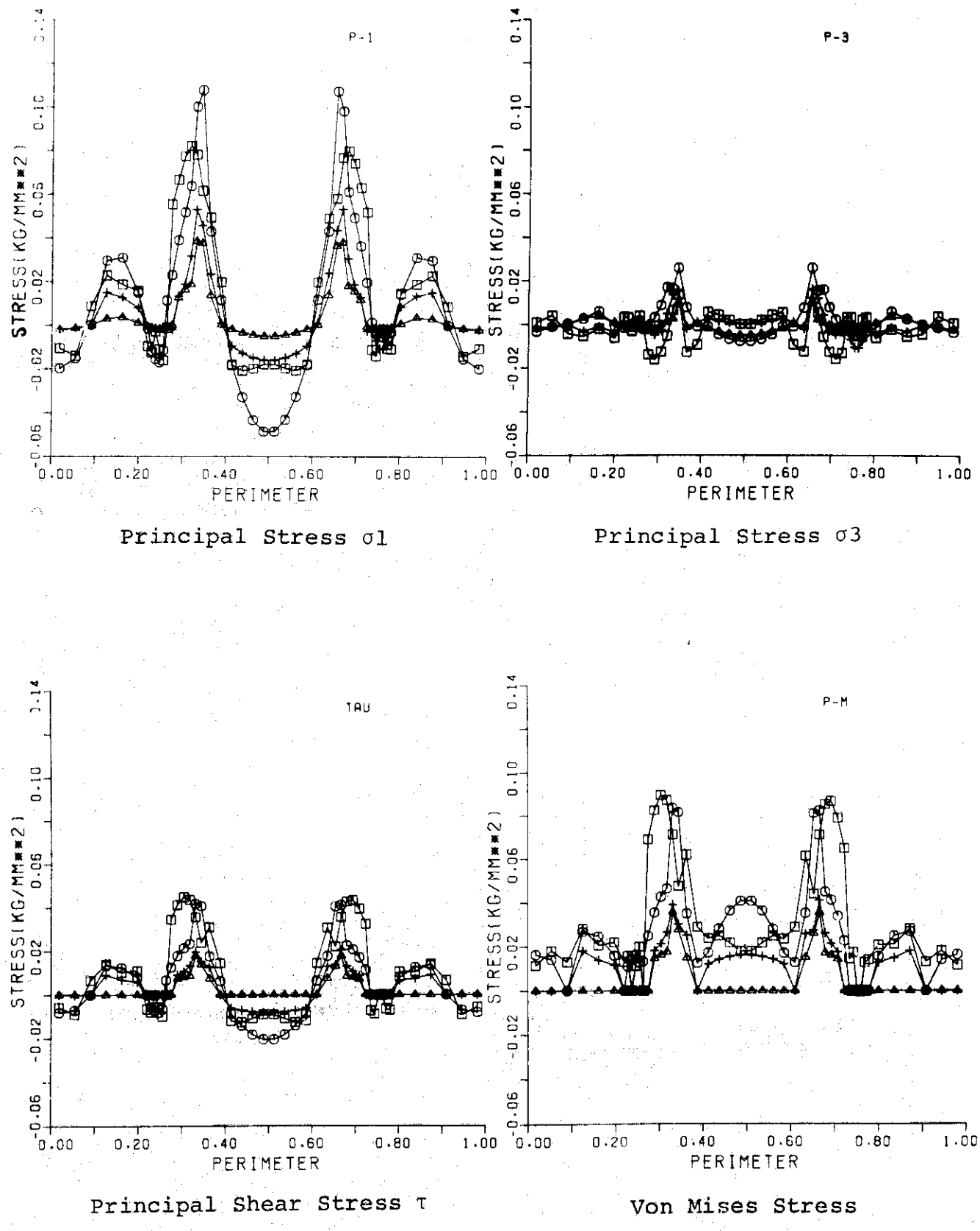

Fig. 32 Stresses in case of seismic force and two points support

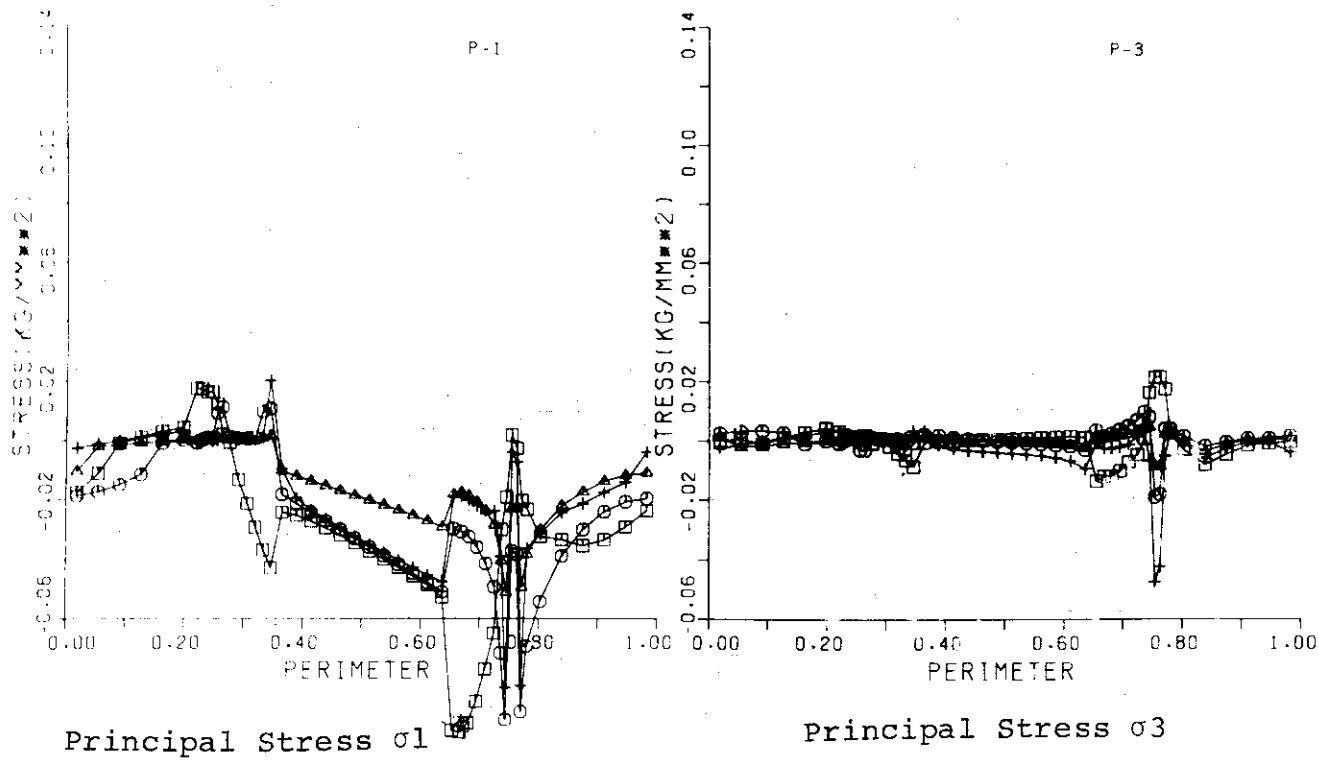

Principal Stress σ1

Principal Stress σ3

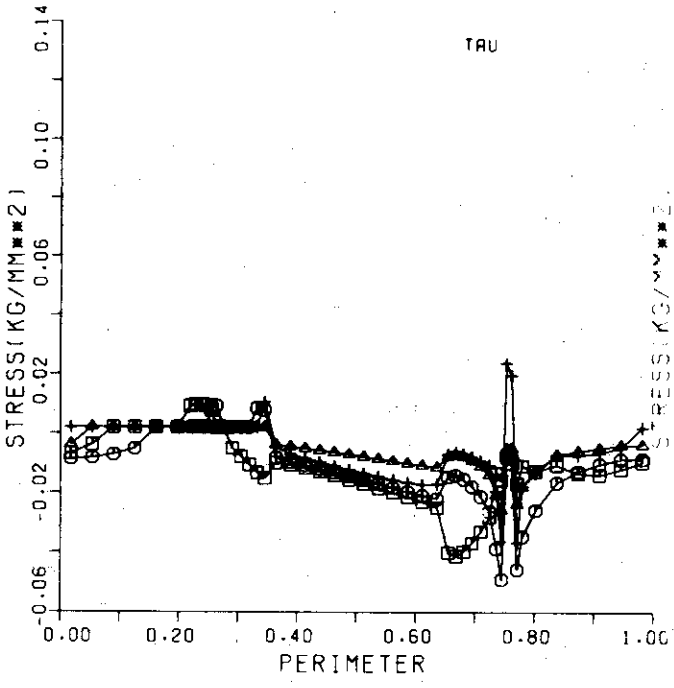

Principal Shear Stress τ

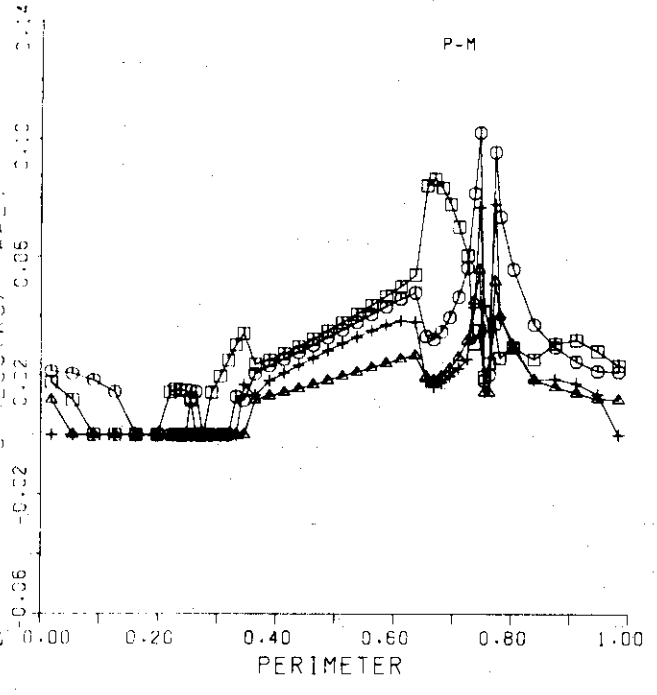

Von Mises Stress

Fig. 33 Stresses in case of gravitational force and continuous support

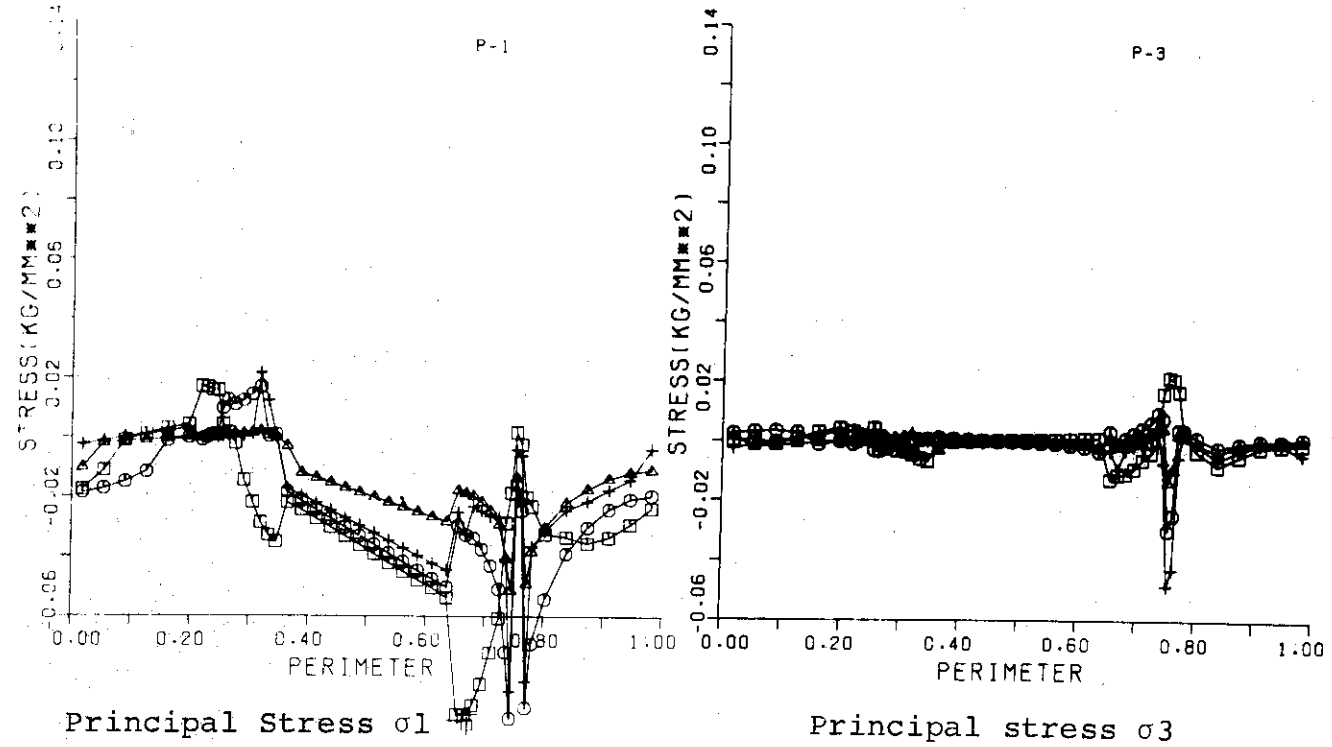

Principal Stress σ1

Principal stress σ3

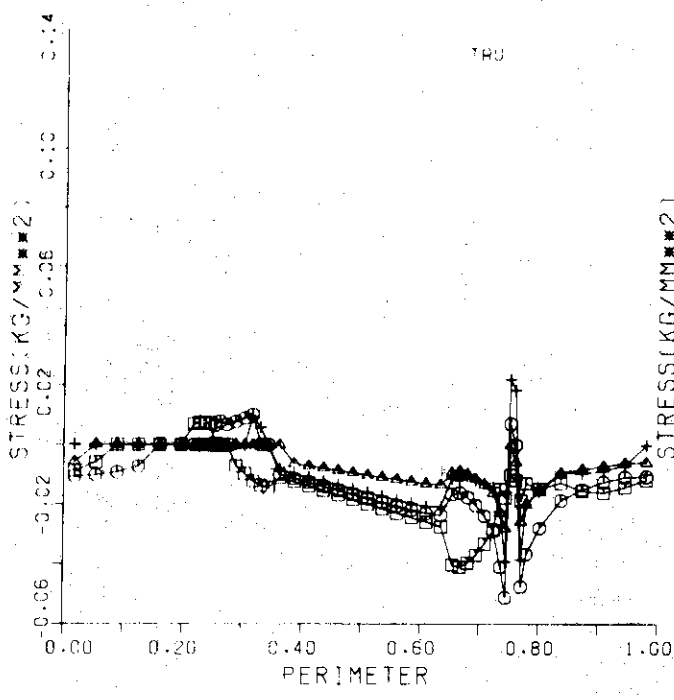

Principal Shear Stress τ

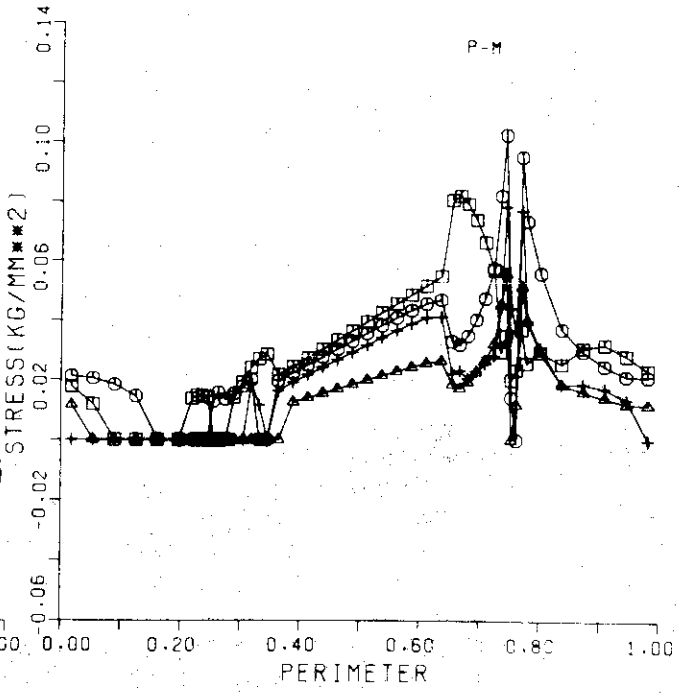

Von Mises Stress

Fig. 34 Stresses in case of gravitational force and two points support

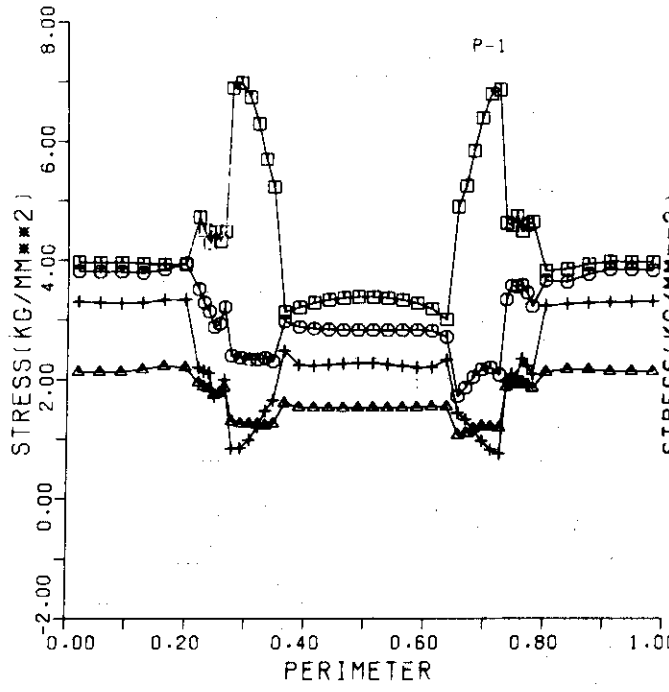

Principal stress σ1

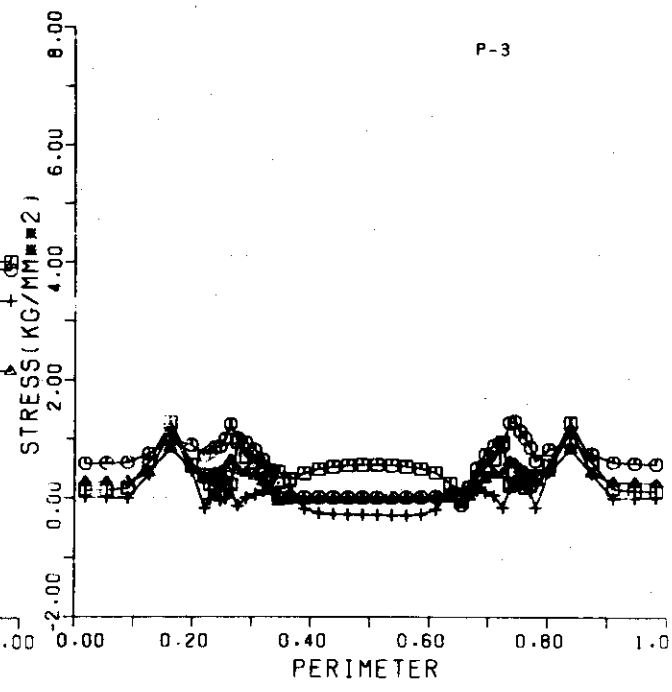

Principal Stress σ3

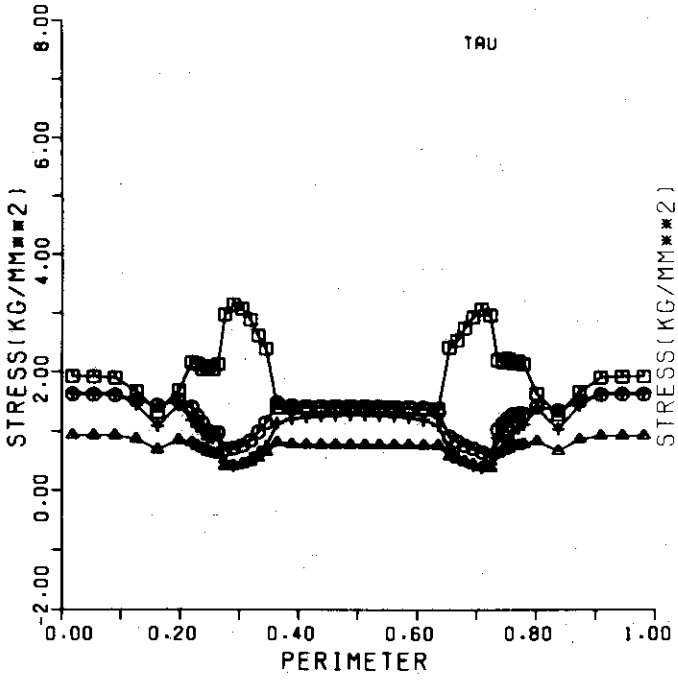

Principal Shear Stress τ

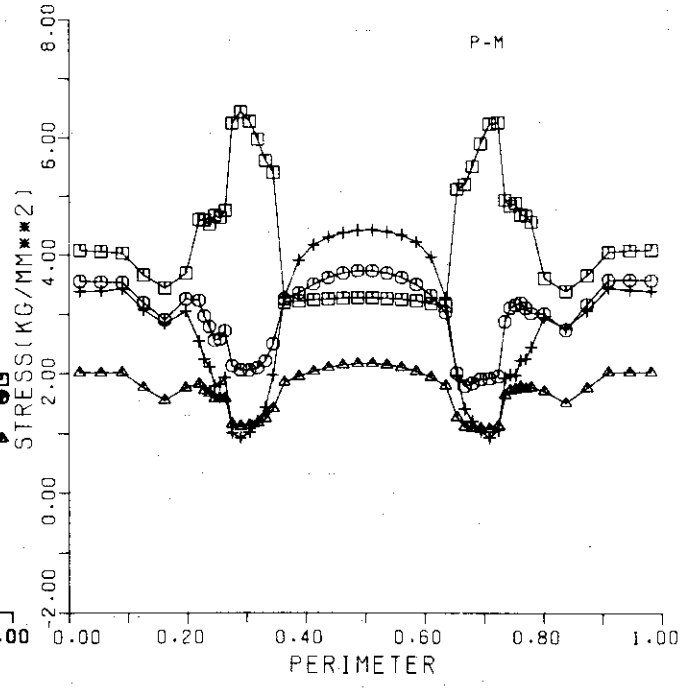

Von Mises Stress

Fig. 35 Stresses in case of inner OH coils, isotropy and continuous support

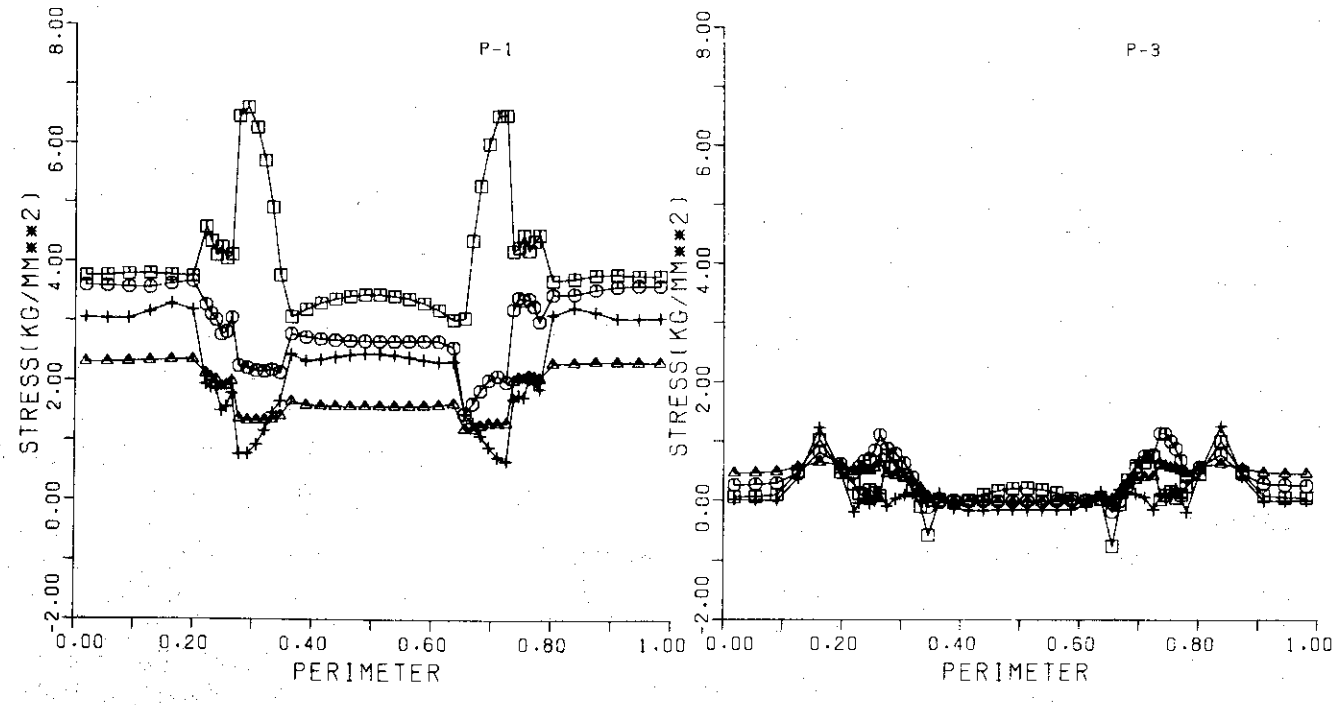

Principal Stress σ1

Principal Stress σ3

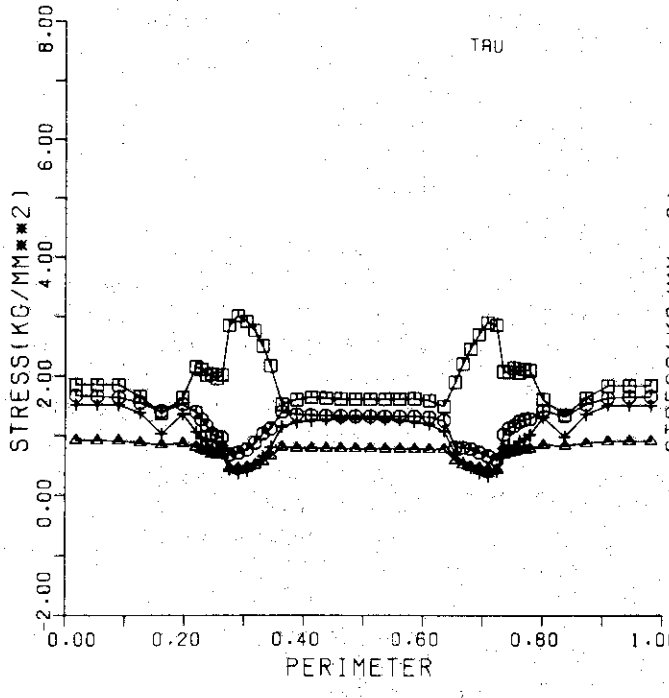

Principal Shear Stress τ

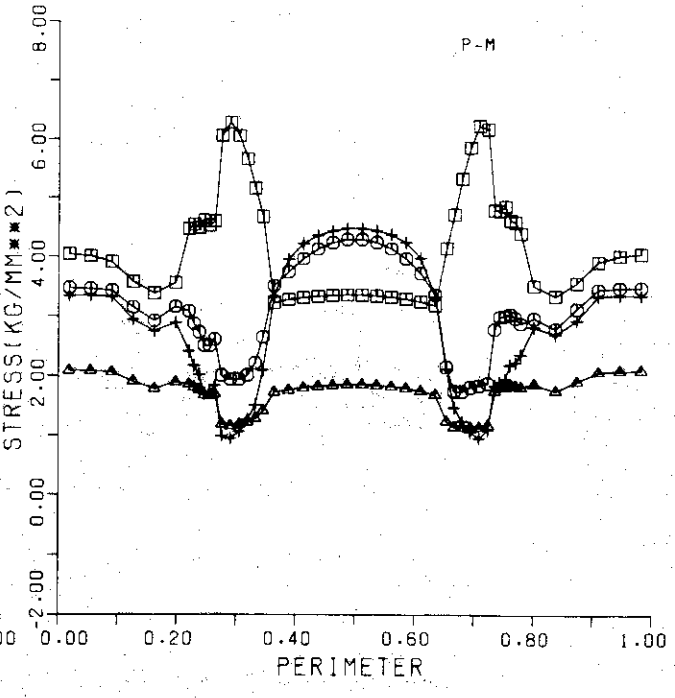

Von Mises Stress

Fig. 36 Stresses in case of inner OH coils, anisotropy and continuous support

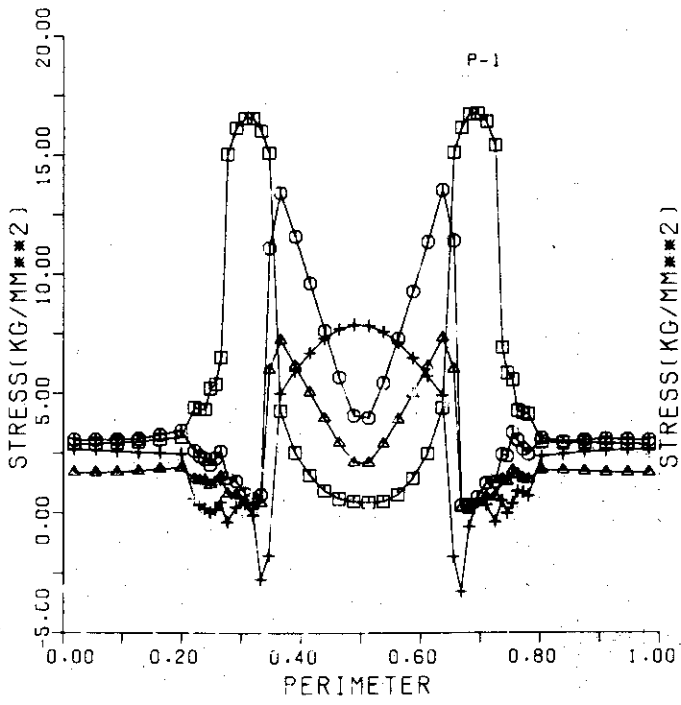

Principal Stress σ1

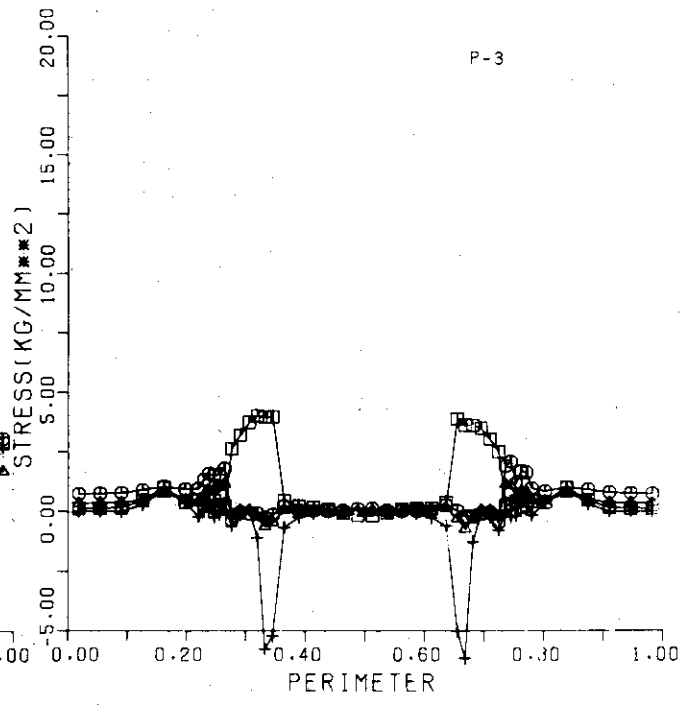

Principal Stress σ3

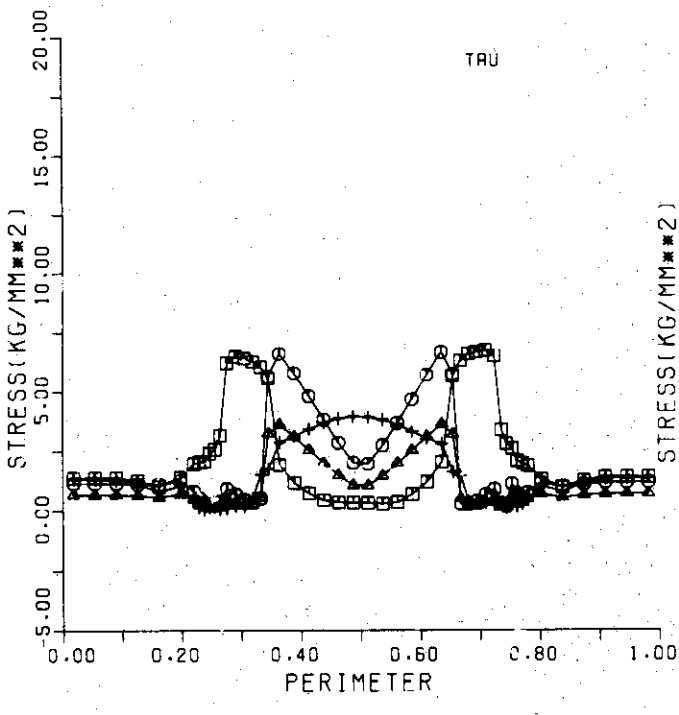

Principal Shear Stress τ

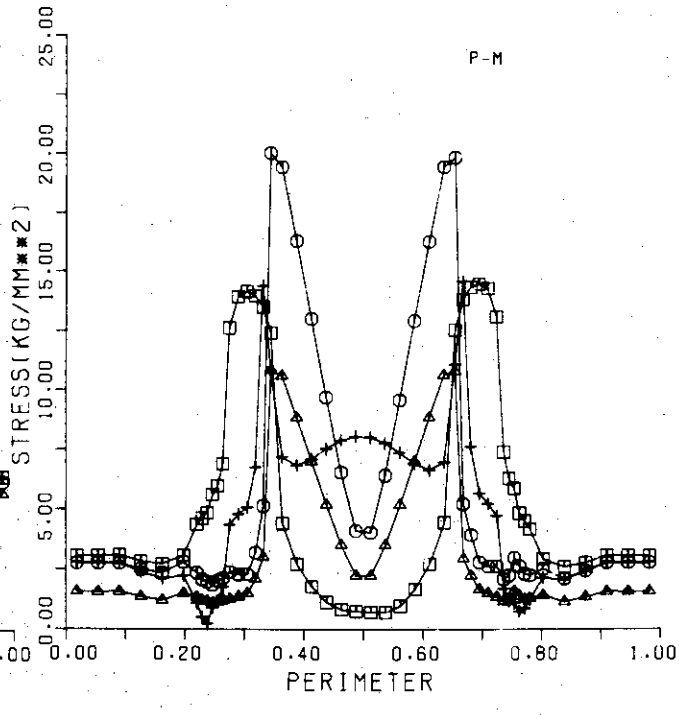

Von Mises Stress

Fig. 37 Stresses in case of inner OH coils, isotropy and two points support

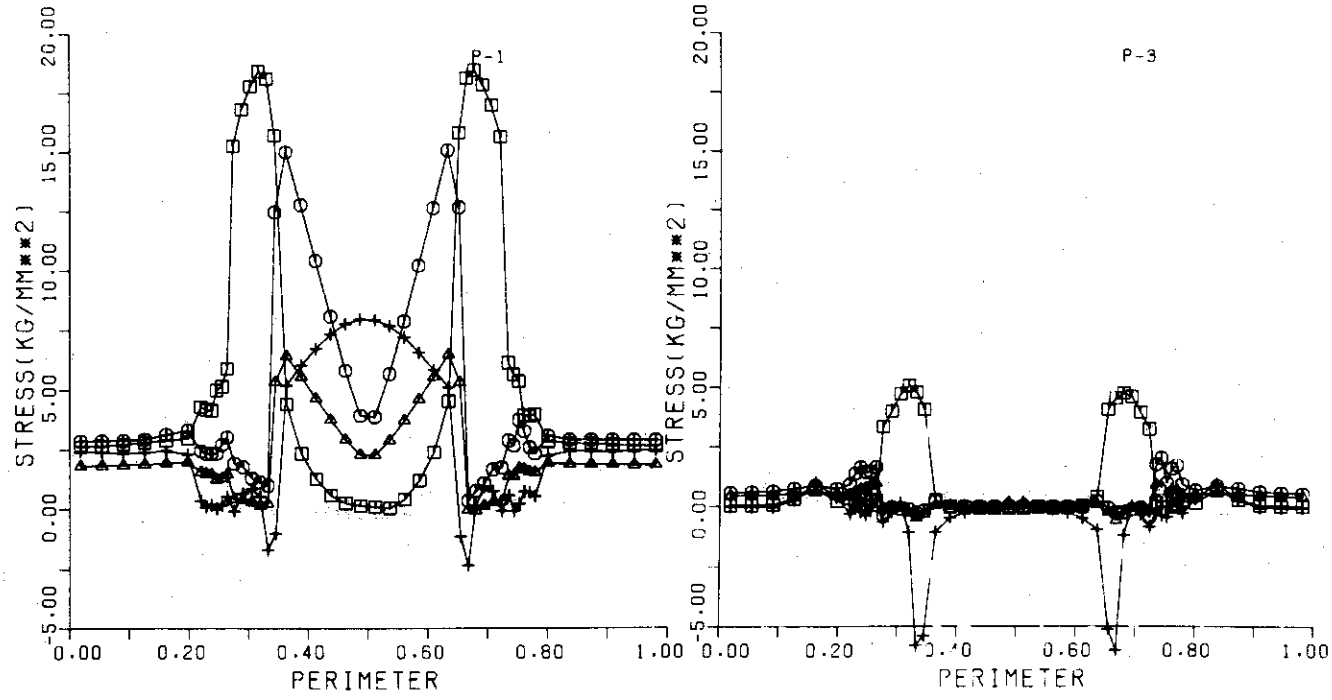

Principal Stress σ1 principal Stress σ3

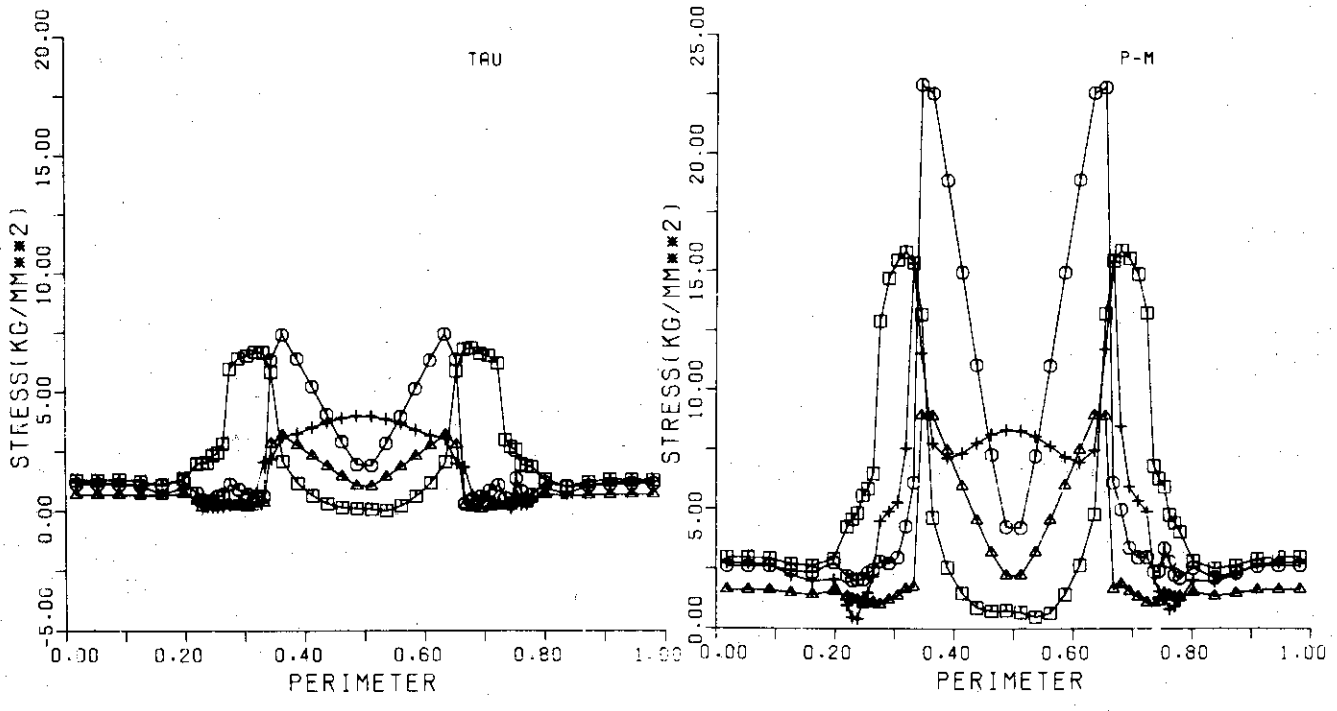

Principal Shear Stress τ Von Mises Stress

Fig. 38 Stresses in case of inner OH coils, anisotropy and two points support

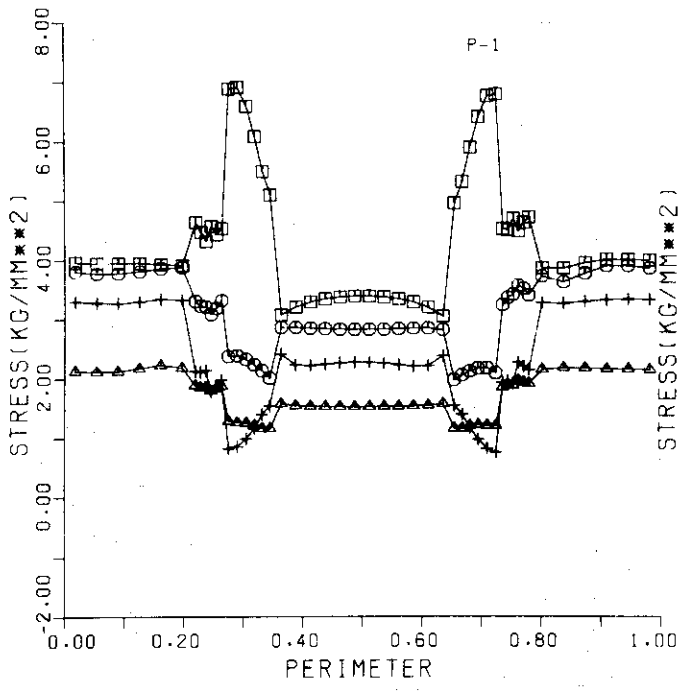

Principal Stress σ1

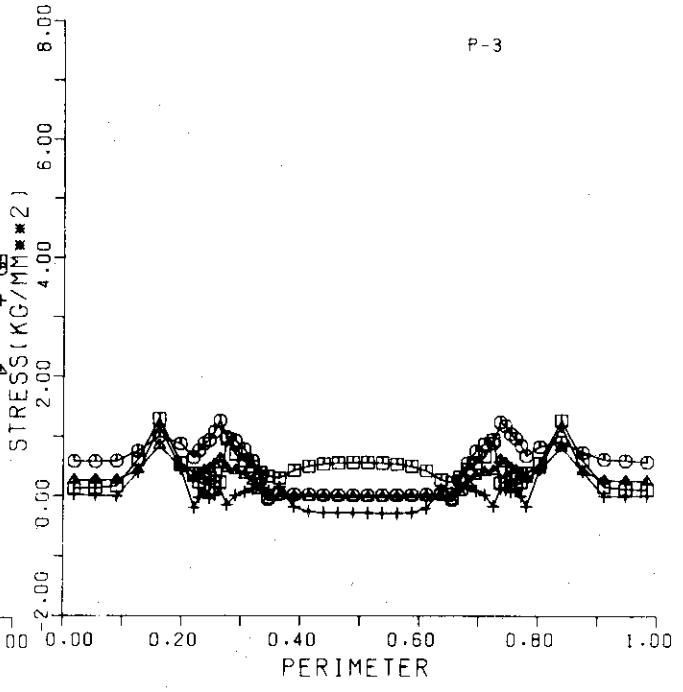

Principal Stress σ3

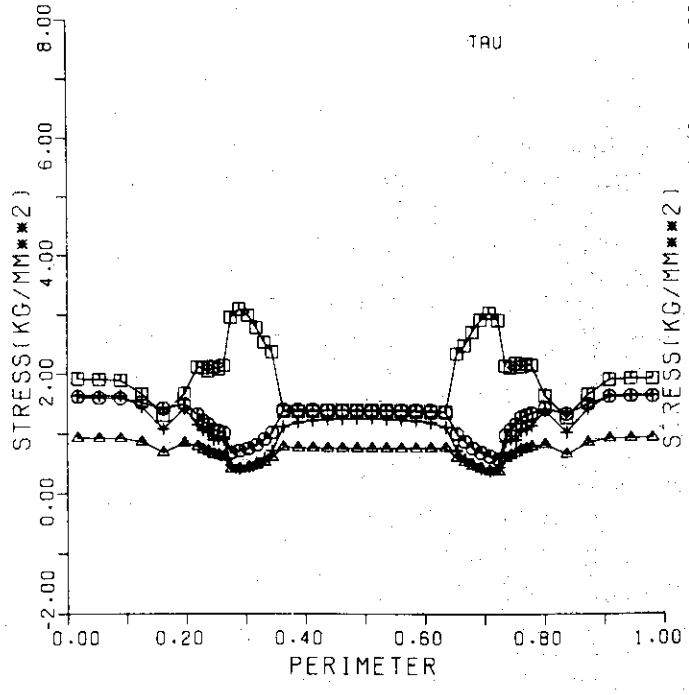

Principal Shear Stress τ

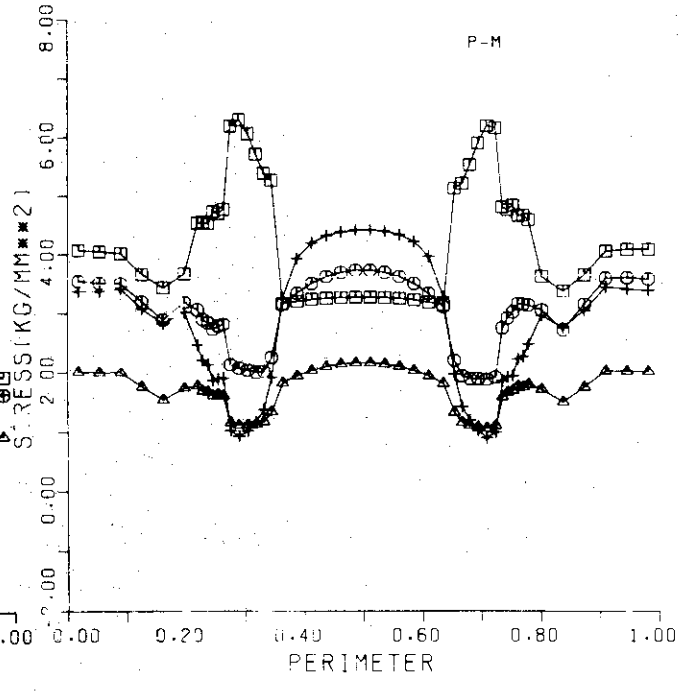

Von Mises Stress

Fig. 39 Stresses in case of inner VF coils, isotropy and continuous support

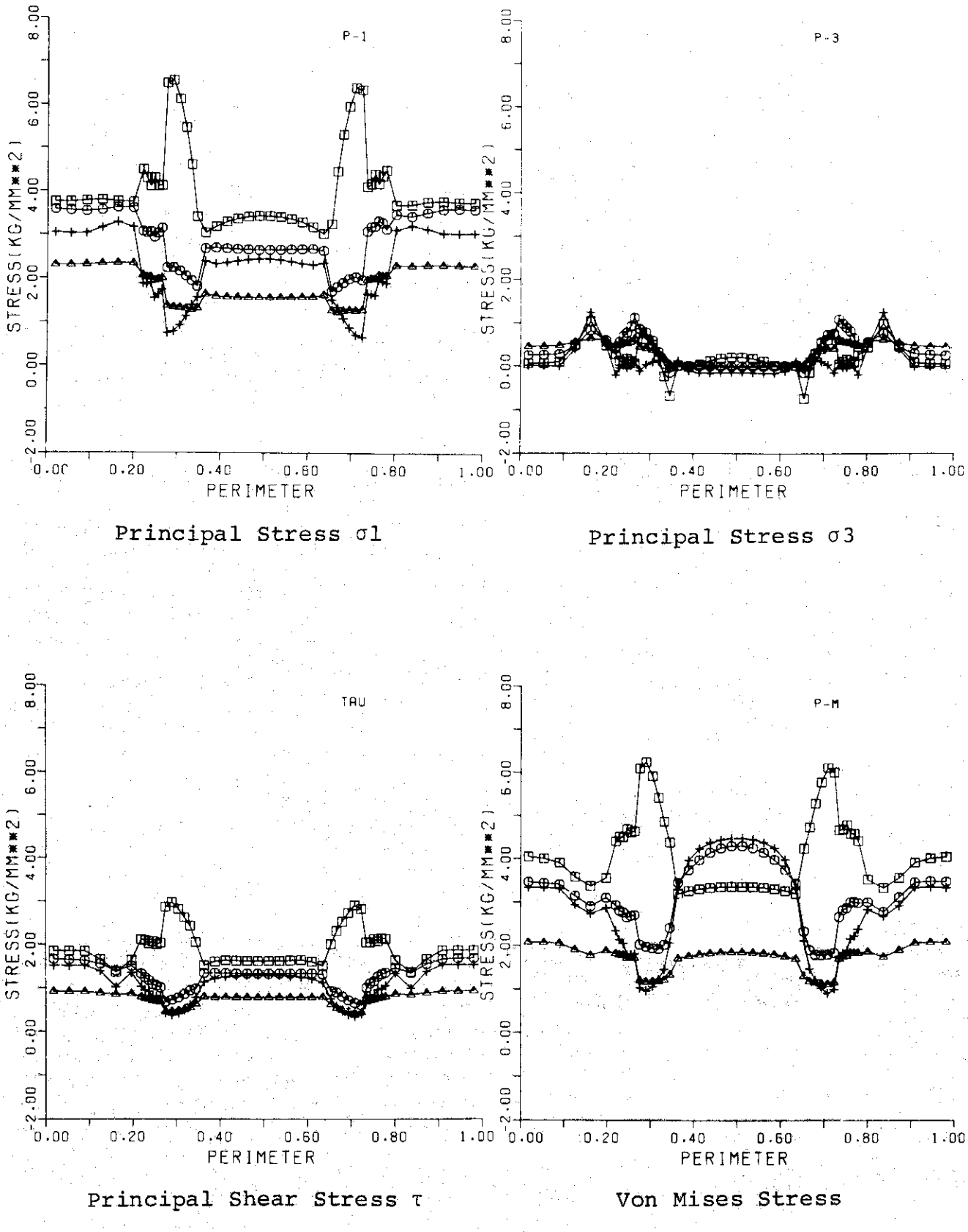

Principal Stress σ1

Principal Stress σ3

Principal Shear Stress τ

Von Mises Stress

Fig. 40 Stresses in case of inner VF coils, anisotropy and continuous support

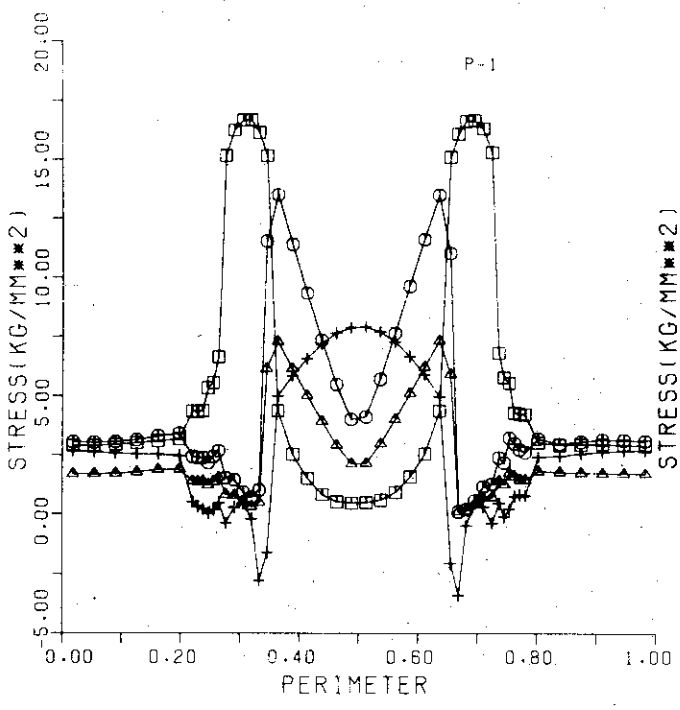

Principal Stress σ1

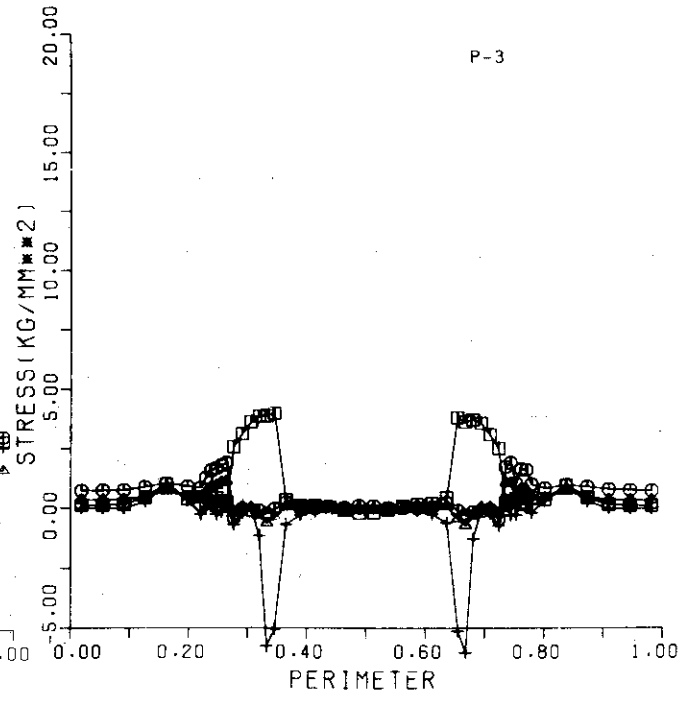

Principal stress σ3

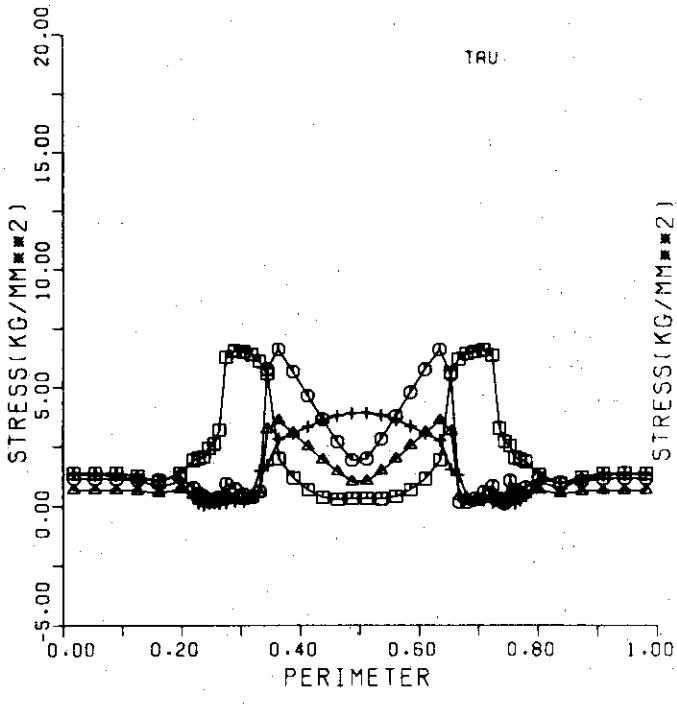

Principal Shear Stress τ

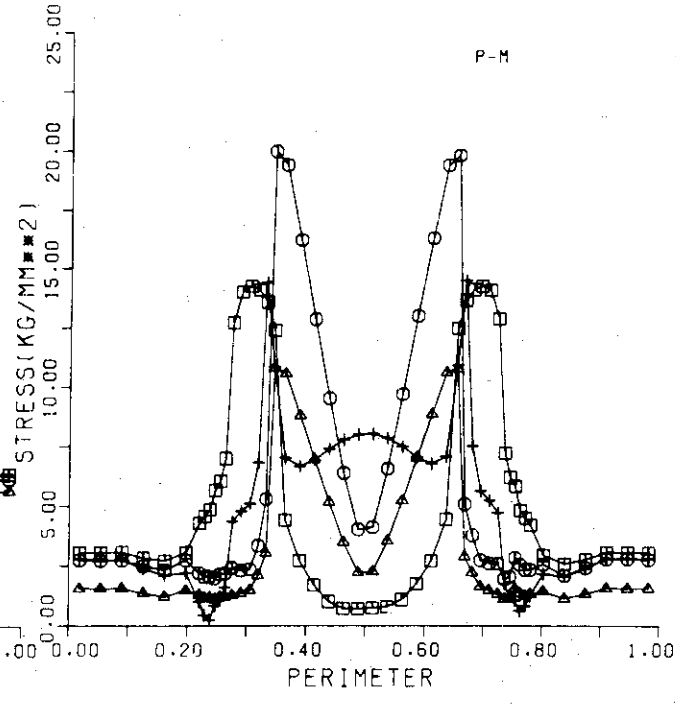

Von Mises Stress

Fig. 41 Stresses in case of inner VF coils, isotropy and two points support

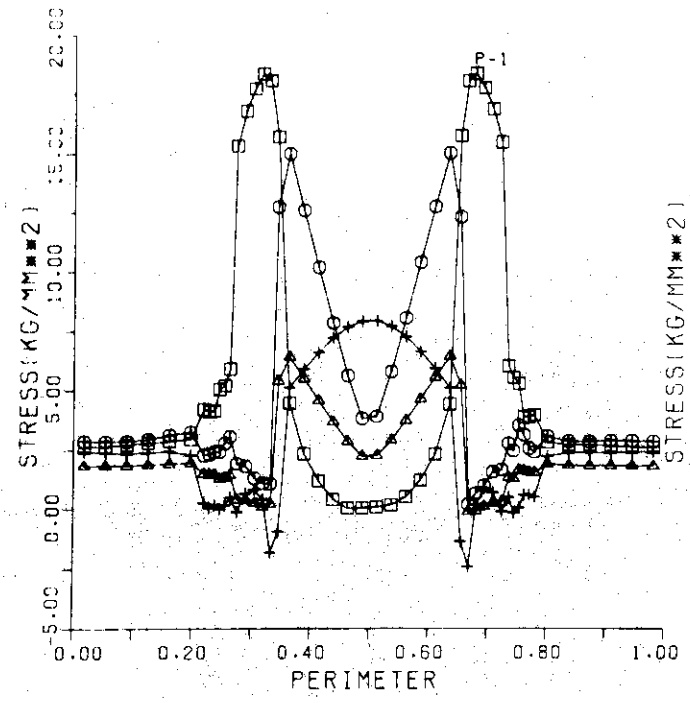

Principal Stress σ1

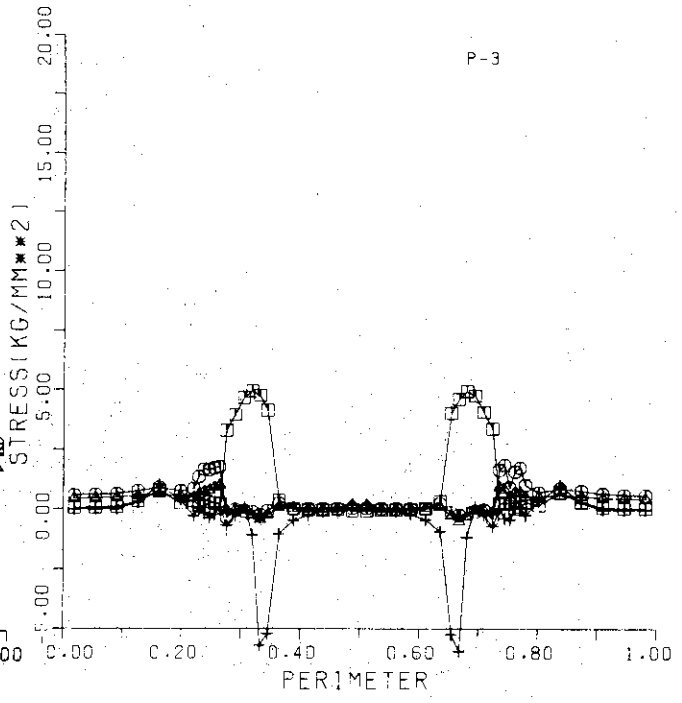

Principal Stress σ3

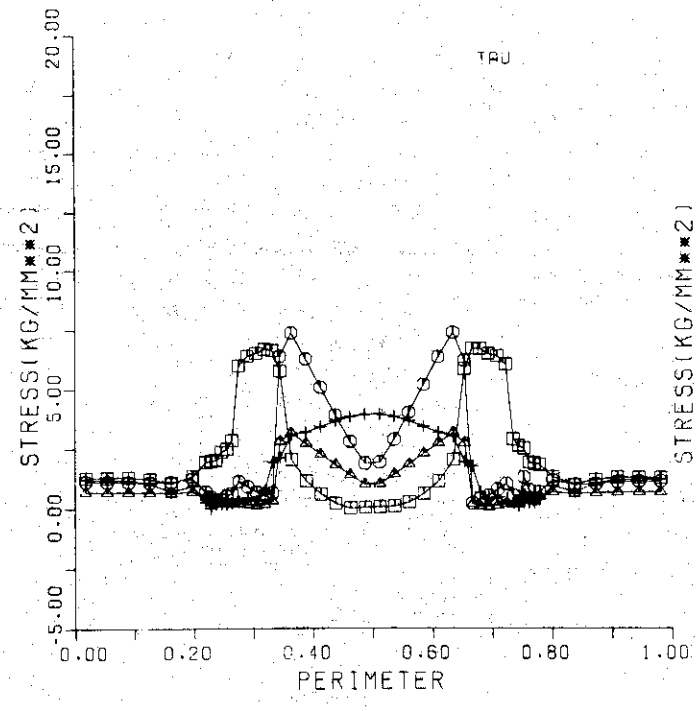

Principal Shear Stress τ

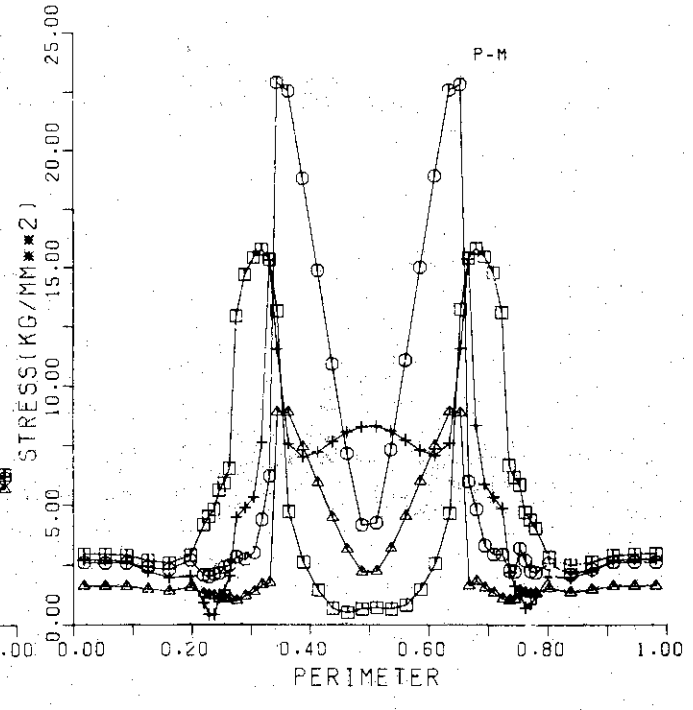

Von Mises Stress

Fig. 42 Stresses in case of inner VF coils, anisotropy and two points support

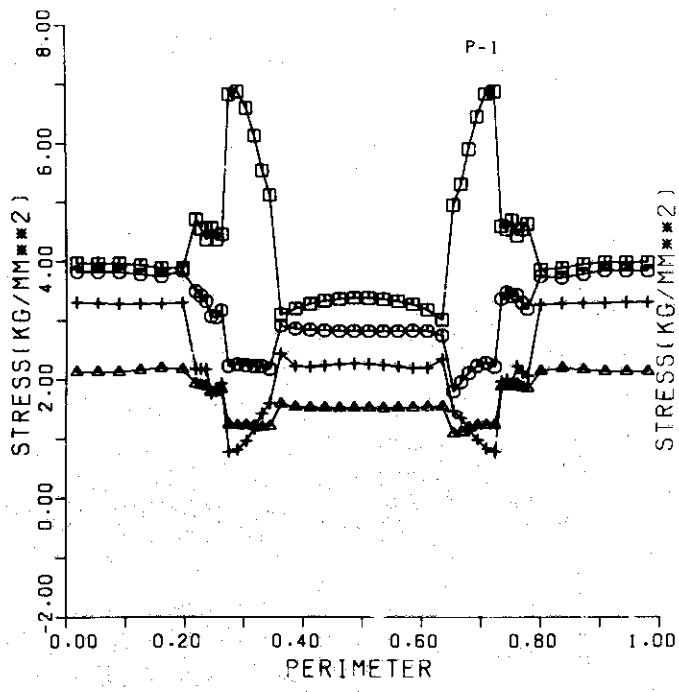

Principal Stress σ1

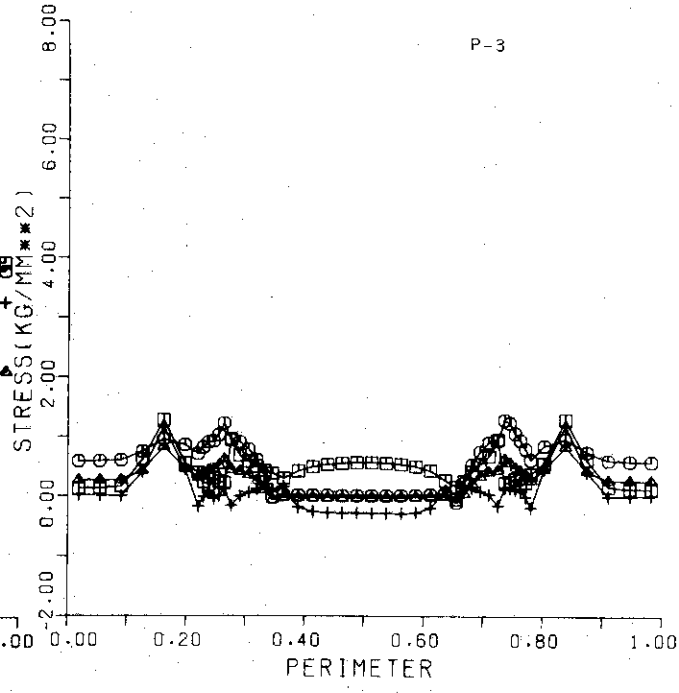

Principal Stress σ3

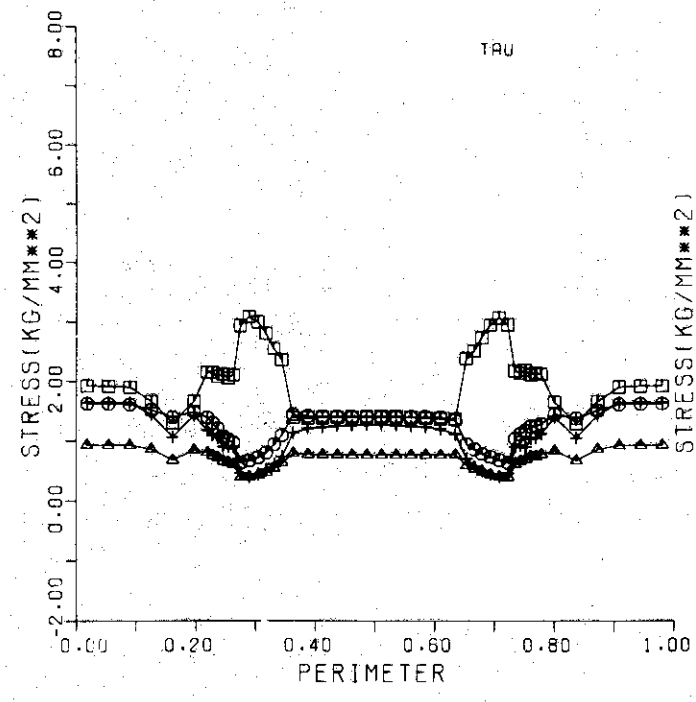

Principal Shear Stress τ

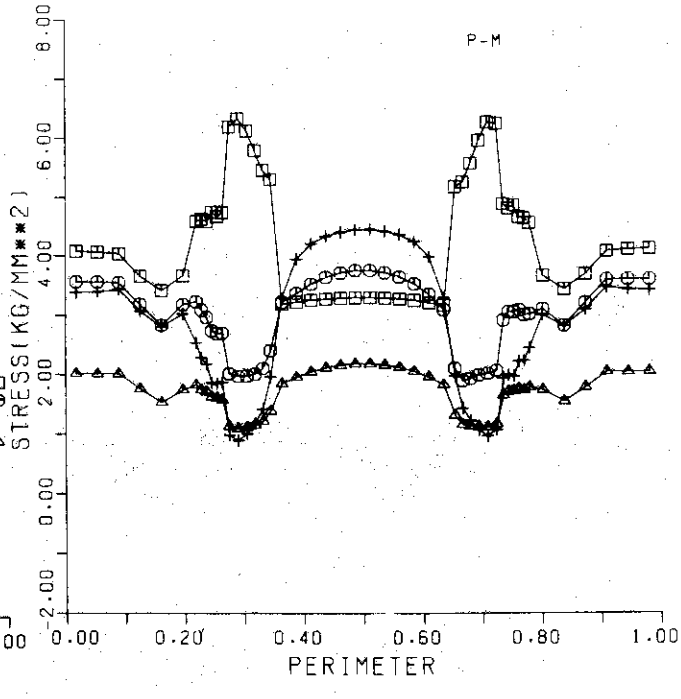

Von Mises Stress

Fig. 43 Stresses in case of outer OH coils, isotropy and continuous support

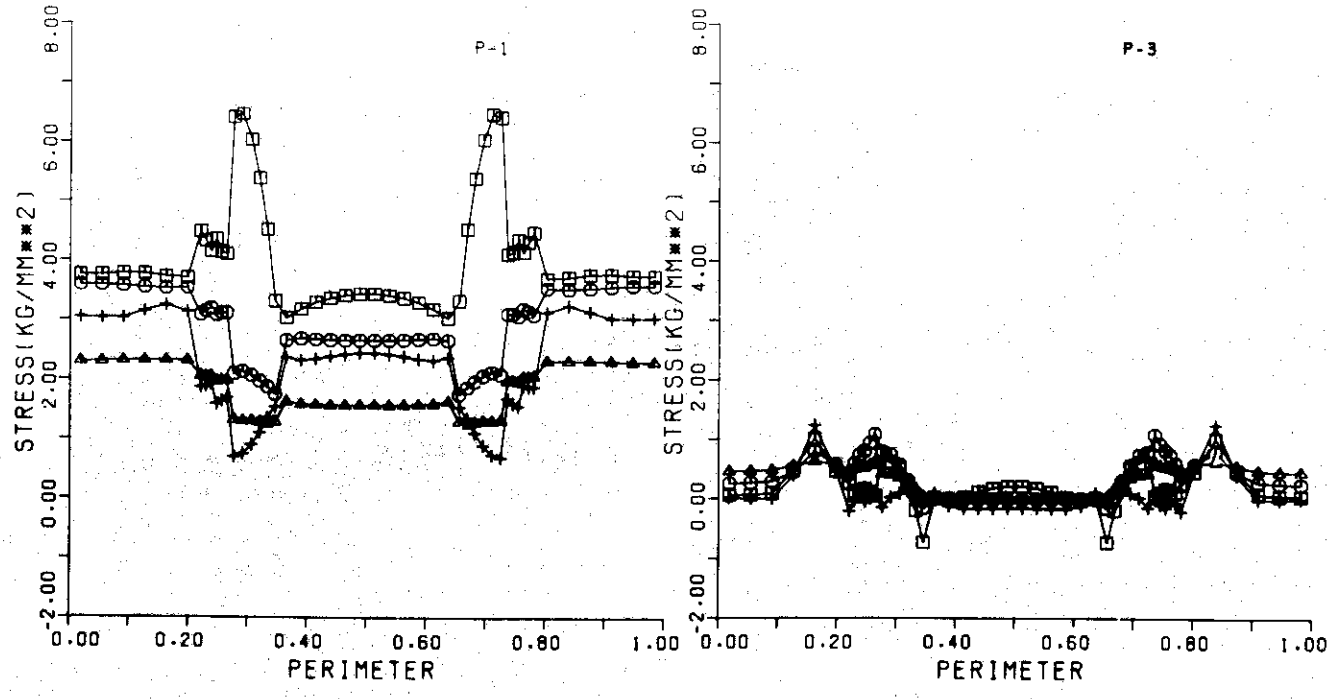

Principal Stress σ1

Principal Stress σ3

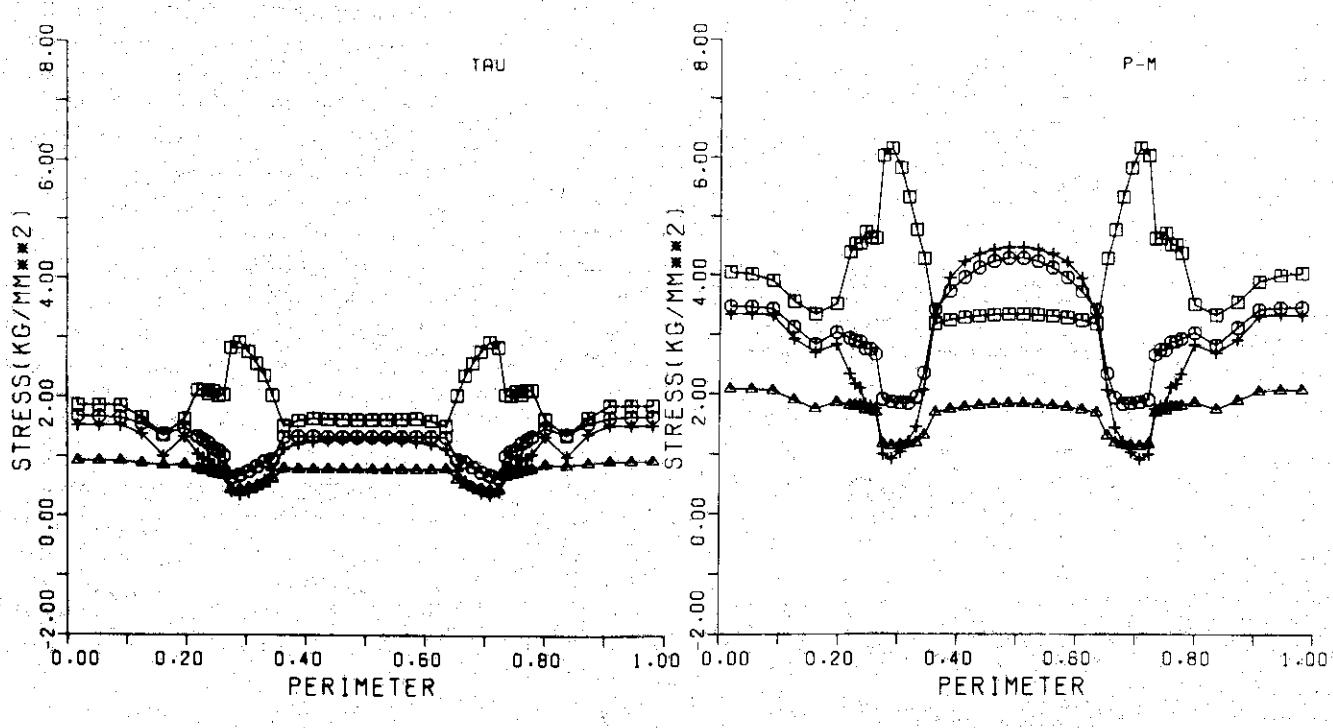

Principal Shear Stress τ

Von Mises Stress

Fig. 44 Stresses in case of outer OH coils, anisotropy and continuous support

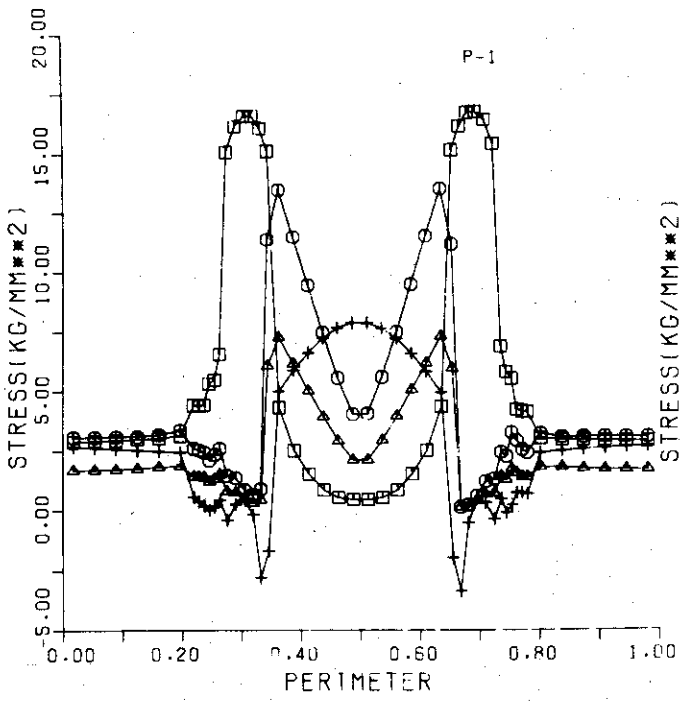

Principal Stress σ1

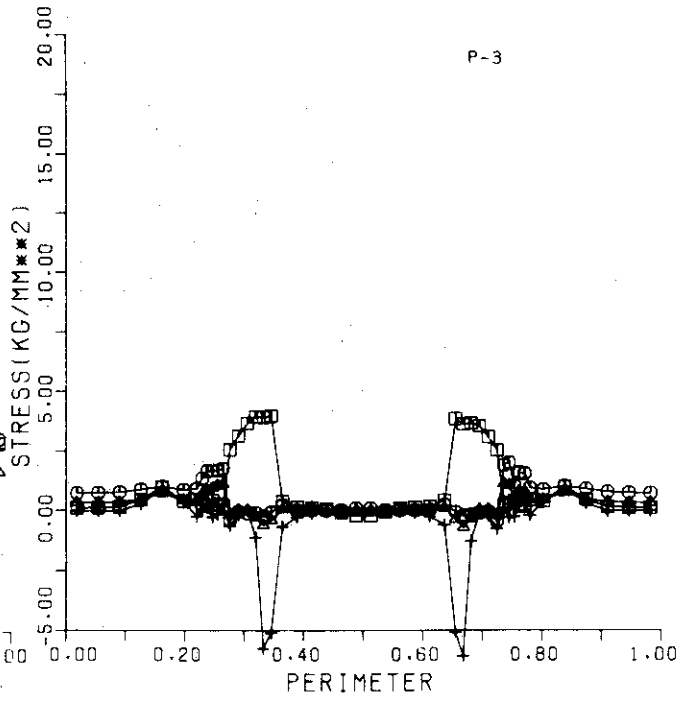

Principal Stress σ3

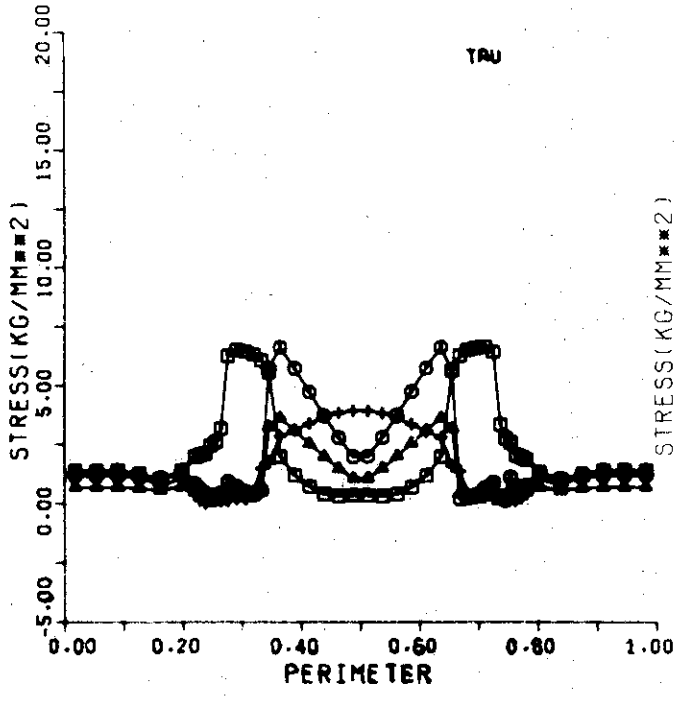

Principal Shear Stress τ

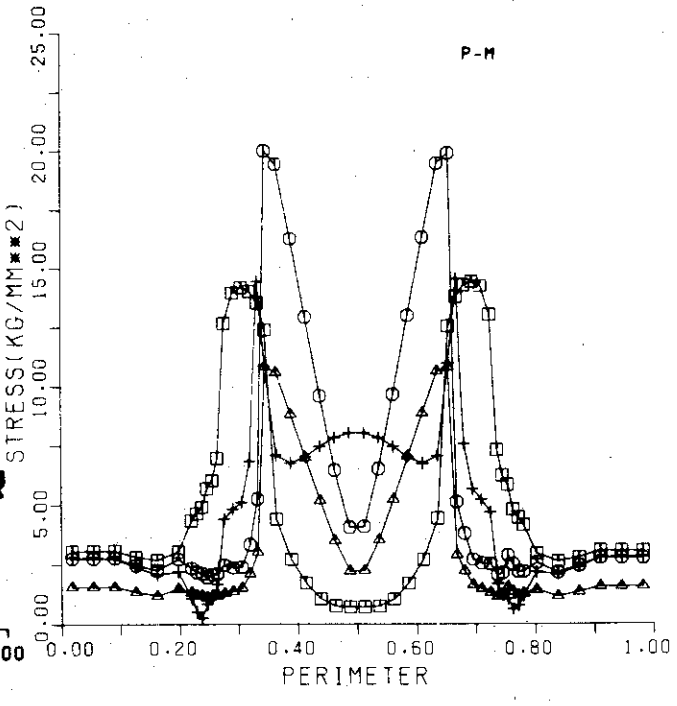

Von Mises Stress

Fig. 45 Stresses in case of outer OH coils, isotropy and two points support

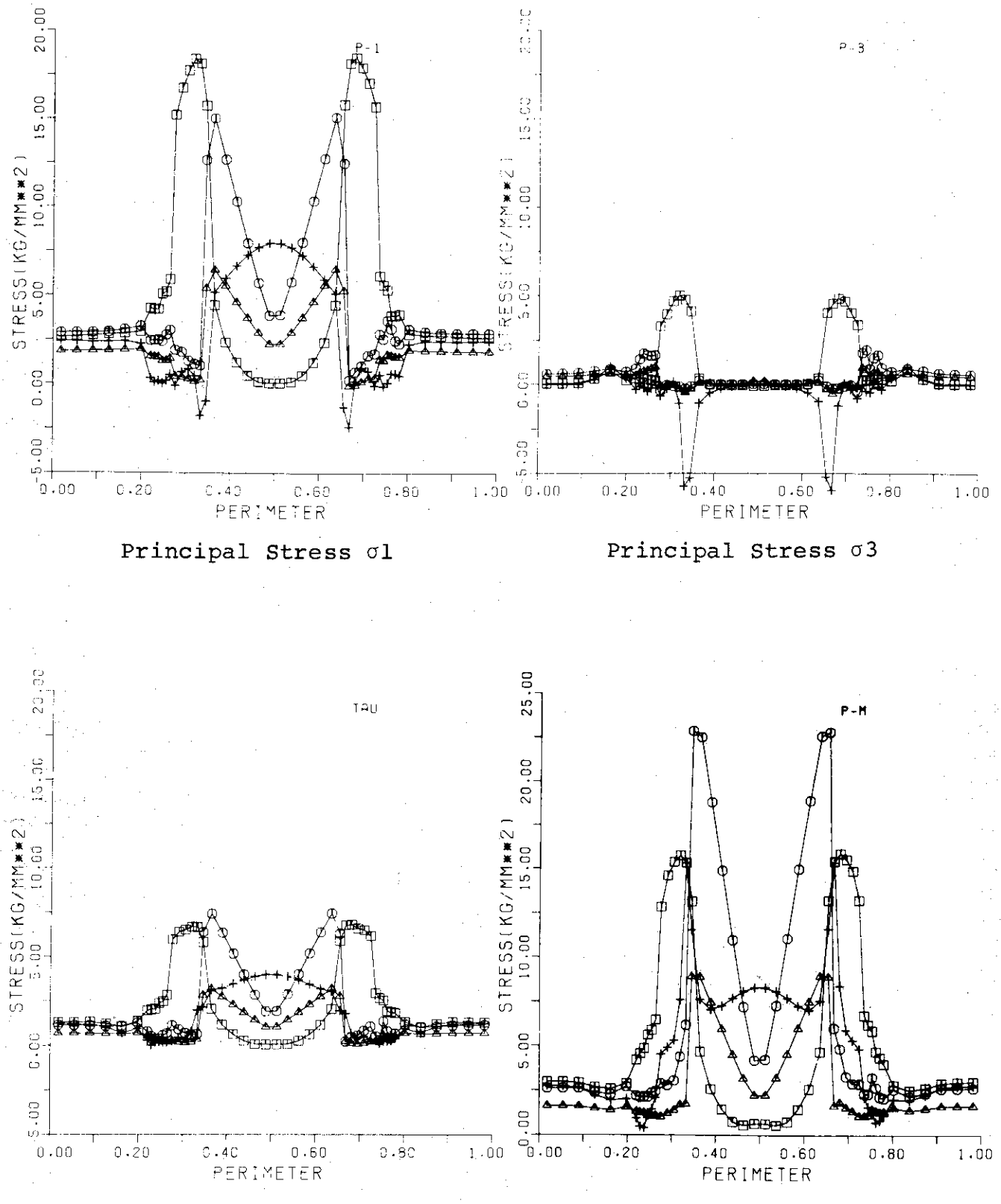

Principal Stress σ1

Principal Stress σ3

Principal Shear Stress τ

Von Mises Stress

Fig. 46 Stresses in case of outer OH coils, anisotropy and two points support

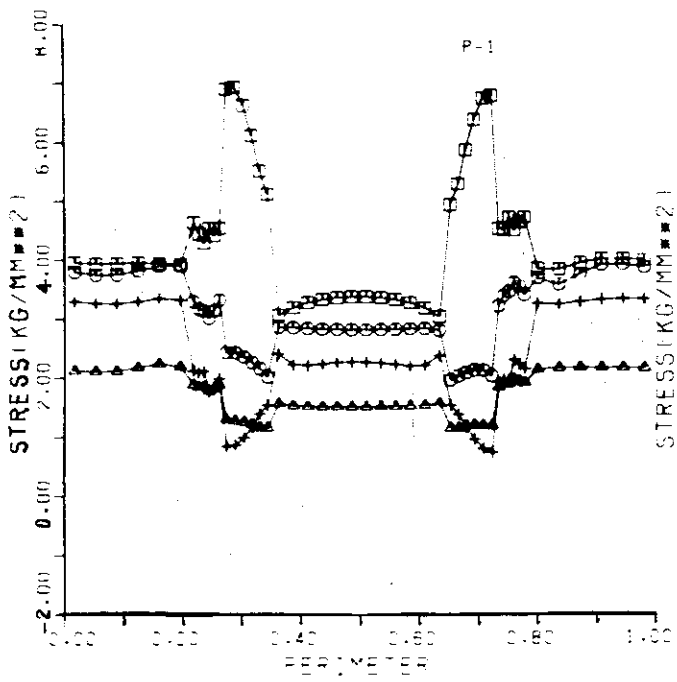

Principal Stress σ1

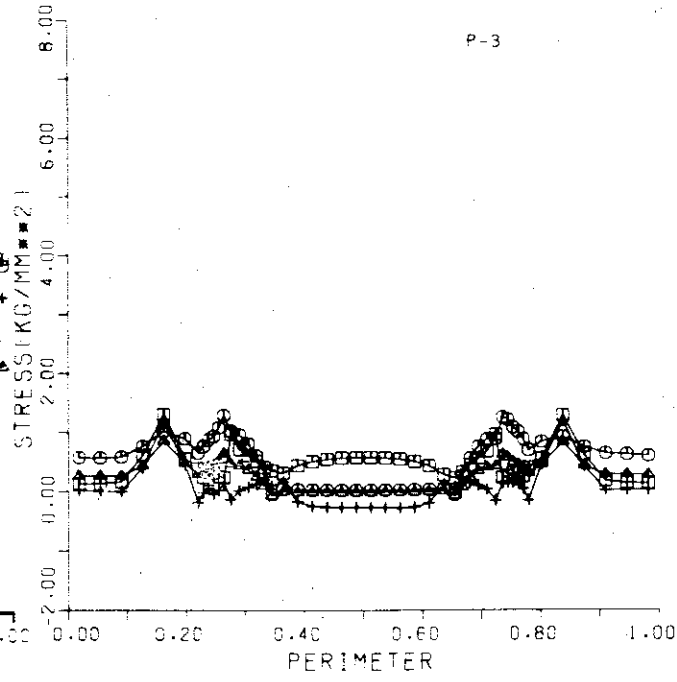

Principal Stress σ3

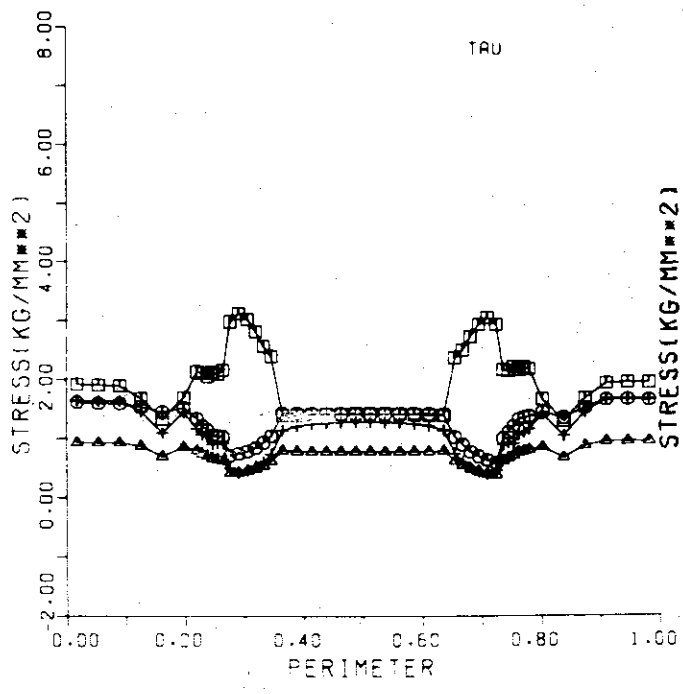

Principal Shear Stress τ

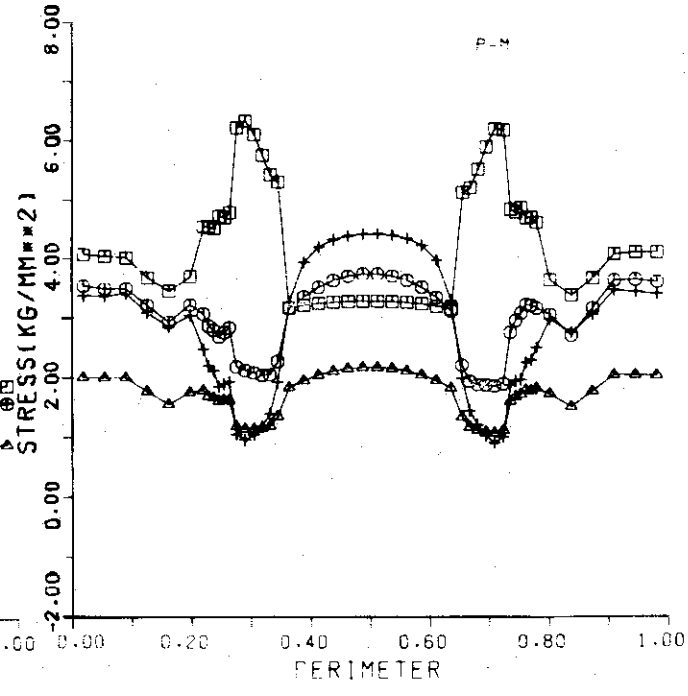

Von Mises Stress

Fig. 47 Stresses in case of outer VF coils, isotropy and continuous support

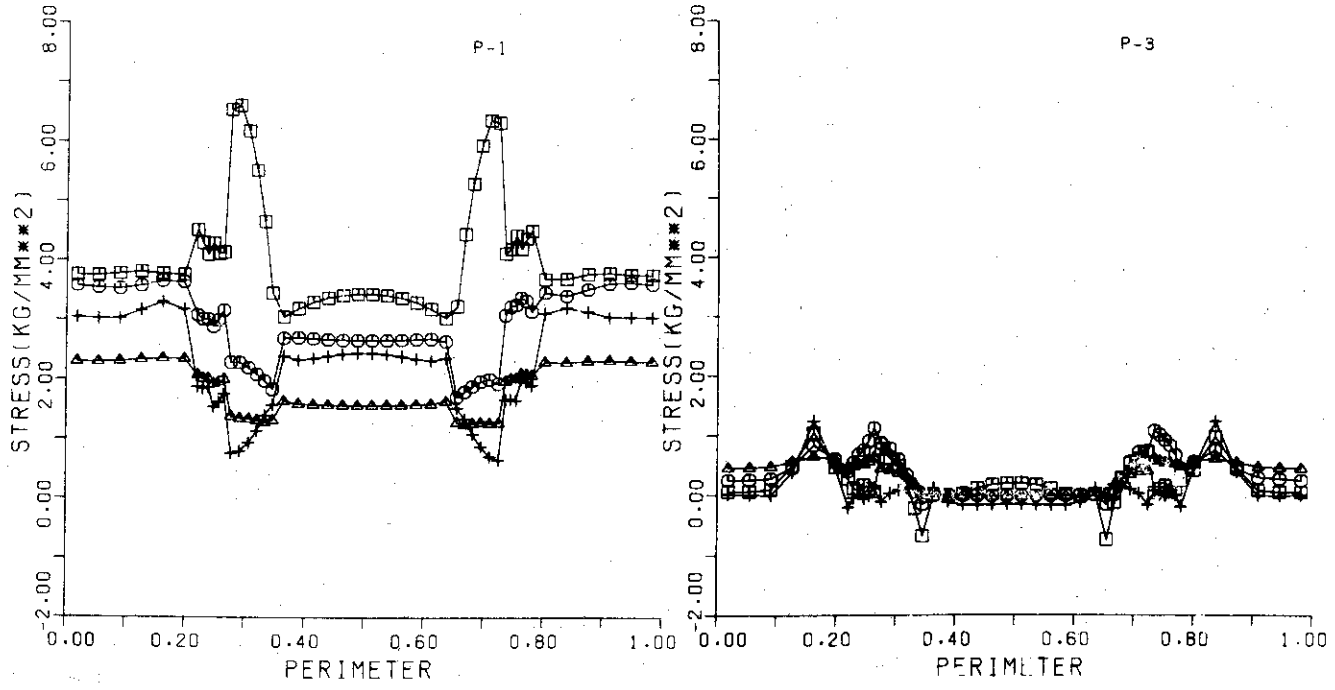

Principal Stress σ1

Principal Stress σ3

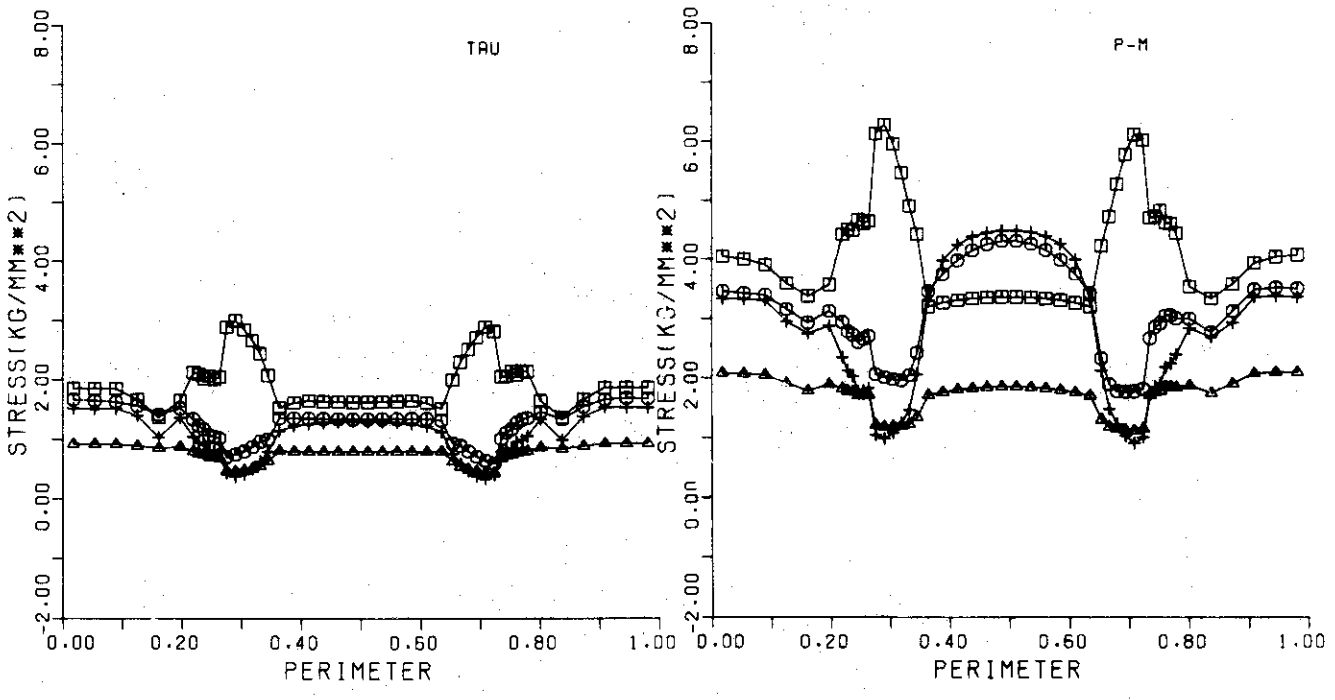

Principal Shear Stress τ

Von Mises Stress

Fig. 48 Stresses in case of outer VF coils, anisotropy and continuous support

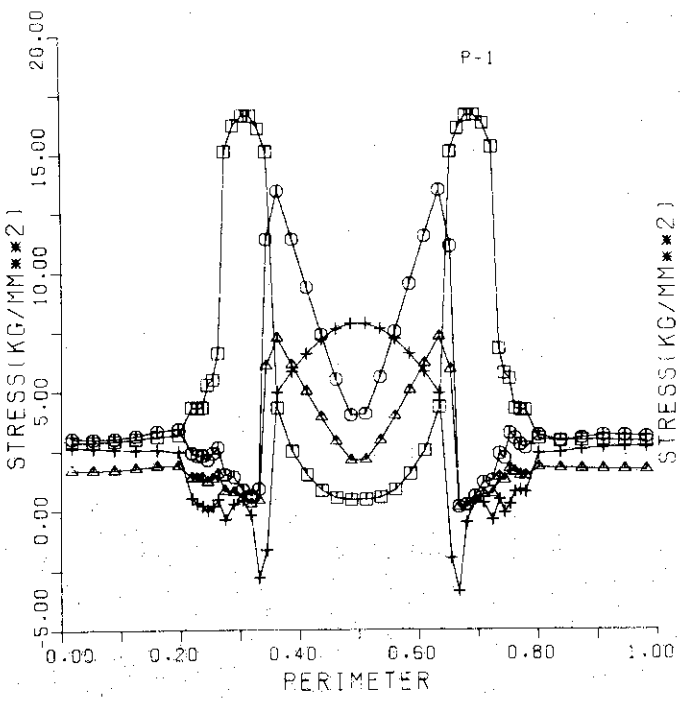

Principal Stress σ1

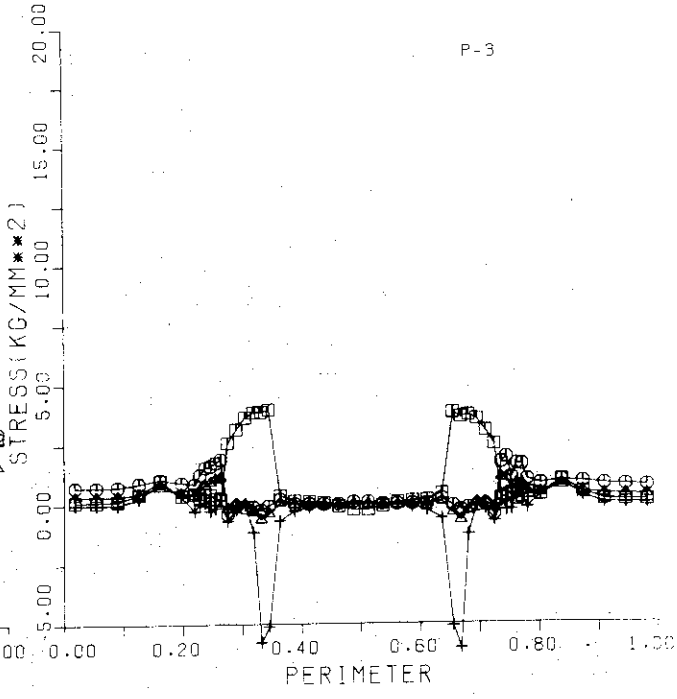

Principal Stress σ3

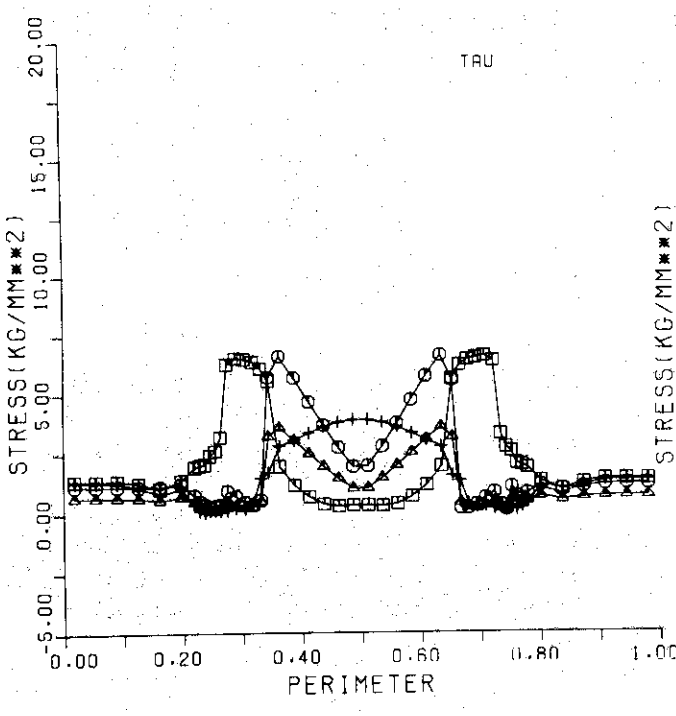

Principal Shear Stress τ

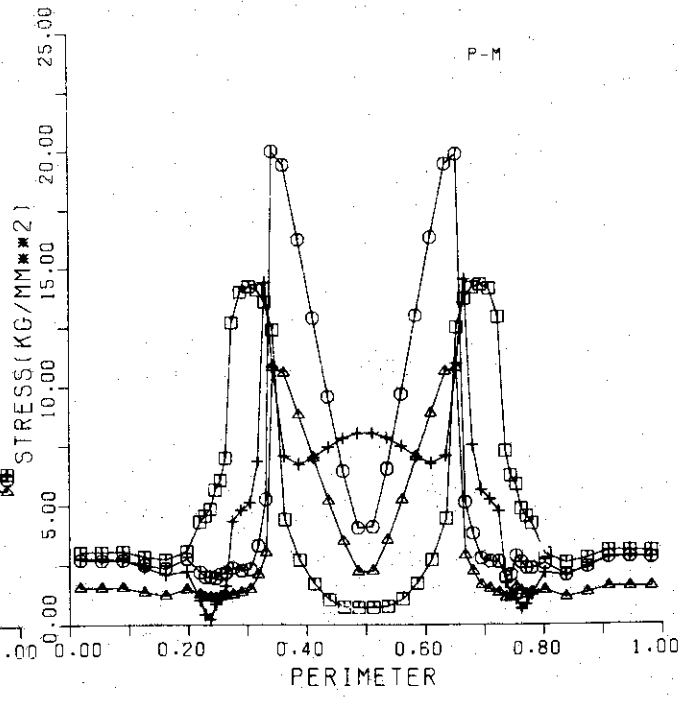

Von Mises Stress

Fig. 49 Stresses in case of outer VF coils, isotropy and two points support

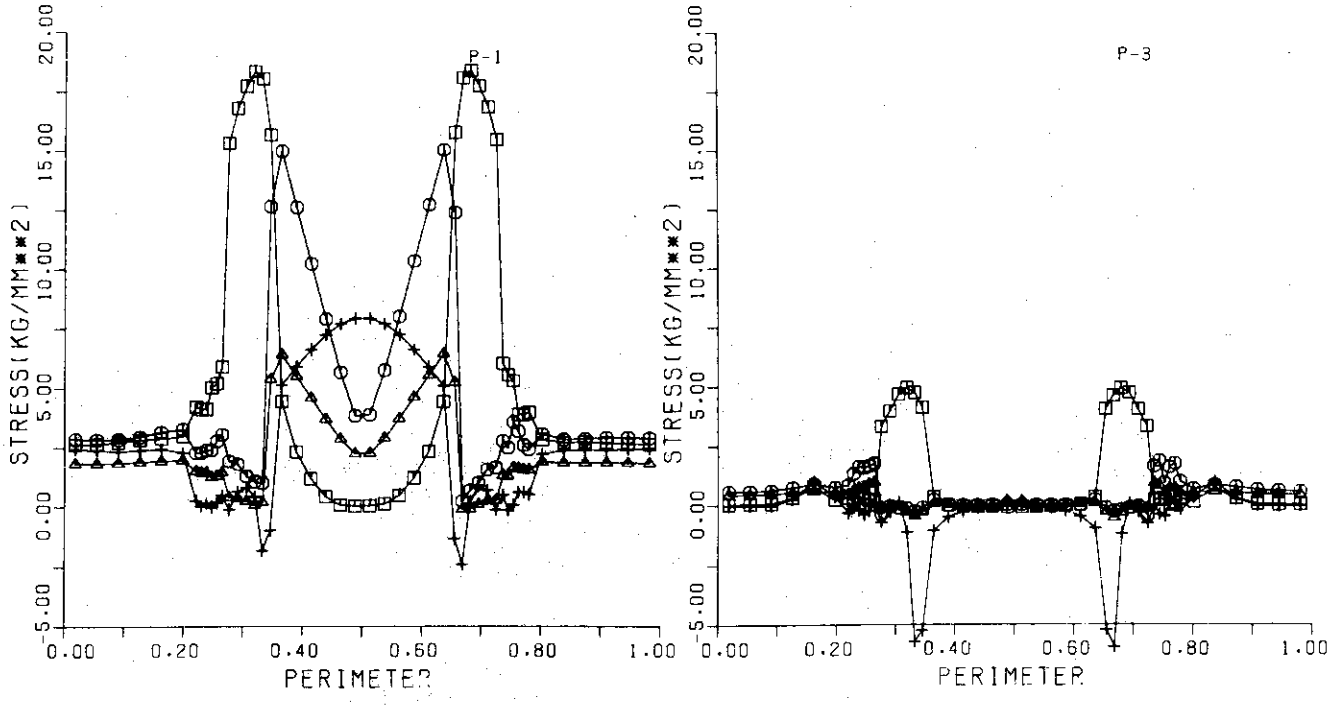

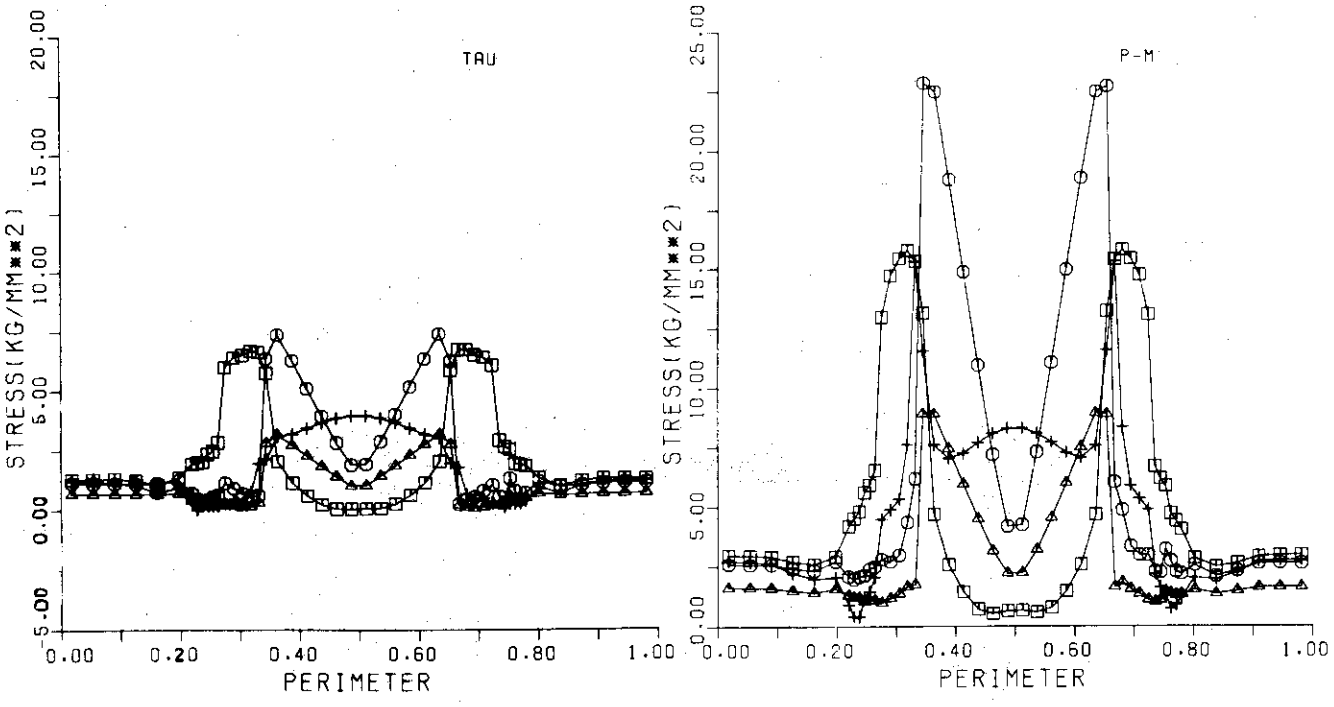

Fig. 50 Stresses in case of outer VF coils, anisoropy and two points support

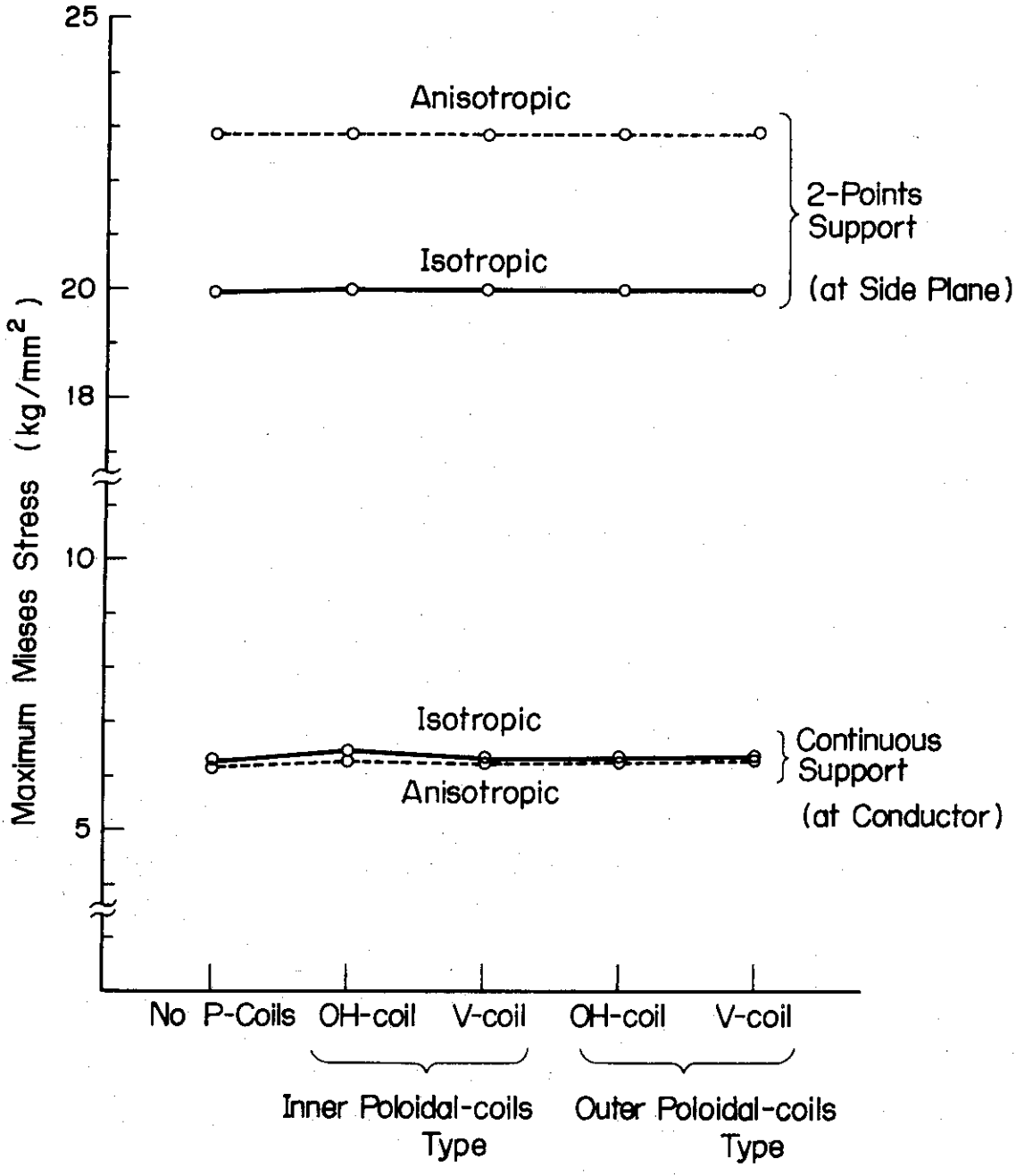

Fig. 51 Summarization of detailed data with maximum Von Mises stress